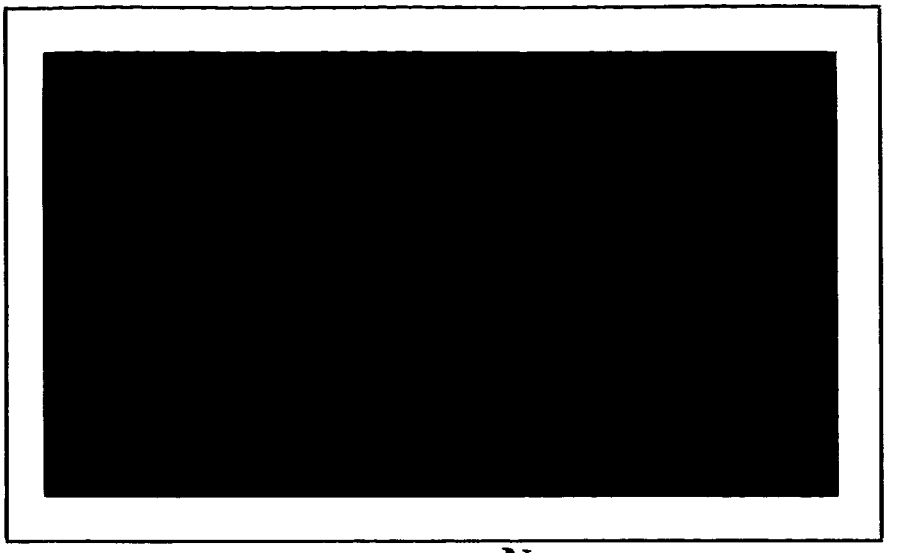

GPO PRICE $ _____

CFSTI PRICE(S) $ _____

Hard copy (HC) 3.00

Microfiche (MF) .65

ff 653 July 65

UNIVERSITY OF PENNSYLVANIA

ELECTROCHEMISTRY LABORATORY

PHILADELPHIA, PENNSYLVANIA 19104

REPORT NO. 11

SEMI-ANNUAL PROGRESS REPORT

1 July 1967 to 31 December 1967

STUDIES IN FUNDAMENTAL CHEMISTRY OF FUEL CELL REACTIONS

NsG-325

Submitted to:

NATIONAL AERONAUTICS AND SPACE ADMINISTRATION

Washington 25, D.C.

Submitted by:

Professor John O'M. Bockris

The Electrochemistry Laboratory
The University of Pennsylvania
Philadelphia, Pa. 19104

NOTICE

This report was prepared as an account of Government sponsored work. Neither the United States, nor the National Aeronautics and Space Administration (NASA), nor any person acting on behalf of NASA:

(a) Makes any warranty or representation, expressed or implied, with respect to the accuracy, completeness, or usefulness of the information contained in this report, or that the use of any information, apparatus, method, or process disclosed in this report may not infringe privately owned rights; or

(b) Assumes any liabilities with respect to the use of or for damages resulting from the use of any information, apparatus, method, or process disclosed in this report.

As used above, "person acting on behalf of NASA" includes any employee or contractor of NASA, or employee of such contractor, to the extent that such employee or contractor of NASA, or employee of such contractor, prepares, disseminates, or provides access to, any information pursuant to his employment or contract with NASA, or his employment with such contractor.

TABLE OF CONTENTS

PROJECT PERSONNEL

Section I

Mr. Boris Cahan, Pre-doctoral Research Fellow

Dr. John O' M. Bockris, Supervisor

Section II

Dr. Ying-Chech Chiu, Post-doctoral Research Fellow

Dr. M. Genshaw, Supervisor

Section III

Mr. Shyam Argade, Pre-doctoral Research Fellow

Dr. John O' M. Bockris, Supervisor

Section IV

Dr. Ljerka Duic, Post-doctoral Research Fellow

Dr. Aleksandar Despic, Supervisor

Section V

Mr. John Diggle, Post-doctoral Research Fellow

Dr. Aleksandar Despic, Supervisor

Section VI

Dr. Divna Cipris, Post-doctoral Research Fellow

Dr. Marvin Genshaw, Supervisor

Section VII

Dr. S. Srinivasan, State University of New York,
Downstate Medical Center, Brooklyn, New York 11203

Section VIII

Dr. A. K. N. Reddy, Indian Institute of Science,
Bangalore 12, India

SECTION I. THE MECHANISM OF POROUS ELECTRODES

The experimental work of this section has been completed, and the essential results of the study are summarized. Papers and a complete write-up are being prepared and will be submitted when complete.

The thesis will be completed and submitted under separate cover within several weeks.

SECTION II. DEVELOPMENT OF A NEW TECHNIQUE TO STUDY ION ADSORPTION

I. Introduction

As electrical double layer and ion adsorption play an important role in electrochemistry, information concerning the structure of the double layer and the amount of its adsorbed ions is highly desirable. Up to the present time, there are only a limited number of methods employed in the study of ion adsorption and there has not been a very successful method for measuring ion adsorption on solid metal. The radiotracer method developed by the Russian workers is subject to the limitation of low concentration and the availability of the radioactive isotopes. The other methods all have their own limitations. The electrocapillary method, which gives a satisfactory result for the amount of ion adsorbed on liquid metal, is not suitable for the same study on solids. Therefore, the development of a new method for studying ion adsorption is demanded. This research is designed to accomplish this, and some qualitative indication of the success of using ellipsometry in the study of ion adsorption on platinum has been presented prior to this reporting period.[1,2] A quantitative interpretation of data constitutes the main work of this project up to this moment. During this reporting period, ellipsometry has been successfully applied to the study of ion adsorption on mercury, the result of which was compared with that obtained

by electrocapillary measurement. A satisfactory agreement was obtained between these two methods. This indicates further the suitability of using ellipsometry in the study of ion adsorption.

II. Experimental

A. Apparatus

The apparatus used in this measurement is shown in Figure 1. The ellipsometer was made by O.C. Rudolph & Sons, Inc. (Model 437-200E).

B. Cell

The cell is made of quartz and has a Teflon top having holes to keep tubing and electrodes in position (Figure 2).

C. Preparation of the mercury surface

In order to minimize mechanical vibration, a thin layer of mercury on gold foil was used as the reflecting surface. Gold foil (30 mm × 38 mm × 0.0007 in. thick, Arthur H. Thomas Co., Philadelphia) was mounted on a piece of microscope glass slide (2" × 1") and was soaked in 1:8 H_2SO_4 overnight. After washing with water, distilled water, and conductivity water, the gold foil (mounted on glass) was soaked in acetone overnight. Immediately before the experiment, the gold foil was taken out from the acetone bath. After evaporating off the adhering acetone, the gold foil was dipped in a mercury pool and the surface was

amalgamated, and a thin layer of mercury was also carried out from the pool, which serves as the reflecting surface.

D. Procedures for making a measurement

After the mercury surface was prepared and all the accessories were put in the proper position, the cell was immediately connected to the potentiostat and the potential was maintained at -1.0 V (vs. Sat. Cal. electrode). Then the alignment of the cell was made to obtain a proper reflection (the angle of incidence was 68.2° to the reflecting surface) and the quarter wave plate was fixed at 45°. The potential was then changed to -0.7 V. An extinction setting of the optical components of the ellipsometer was first found by a swing method. The condition of the experiment was then varied by changing the potential and concentration of the solution. The change of adsorption state was registered by a Sanborn Recorder as a change of intensity of light at the extinction setting of analyzer and about 4° away from extinction of the polarizer.[3] The change in intensity was then calibrated against the readings of the polarizer, and it is directly proportional to the change in polarizer reading in the range of the experimental conditions.

III. Result and Discussion

A. Result

Adsorption study was made with sodium thiocyanate (Baker Analyzed

Reagent) solution. Data of five different solutions of sodium thiocyanate are shown in Figure 3.

B. Method of calculation

(1) Calculation of Δ and ψ from polarizer and analyzer reading.

Δ and ψ for this set-up of the ellipsometer are calculated according to the following equations:

$$\Delta = 2 \times (\text{reading of polarizer}) + 90°$$

$$\psi = \text{reading of analyzer.}$$

(2) Calculation of refractive index of mercury surface.

The refractive index was calculated from the following equation:[4]

$$n_2^2 = (n + iK)^2 = n_1 \tan \phi_1 \left[1 - \frac{4\rho \sin^2 \phi_1}{(\rho + 1)^2}\right]^{\frac{1}{2}}$$

where

n_2 = the refractive index of the mercury,

n = the real part of n_2,

K = the imaginary part of n_2,

n_1 = refractive index of solution,

ϕ_1 = angle of incidence,

$\rho = \tan \psi e^{i\Delta}$.

The Δ, ψ values were obtained from 0.64 NaF solution at -0.7 V vs. Sat. Cal. electrode where no adsorption of ion is expected. The n value is 1.45 and K is -5.31.

(3) Calculation of refractive index of ion.

The refractive index of ion was calculated from the Lorentz-Lorenz equation:[5]

$$R = V_m \frac{n^2 - 1}{n^2 + 2}$$

where

R = molar refractivity,

V_m = molar volume,

n = refractive index.

For CNS^-, V_m = 40.4 cc/q-ion.[6] R_{CNS^-} was calculated from the following equations:

$$R_{salt} = R_{cation} + R_{anion} \quad (7) = \frac{M}{d}\left(\frac{n^2_{salt} - 1}{n^2_{salt} + 2}\right)$$

R_{NH_4CNS} was calculated to be 22.2 (using M = 76.13, d = 1.305, n = 1.685)[8]

$R_{NH_4^+}$ = 4.65 cc/g-ion[9]

R_{CNS^-} = 22.2 - 4.65 = 17.55 cc/g-ion .

By solving the Lorentz-Lorenz equation, n_{CNS^-} is calculated to be 1.84.

(4) Calculation of surface coverage of adsorbed ion.

The surface coverage of adsorbed ion was calculated by using the Drude exact equation[10] in the following way:

(a) A constant film thickness of 5.5Å[11] was taken for the adsorbing film of CNS^- for all the coverages below monolayer.

(b) The surface film was assumed to be constituted from adsorbed

CNS^- and water molecules. The refractive index was calculated assuming a linear combination of the refractive indices of CNS^- and water as:

$$n_{film} = n_{H_2O}(1 - \theta) + n_{CNS^-}\theta \quad ,$$

where

$n_{H_2O} = 1.33$

θ = surface coverage of CNS^-.

(c) The Δ and ψ values were calculated for different refractive indices of the film by using the exact ellipsometry equations through an electronic computer. The calculated change of Δ at different θ values was plotted as a calibration curve in Figure 4. There are two curves in Figure 4; the lower one is for solution of high concentration (1 N) where the refractive index of solution was taken as 1.35, and the upper one is for solution of low concentrations (10^{-1} N or less) where the refractive index of solution was taken as 1.33. The experimental value of the change of Δ was then applied to Figure 4 and the θ value was obtained from the curve.

The experimental θ was compared with Kovac's result[12] in Figure 5. Kovac's determination of adsorbed ion was made by electrocapillary method, which is well justified for adsorption measurements on liquid metal. The agreement shown in Figure 5 is good in general. At large negative potential, where the adsorption is low, the ellipsometry seems to give lower values of θ. This is due to the difficulty of choosing

the absolute zero point for comparison of data. The ellipsometer is sensitive to $\pm 0.01°$, which amounts to about ± 0.04 of θ in this case. The deviation of ellipsometry θ from that of the electrocapillary method seems to lie within this experimental limit. The agreement could be improved if the sensitivity of the ellipsometry is increased to $\pm 0.001°$ either by using multiple reflection or by minimizing the noise level of the whole experimental set-up. The agreement could also be improved by choosing better values of the constants involved in the calculation or by using some other assumptions about the refractive index of the film.

IV. Plan for the Future

A. More experiments will be made on the thiocyanate adsorption on mercury in order to check the reproducibility and the reliability of the method.

B. The study of ion adsorption on solid metal will be undertaken.

REFERENCES

1. Technical Report ECOM-01291-7, 7th Quarterly Report, April, 1967, United States Army Electronics Command, Fort Monmouth, N.J.

2. Technical Report ECOM-01291-F, Final Report, November, 1967, United States Army Electronics Command, Fort Monmouth, N.J.

3. J.O'M. Bockris, M.A.V. Devanathan, and A.K.N. Reddy, Proc. Roy. Soc., 279, 327 (1964).

4. Ellipsometry in the Measurement of Surfaces and Thin Films, Symposium Proceedings, National Bureau of Standards Miscellaneous Publication 256, p. 62.

5. E.A. Moelwhyn-Hughes, Physical Chemistry, Pergamon Press, 1961, p. 382.

6. Ibid., p. 878.

7. J.R. Tessman and A.H. Kahn, Phys. Rev., 92, 890 (1953).

8. N.A. Lange, Handbook of Chemistry, Ninth Ed., p. 220.

9. E.A. Moelwhyn-Hughes, Physical Chemistry, Pergamon Press, 1961, p. 400.

10. Ellipsometry in the Measurement of Surfaces and Thin Films, Symposium Proceedings, National Bureau of Standards Miscellaneous Publication 256, p. 61.

11. H. Wroblowa, Z. Kovac, and J.O'M. Bockris, Trans. Faraday Soc., 61, 1523 (1965).

12. Z. Kovac, Ph.D. Thesis, University of Pennsylvania, 1964.

CAPTIONS

Fig. 1. Schematic diagram of the apparatus.

Fig. 2. The cell.

Fig. 3. Change of polarizer reading with potential.

Fig. 4. Calibration curve.

Fig. 5. Comparison of θ obtained from ellipsometry and electrocapillary method.

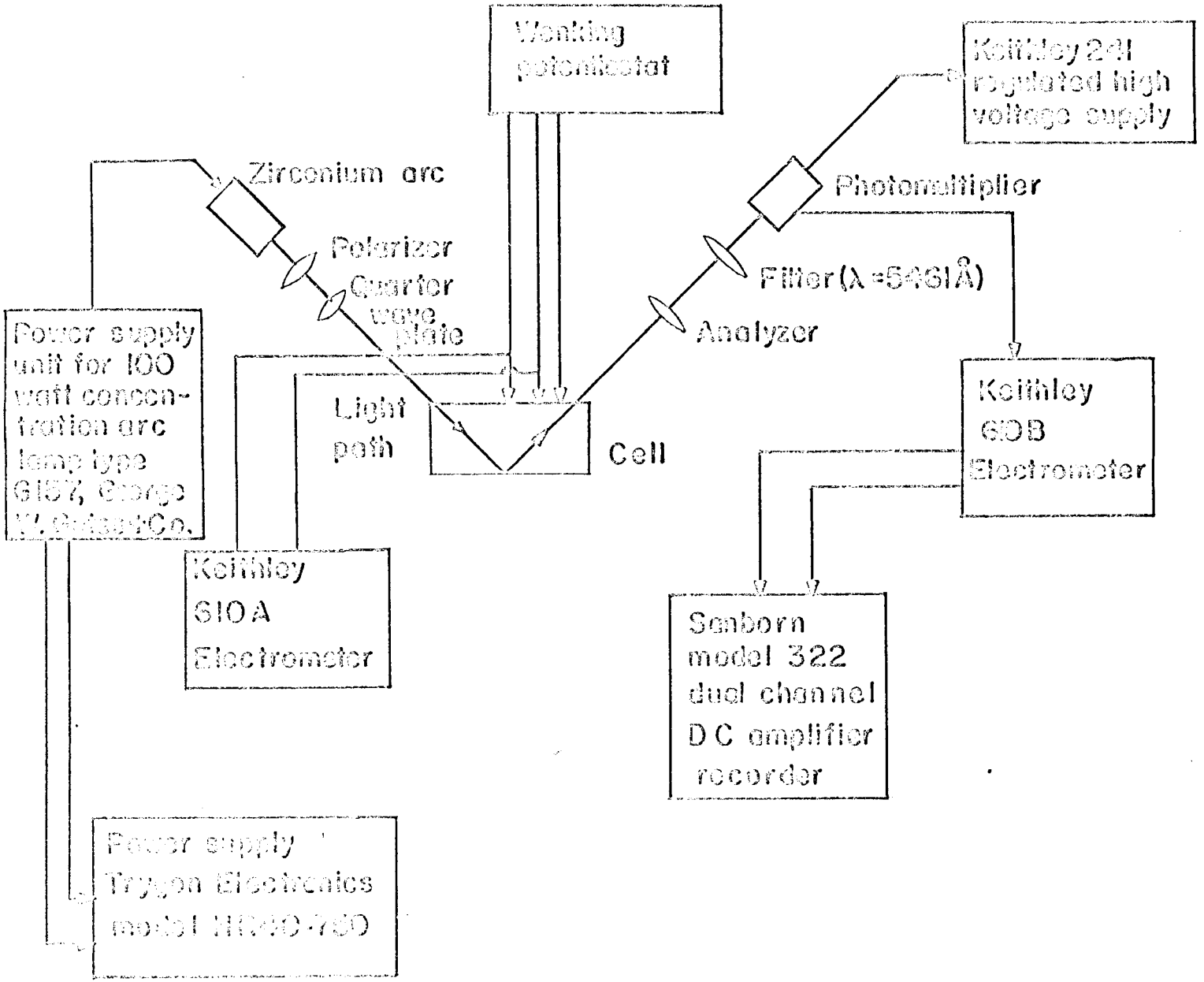

Fig.1 Schematic diagram of the apparatus.

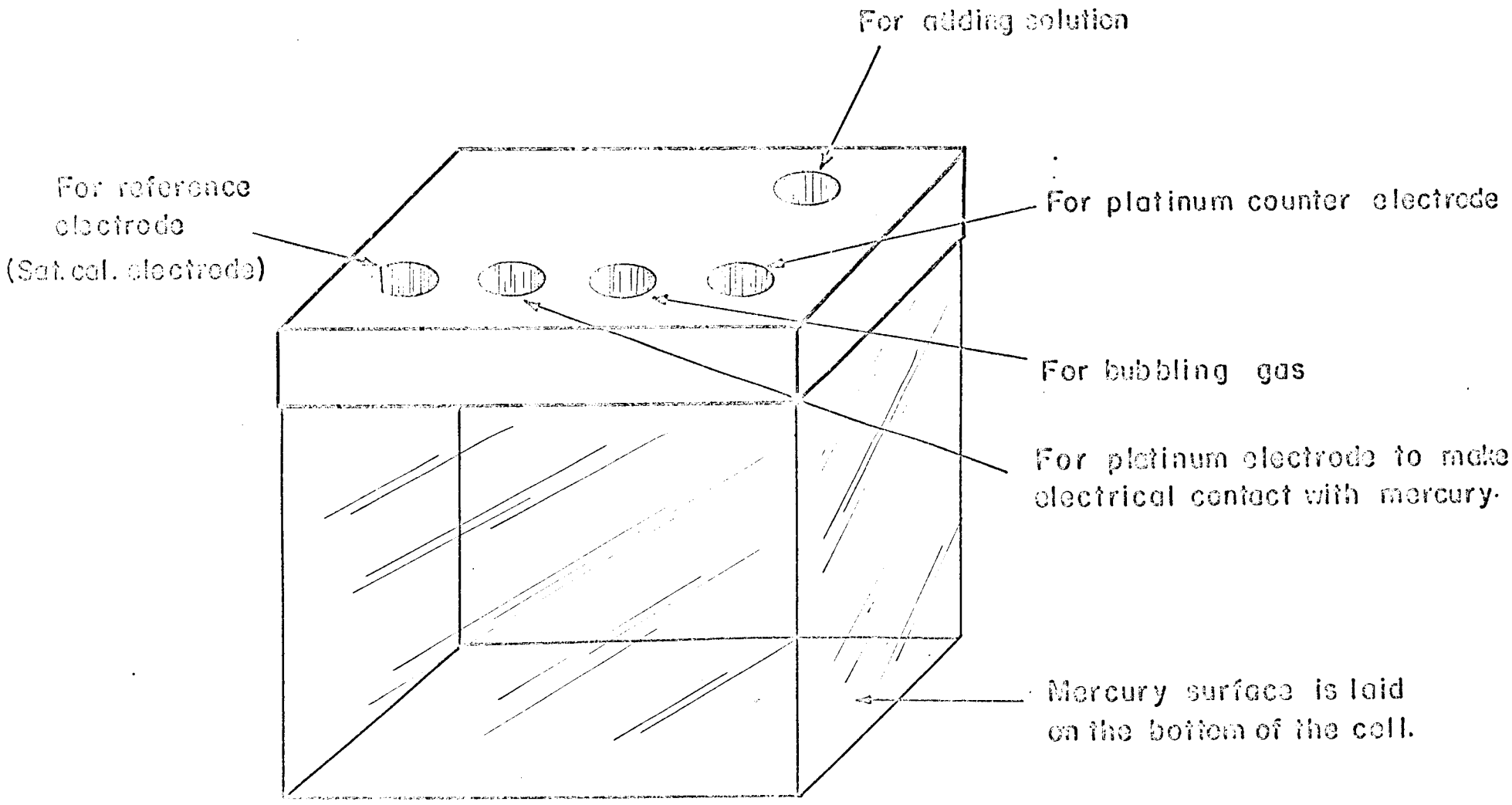
For adding solution
For reference electrode (Sat. cal. electrode)
For platinum counter electrode
For bubbling gas
For platinum electrode to make electrical contact with mercury.
Mercury surface is laid on the bottom of the cell.

Fig. 2 Cell

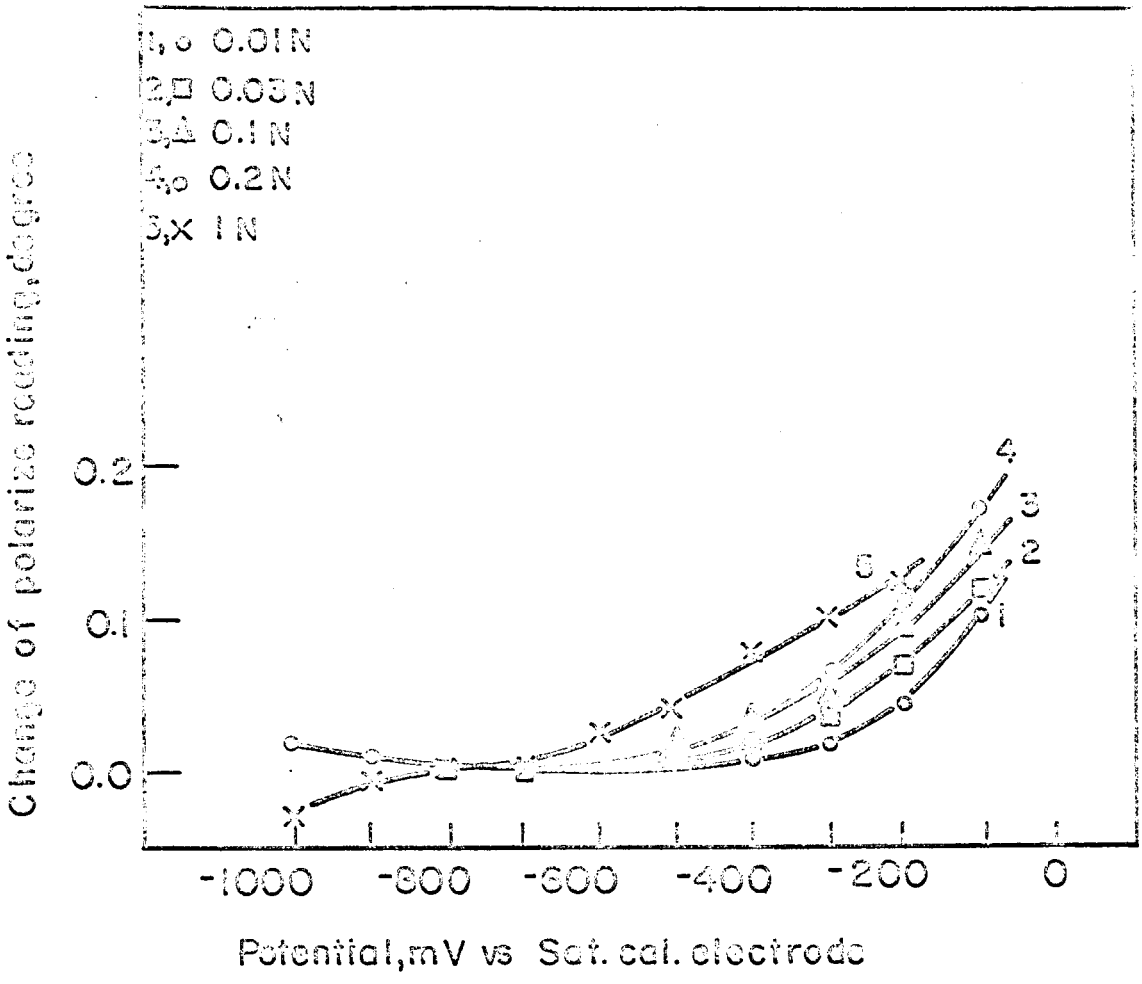

Fig. 3 Change of polarizer reading with potential

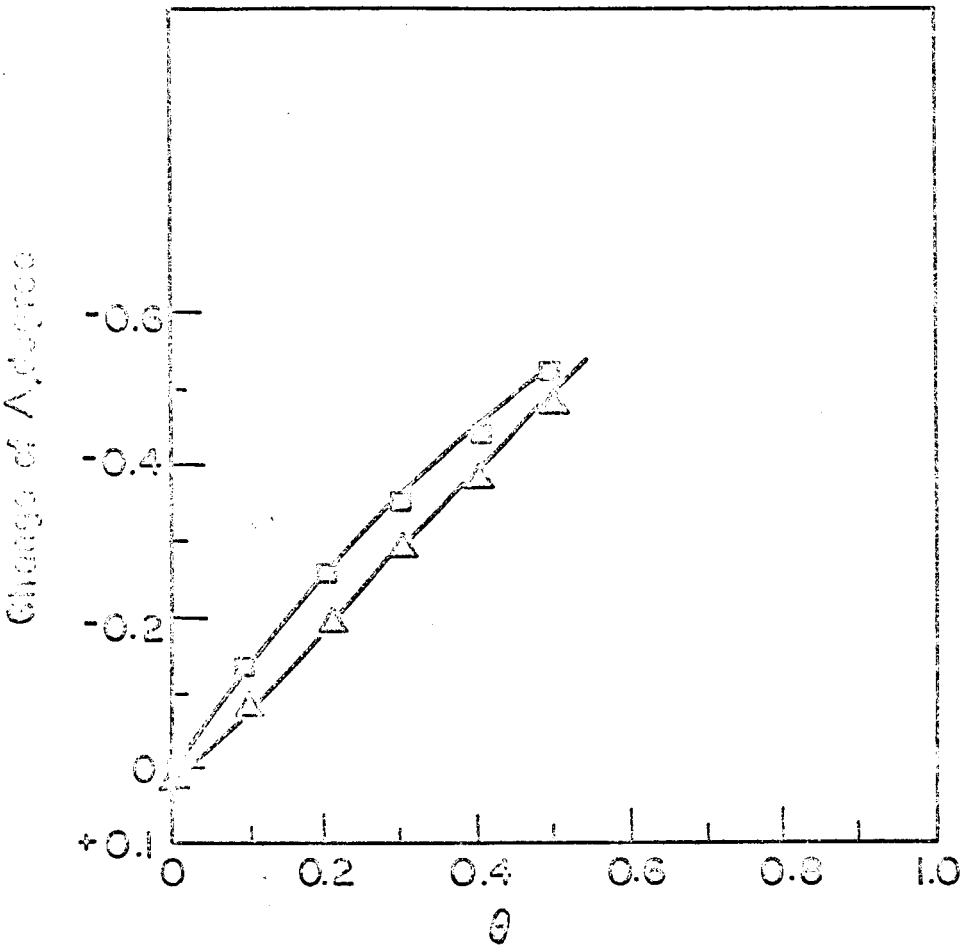

Fig. 4 Calibration curve

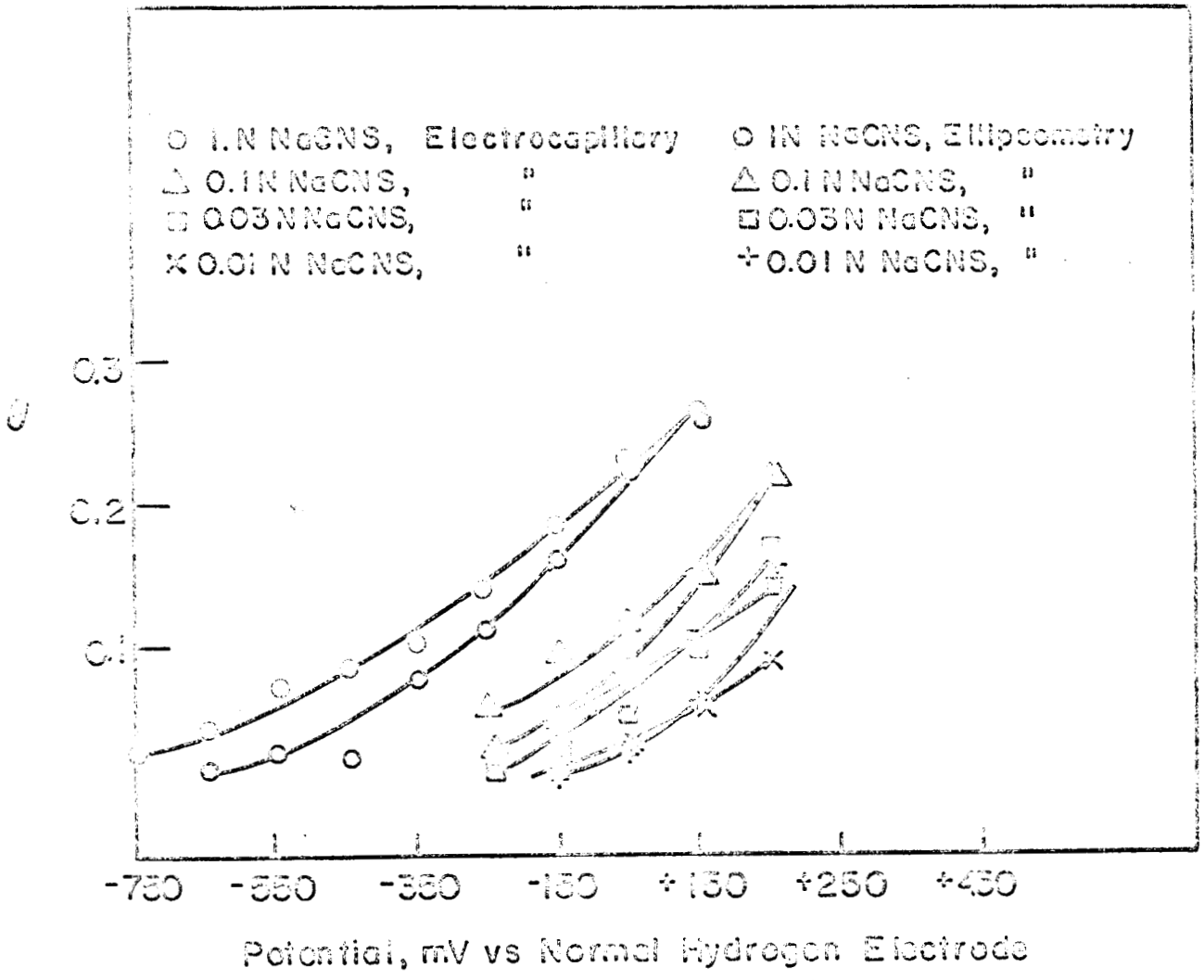

Fig. 5 Comparison of θ obtained from ellisometry and electrocapillary method.

SECTION III. POTENTIAL OF ZERO CHARGE DETERMINATION

1. General Objectives

The data in the literature for potentials of zero charge are discrepant from method to method and discordant from author to author. Since potential of zero charge is one of the important electrochemical parameters, it is sought to obtain concordant results by three independent methods for a number of systems. Also this will enable us to apprehend the double layer at a solid-solution interface to a better extent.

2. Present Period

In the present report period, a rebuttal to Frumkin's criticism of our work on potential of zero charge on platinum was prepared. An attempt was also made to explain the discrepancies in the two values of potential of zero charge on platinum.

I. Facts

1. The value of the $V_{p.z.c.}$ obtained in the Russian work is about 0.2 v. (N.H.S.). It is independent of pH.

2. The value of $V_{p.z.c.}$ obtained in this laboratory is 0.5v, but varies with pH according to the equation

$$V_{p.z.c.} = 0.55 - 0.066pH. \quad (1)$$

3. The methods used in the Russian work are: capacitance minimum; repulsion between double layers; equal ionic adsorption of cations and anions.

The methods used in the Electrochemistry Laboratory are: capacitance minimum; dependence of friction on potential; potential at which organic adsorption is equal with different concentration of the electrolyte.

4. There is a considerable difference in the platinum-solution interface. In the work done in Frumkin's laboratory, the hydrogen on the platinum surface is in equilibrium with dissolved hydrogen in the metal and protons in the solution. In the work from this laboratory, no hydrogen is intentionally present in the solution, and a negligible quantity is in the metal (see calculations given in Appendix I). Moreover, no equilibrium is established between protons in solution and hydrogen on surface.

5. Burshtein et al. observe a capacitance minimum at 0.5 v <u>in concentrated solutions</u>.

II. <u>Frumkin's criticisms of our work</u>

1. He has stated that in his opinion the minimum observed by Argade is in fact a pseudo-capacitance minimum, and thus does not refer to the situation necessary for the determination of potential of zero charge.

2. He points to the pH dependence of our p.z.c. implying that, if such a dependence exists, the quantity to which it refers cannot be a potential of zero charge.

3. It is implied that, because the method first originated by Dahms and Green has been used (equality of organic adsorption at different ionic strengths), the values obtained therefrom cannot be valid. It is implied that the adsorption of organic compounds is not dependent upon the electrostatic considerations primarily (used as a basis of the Dahms and Green method) but must be connected with the presence of H and O on the surface.

III. Defensive remarks concerning Frumkin's criticisms

1. Pseudocapacitance

The pseudocapacitance criticism does not have validity, because the comparison is made for two different surfaces of Pt at two different concentrations.

Thus, the capacitance minimum observed at 0.5 v by Burshtein et al. was obtained by carrying out capacitance measurements on active platinum in 0.1 N H_2SO_4 solution, where the possibility of getting a minimum corresponding to the p.z.c. is exceedingly small.

On the other hand, Mr. Argade's minima for the capacitance were obtained in 10^{-3} N perchloric acid, with deactivated electrodes which contained "no hydrogen" (see Appendix I). It is, therefore, not tenable

to criticize Argade's values on the basis which Frumkin has published. Further evidence to support this view is as follows:

a. Capacitance-frequency relationships

A variation of capacitance with frequency was observed by Argade, and at first one might naively assume that this might be evidence for a pseudocapacitance contribution to the capacitance which he observed. This hypothesis has been examined, and in Appendix II the evidence that it is not a pseudocapacitance, but in fact arises probably from relaxation phenomena of the water dipoles, or possibly from some effect corresponding to the spreading of current lines along a liquid layer on the electrode in contact with the glass holder, is presented.

b. Concentration variation

It is of course possible to examine the degree of pseudocapacitance observed by Mr. Argade by varying the concentration of the electrolyte, and in Appendix III the results, which do not support a pseudocapacitance nature of his minima, are given.

One can see that the evidence given on these two diagnostic criteria of the pseudocapacitance is unambiguous.

2. pH dependence of the potential of zero charge

Specific adsorption of H_3O^+ or OH^- ions may give rise to pH dependence of the potential of zero charge. Electrocapillary thermodynamics for the platinum-solution polarizable interface has been worked out in Appendix IV and it is shown that:

$$\left(\frac{\partial E}{\partial \ln a_{OH^-}}\right)_{q^m=0} = -\frac{RT}{F}\left\{\left(\frac{\partial q_{OH^-}}{\partial q^m}\right)_{a_{NaOH}} + 1\right\} \qquad (2)$$

where E is the potential of zero charge on the normal hydrogen scale, a is the chemical potential, q_{OH^-} is the amount of OH^- ions adsorbed, and q^m is the charge on the metal. If the first term in equation (2) is negligible, then the slope of the p. z. c. versus pH plot seems to be $-RT/F$, in accordance with the experimental facts.

The independence of the amount of adsorbed ions with charge on the metal, appears to have some qualitative confirmation near the potential of zero charge. Thus, for example, cations like Na^+, Cs^+ in alkaline iodide solutions behave in this way. An analogous situation arises in SO_4^{2-} adsorption on platinum from 10^{-2} N H_2SO_4 + 10^{-2} N $CdSO_4$ and I^- adsorption on Pt from 10^{-3} N NaI + 10^{-3} N H_2SO_4 (Frumkin et al., J. Electrochem. Soc., 113, 1011 (1966)).

Thus, the pH-dependence of p. z. c. as observed in our work need not be connected with hydrogen and oxygen adsorption, but may arise from the independence of the amount of adsorbed ions with the charge on the metal near the potential of zero charge.

3. Dahms and Green method

According to this method, at p. z. c., adsorption of an organic substance is independent of the electrolyte concentration. This method depends upon purely electrostatic considerations, i.e., variation of Γ_{org} (surface concentration) with charge on the metal.

According to Frumkin's theory that organic adsorption is dependent predominantly on H and O adsorption (Frumkin's notation),

$$\left(\frac{\partial \Delta G}{\partial \psi}\right)_{\Gamma_{org}} = -\left(\frac{\partial \varepsilon}{\partial \Gamma_{org}}\right)_{\psi} + \left(\frac{\partial A_H}{\partial \Gamma_{org}}\right)_{\psi} , \qquad (3)$$

where ψ is the potential on some scale. Further, $\left(\frac{\partial \Delta G}{\partial \psi}\right)_{\Gamma_{org}}$ will be determined by the magnitude of the ratio between ε and A_H. If one considers an equilibrium between adsorbed hydrogen and protons in solution, then the coverage of hydrogen in a solution of pH = 3 at 0.4 v is found to be about 2×10^{-7}.* This corresponds to an adsorbed charge of 4×10^{-5} μ coul cm^{-2} which in comparison with the charge on the metal ε of about a few μ coul cm^{-2} is negligible. Thus, the effect of $(\partial A_H/\partial \Gamma_{org})_{\psi}$ on $(\partial \Delta G_{org}/\partial \psi)$ is seen to be exceedingly small in the potential range of the adsorption maximum and p. z. c. Moreover, in these experiments, the pH of the solution was kept constant and the concentration of the neutral salt was varied. Thus, any effect of H and O on the adsorption of the organic substance would remain exceedingly small and constant.

Thus, the adsorption of organic molecules in the range used in the Dahms and Green method is probably effected by electrode potential largely in a direct way.

---

*Assuming Langmuir conditions for H-adsorption equilibrium, one obtains $\theta/(1-\theta) = (\theta/(1-\theta))_0 C_{H^+}/(C_{H^+})_0 \exp -(V - V_0)F/RT$, $\theta_0 = 0.3$, $V_0 = 0.2$ v, $C_{H^+} = 1$ N acid; for $V = 0.4$v and $C_{H^+} = 10^{-3}$ N acid, $\theta = 2 \times 10^{-7}$. (Assuming a Temkin behavior won't make much difference.—low concentration.)

4. Results of the friction method

The friction method is of course not dependent upon the same kind of criticisms as those which Frumkin has made. However, (a) it gives good agreement with the results of the other two methods (see Appendix V), and (b) it gives the same pH variation as the other two methods (Appendix V). It would need a rather considerable coincidence, surely, for the errors of the pseudocapacitance to show with an equal degree in the friction method.

In summarizing the situation as seen at the moment, therefore, one might say: The results of both investigations probably measure a potential of zero charge, and the investigation should be shifted to why the difference in conditions used gives differences in the potential of zero charge.

IV. Differences in condition of materials used in the work in Moscow and in Philadelphia

In Moscow work the conditions are: The H on platinum surface is in equilibrium with hydrogen ions in the solution. The amount of hydrogen absorbed in the electrodes used by Voropaeva, Deryagain and Kubanov, for example, may be roughly estimated. This has been done, with certain stated assumptions, in Appendix VI. It is of the order of 33% of saturation, some seventeen minutes after the coverage of hydrogen on the Pt surface is made zero, for the size of electrodes used.

In the Philadelphia electrodes, the amount of hydrogen is about 10^{-4} of saturation as evidenced by the estimatory calculations given in Appendix I.

Roughly, one has with the Philadelphia electrodes a situation of a polarizable interface; in the case of the Moscow electrodes one has the situation of a non-polarizable interface, because of the activation procedure used.

V. Some interpretive suggestions concerning the change of absolute values under the activated, Moscow, electrodes and the non-activated, Philadelphia, electrodes

(a) An initial model which one might think of as a basis for an interpretation of the difference of p. z. c. values observed, is connected with the difference in the amount of hydrogen present in the two electrodes. However, it is shown in Appendix VII that neither the dissolved hydrogen nor the adsorbed hydrogen is significantly important to account for the discrepancy, under the assumptions involved.

(b) A second model which may be considered arises from the difference in structure of the surfaces in the two works. One may speculate reasoningly upon the different surfaces to which the differing pretreatments give rise. The Moscow electrodes are given a so-called "activation" procedure, namely, holding electrodes at a potential where they have formed a surface phase oxide (cf. Reddy, Genshaw, and Bockris, J. Electroanal. Chem., 8, 406 (1964)). The consequent cathodic pulse

gives rise to an "active" platinum surface which is in a different state from the state it was in before the activational treatment.

The "active" surface is left with vacancies in the surface and they are filled with water molecules. The number of these vacancies can be estimated as follows. Weizer and Girifalco (cf. Phys. Rev., 120, 837 (1960)), have shown by calculations assuming Morse functions for the various interaction potentials, that two vacancies do not attract each other at a distance of >7Å separation. At a smaller distance of separation (<7Å), they probably disappear by becoming divacancies and diffuse into the bulk of the metal. Thus, if one assumes that there will be one vacancy in an area of about $150 Å^2$, the number of vacancies per cm^2 is calculated to be about 6×10^{13} (i.e., the Moscow electrodes). Thus, the essential difference between the surface in the Philadelphia and Moscow electrodes is that the latter have a higher concentration of defects on the surface.

The surfaces with defects will have a different potential of zero charge because the surface electron overlap potential will be changed and the resulting reorientation of water dipoles will be effected.

The change in the χ^m, metal surface potential, can be estimated as follows. The presence of a vacancy will effect a line dipole with an opposite polarity to that of the electron overlap, resulting in a lowering of the surface potential. The line dipole will have a dipole moment of about 1×10^{-18} e.s.u. (see Appendix VIII). Thus, the resulting change in χ^m due to 6×10^{13} vacancies per cm^2 is about 0.24 v. Thus, the

assumption of the essential point of the difference between the structures being related to the defects gives a result in the correct direction for the difference between the p. z. c. 's of the two electrodes, and of the right order of magnitude.

A further less important change in the surface potential may arise from a difference in the orientation of water dipoles. Because of the presence of vacancies (metal surface dipoles with positive end outwards), more water molecules will orient with the oxygen end towards the metal. Assuming the number of water molecules reoriented is the same as the number of vacancies, the change in solution surface potential is worked out to be 0.07 v (see Appendix VIII).

The fact that the model which we have chosen gives the correct difference between the results of about 0.3 volts is, of course, coincidental. It is necessary only to show that it has to be of the order of the right type of result.

3. Future Work

A reply from Frumkin has been received to the above letter which was sent to him. The points that he has reaised will be answered in the next report period. Concurrently, the thesis writing will be continued.

APPENDIX III-I

Calculations to estimate the amount of hydrogen remaining in the Philadelphia electrodes

The treatment that was given to our electrodes was as follows: After an initial reduction of surface oxide on Pt at 300°C for five minutes, the platinum electrodes were further heated at 450°C in high purity argon for a minimum period of three hours. During the initial oxide reduction in hydrogen, some hydrogen diffuses inside. The hydrogen that has diffused into the bulk platinum will diffuse out when the electrode is heated at a higher temperature and for long periods of time. The calculations are based on the considerations of a diffusion problem solved by Genshaw and Fullenwider[1] of this laboratory.

The following boundary conditions pertain to the initial situation, namely, that corresponding to the initial reduction in hydrogen.

$$t \leq 0\,,\ x = 0\,,\ c = 0$$

$$t > 0\,,\ x = 0\,,\ c = c_0$$

If one applies these boundary conditions to Fick's second law of diffusion and assumes the electrode to be semi-infinite, one obtains

$$c_x = c_0 \operatorname{erfc} \frac{x}{2\sqrt{Dt}}$$

where c is the concentration of H in Pt as a function of distance x and time t; D is the diffusion coefficient of hydrogen in platinum.

The diffusion coefficient at the elevated temperatures was obtained by extrapolation of the D values determined from 50°C to 70°C and the energy of activation for the diffusion process.

Derivation of the diffusion equation for H diffusing out of platinum

Boundary conditions;

$$t < o_-;\ c_x = c_0 \operatorname{erfc} \frac{x}{2\sqrt{Dt_0}} \tag{1}$$

$$t = o_+;\ c(o, t) = 0 \tag{2}$$

Fick's second law, $D\frac{\partial^2 c(x,t)}{\partial x^2} = \frac{\partial c(x,t)}{\partial t}$ (3)

Assume, $c(x, t) = X(x)\,T(t)$. (4)

From equations (3) and (4),

$$X''(x)\,T(t) = \frac{1}{D}XT'(t) \tag{5}$$

where T' and X'' are first derivative of T(t) and second derivative of X(x) respectively

Dividing both sides of equation (5) by $X(x)\,T(t)$,

$$\frac{X''}{X} = \frac{1}{D}\frac{T'}{T} \tag{6}$$

Since x and t are independent variables, X''/X and T'/DT must equal some constant, say λ^2

$$\frac{X''}{X} = \frac{T'}{DT} = \lambda^2 \tag{7}$$

(1) when $\lambda^2 > 0$;

Now $\frac{T'}{T}dt = D\lambda^2 dt \quad \ln T = D\lambda^2 t + c_1$ (8)

(8) can be written as

$$T = C_1 e^{\lambda^2 Dt} \tag{9}$$

Equation (9) is physically absurd because $c(x, t) = XT$ increases beyond all the boundary conditions as t increases.

(2) $\lambda^2 = 0$;

$$X'' = 0;\ T' = 0, \tag{10}$$

$$X = Ax + B;\ T = C \tag{11}$$

Equations (10) and (11) for the case $\lambda^2 = 0$ are trivial because physically it is suggested that as t increases, c(x, t) remains constant. This can be seen as follows.

$$t \geq 0,\ x = 0,\ c = 0$$

$$\therefore B = 0.$$

From (10), (11), and (4) one obtains

$$c(x) = AC\,x \tag{12}$$

Concentration increases with x continuously, which is an impossibility, and this solution is rejected.

(3) $\lambda^2 < 0$;

From (7) one can write

$$X'' = -\lambda^2 X;\ T' = -\lambda^2 DT \tag{13}$$

$$X = A' \cos \lambda x + B' \sin \lambda T;\ T = C' e^{-\lambda^2 Dt} \tag{14}$$

$$c(x, t) = XT$$

$$= (A' \cos \lambda x + B' \sin \lambda x)\, C' e^{-\lambda^2 Dt}$$

$$= (A \cos \lambda x + B \sin \lambda x) e^{-\lambda^2 Dt} \tag{15}$$

$x = 0$, $c = 0$ and (15) gives

$$Ae^{-\lambda^2 Dt} = 0. \quad \therefore A = 0 \tag{16}$$

$$c(x, t) = B e^{-\lambda^2 Dt} \sin \lambda x \tag{17}$$

It is seen that λ can assume a number of values and each value of λ will specify a given $c(x, t)$. In order to get the entire function $c(x, t)$ equation (17) will have to be integrated over all the values of λ. Thus,

$$c(x, t) = \int_{-\infty}^{\infty} B(\lambda) e^{-\lambda^2 Dt} \sin \lambda x \, d\lambda \tag{18}$$

Now, we have the condition (1) at $t = 0$,

$$c(x, t) = c_0 \operatorname{erfc} \frac{x}{2\sqrt{Dt_0}} = \int_{-\infty}^{\infty} B(\lambda) \sin \lambda x \, d\lambda \tag{19}$$

Now, the Fourier transform is given as

$$[f(t) = \int_{-\infty}^{\infty} g(w) \sin wt \, dw, \text{ is transformed into } g(w) = \frac{1}{\pi} \int_{-\infty}^{\infty} f(s) \sin ws \, ds] \tag{20}$$

Applying (20) to (19),

$$B(\lambda) = \frac{c_0}{\pi} \int_0^{\infty} \operatorname{erfc} \frac{x}{2\sqrt{Dt_0}} \cdot \sin \lambda x \, dx \tag{21}$$

From mathematical tables (NBS Math. Handbook, eds. Abramowitz et al., p. 303), equation (21) is given as

$$B(\lambda) = \frac{c_0}{\pi \lambda} (1 - e^{-\lambda^2 Dt_0}) \tag{22}$$

From (18) and (22),

$$c(x, t) = \frac{c_0}{\pi} \int_{-\infty}^{\infty} \frac{1}{\lambda} (1 - e^{-\lambda^2 Dt_0}) e^{-\lambda^2 Dt} \times \sin \lambda x \, d\lambda \tag{23}$$

Rearranging (23),

$$c(x, t) = \frac{c_0}{\pi} \int_{-\infty}^{\infty} \frac{\sin \lambda x}{\lambda} e^{-\lambda^2 Dt} \, d\lambda - \frac{c_0}{\pi} \int_{-\infty}^{\infty} \frac{\sin \lambda x}{\lambda} e^{-\lambda^2 D(t+t_0)} \, d\lambda \tag{24}$$

$$= \frac{c_0}{\pi} \cdot \pi \operatorname{erf} \frac{x}{2\sqrt{Dt}} - \frac{c_0}{\pi} \pi \operatorname{erf} \frac{x}{2\sqrt{Dt + Dt_0}}$$

$$= c_0 \operatorname{erf} \frac{x}{2\sqrt{Dt}} - c_0 \operatorname{erf} \frac{x}{2\sqrt{Dt + D_0 t_0}} \qquad (25)$$

Equation (25) is plotted in Figure I.1 for $D = 5.3 \times 10^{-6}$ cm^2 sec^{-1} at 450°C, $D_0 = 9.34 \times 10^{-7}$ cm^2 sec^{-1} at 300°C, $t = 10{,}000$ sec (time of heating in A); $t_0 = 300$ sec (time of reduction in H_2).

To calculate the concentration of H in the electrode, one integrates the area under the concentration profile and compares this area with that in the case when the electrode is saturated with hydrogen. The area under the curve shown in Figure I.1, for the case when the electrode was heated in argon for 10,000 sec, is 30 cm^2. The area under the curve when the electrode would be saturated with hydrogen, i.e., $c = c_0$ throughout the electrode, is 2×10^5 cm^2. Thus, the average concentration of hydrogen remaining in the electrode after being heated in A for 3 hours is about $1.5 \times 10^{-4}\ c_0$. If $c_0 = 10^{-5}$ g.a.t. cc^{-1}, $c = 1.5 \times 10^{-9}$ g.a.t. cc^{-1}.

Reference

1. M.A. Genshaw and M.A. Fullenwider, to be published.

APPENDIX III-II

Variation of capacity with frequency

Variation of capacity with frequency as observed in Argade's measurements is in qualitative agreement with the measurements of Borisova and Ershler,[1] Leikis and Kabanov[2] and Tse Chuansin and Iofa.[3] Also, similar variation of capacity with frequency was observed by Argade on gold electrodes where one does not have a psuedocapacity due to reactions and adsorption. A typical plot for the variation of capacity with frequency on platinum and gold is shown in Figure II. 1.

In what follows, an attempt is made to explain the small frequency variation of capacity on the basis of different models.

(a) Pseudocapacity

The dispersion due to the contribution of pseudocapacity to the measured capacity with frequency which one would expect at 0.27 v in 10^{-3} N $HClO_4$, due to adsorption of hydrogen on platinum is calculated as follows. Following a similar calculation shown in Appendix VII b, one finds that the hydrogen coverage is 4×10^{-4} at 0.27 v, under the assumption that there is an equilibrium for hydrogen adsorption and ionization.

Now

$$R_{react} = \frac{RT}{Fi_c'} \tag{1}$$

where

$$i_0' = 4 \times 10^{-4}\, i_0 \quad , \tag{2}$$

i_0 the exchange current when $\theta \simeq 1$, is 0.1 A cm^{-2}.

The adsorption pseudocapacity C_ϕ, is given by

$$C_\phi = k'F/RT \cdot \theta(1 - \theta) \tag{3}$$

where k' is the amount of charge needed for a hydrogen coverage of unity, namely, 2×10^{-4} coul cm^{-2}.

The equivalent circuit used is: C_ϕ and R_{react} in series together in parallel with C_{dl}, double layer capacity, i.e.,

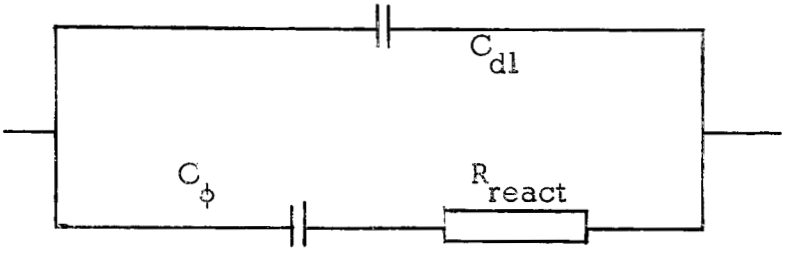

The resolved parallel capacity, C_p, and resistance, R_p, are given as

$$C_p = 1 + R_{react}^2 \omega^2 C_\phi^2 + C_{dl} \tag{4}$$

$$R_p = \frac{1}{\omega^2 C_\phi^2 R_{react}} + R_{react} \tag{5}$$

C_p as a function of frequency is shown in Fig. II.1. C_{dl} value used is taken from the experimental capacity value extrapolated to infinite frequency. There is not a good agreement between our capacitance-frequency plot and that which one gets from the values calculated according to the pseudocapacitance hypothesis. Moreover, the

expected parallel resistance variation with frequency according to equation (5) (i.e., $\partial \ln R/\partial \ln \omega = -2$) is experimentally not observed. The experimental log R vs. log ω plot is shown in Fig. II.2.

This is a qualitative discrepancy which makes us reject a pseudo-capacity explanation of the capacitance variation with frequency in our case. This also supports the contention that the observed capacity was indeed the double layer capacity in Argade's work.

(b) Dipole relaxation in the double layer[4,5]

Equations have been derived for the effect of dielectric relaxation on the variation of resistance and capacity with frequency.[5] For the equivalent parallel R and ΔC are given as follows:

$$R = \frac{1}{\Delta\varepsilon C_0}\left\{\frac{1}{\cos(\beta\pi/2)}\left[\frac{\tau_0^{1-\beta}}{\omega^{\beta}} + \frac{\tau_0^{\beta-1}}{\omega^{2-\beta}}\right] + \frac{2}{\omega}\tan\frac{\beta\pi}{2}\right\} \tag{6}$$

$$\Delta C = \Delta\varepsilon C_0 \frac{1 + (\omega\tau_0)^{1-\beta}\sin(\beta\pi/2)}{1 + (\omega\tau_0)^{2-2\beta} + 2(\omega\tau_0)^{1-\beta}\sin\beta\pi/2} \tag{7}$$

where τ_0 is the mean relaxation time, β signifies the distribution of relaxation times (e.g., $\beta = 0$, all τ values are equal to τ_0; when $\beta = 1$, there is an infinitely wide distribution of relaxation times); $\Delta\varepsilon \equiv \varepsilon_s - \varepsilon_\infty$ and $\Delta C = C \simeq \varepsilon_\infty C_0$; ε_s is the dielectric constant at a given frequency and C_0 is the capacity of the condenser. ΔC is the total change in capacity between actual frequency and $\omega >> \tau_0^{-1}$. The real variation of the capacity with frequency as the frequency increases will be referred to the condition $\omega \to 0$.

$$\delta\Delta C = \Delta\varepsilon C_0 - \Delta C \tag{8}$$

At $\omega \ll \tau_0^{-1}$, (7) reduces to

$$\delta\Delta C = \Delta\varepsilon C_0(\omega\tau_0)^{1-\beta} \sin\left(\frac{\beta\pi}{2}\right) \tag{9}$$

and

$$R = \frac{\tau_0^{\beta-1}}{\Delta\varepsilon C_0\, \omega^{2-\beta} \cos \beta\pi/2} \tag{10}$$

$$-(\partial \log R/\partial \log \omega) = 2 - \beta \tag{11}$$

The dispersion of capacity with frequency on this model is shown in Figure II. 2, assuming $\tau_0 = 10^{-5}$ sec and $\beta = 0.9$; $\Delta\varepsilon C_0$ is obtained from R_p vs. ω experimental relationship. Also $\log R_p$ vs. $\log f$ is plotted in Figure II. 2.

It is seen that the frequency dispersion of capacity is in close correspondence to the observed experimental variation. The parallel equivalent resistance variation with frequency is in good agreement with this model.

Thus, it seems to us that the frequency dispersion of capacity may be due to dipole relaxation in the double layer.

(c) Electrolyte penetration effect[6]

Capacitance variation with frequency may be associated with the penetration of electrolyte into the annular space between the electrode wire and the glass mount. An equivalent circuit of a transmission line has been used to calculate the frequency dispersion of the capacitance due to the penetration effect.[6] It is shown that, for dilute solutions,

$$C = C_{dl} + \sqrt{C_0/2\omega r_0} \qquad (12)$$

where C is the measured capacity, C_{dl} is the double layer capacity, C_0 is the capacity per unit length of penetration, and r_0 is the resistance per cm of the penetration. For a thickness of the film of electrolyte of 4×10^{-4} cm, the r_0 was calculated as about $8 \times 10^5\ \Omega cm^{-1}$ and the appropriate C_0 was found to be $1.16\ \mu F\ cm^{-2}$. The calculated C is plotted as a function of frequency in Figure II. 1. There is a fair agreement between calculated and observed capacity values. Moreover, the slope $(\partial \log R_p/\partial \log f)$ on this model is expected to be between -0.5 and -1.0. The experimental slope is about -1.0, in good agreement with this model.

Thus, the frequency dispersion of capacitance may be due either to electrolyte penetration effect or to the dipole relaxation in the double layer.

References

1. Borisova and Ershler, Zh. Fiz. Khim., 24, 337 (1950).

2. Leikis and Kabanov, Trudy Inst. Fiz. Khim. Akad. Nauk SSSR, 6, 5 (1957).

3. Tsa Chuan-sin and Iofa, Dokl. Akad. Nauk, 131, 137 (1960).

4. Bockris and Conway, J. Chem. Phys., 28, 707 (1958).

5. Bockris, Gileadi, and Muller, J. Chem. Phys., 44, 1445 (1966).

6. Leikis, Sevastyanov, and Knots, Zh. Fiz. Khim., 38, 1833 (1964).

APPENDIX III-III

Capacitance minimum and variation of the concentration of the electrolyte

One of the important characteristics of the capacitance minimum (if it represents the potential of zero charge) is that it should disappear as the concentration of the electrolyte is increased.

The capacitance of a platinum electrode was measured as a function of concentration of the electrolyte: (a) keeping the pH constant and varying the $KClO_4$ concentration in acid and alkaline solutions; (b) concentration of perchloric acid was varied.

In each of these cases the capacitance minimum was found to disappear as the concentration of the electrolyte was increased. See Figures IV.1, IV.2, IV.3. Figures IV.1 and IV.2 show the effect of $KClO_4$ concentration variation on the capacitance-potential plot in ph = 3 and pH = 10 solutions, respectively. Figure IV.3 shows capacitance-potential plots at various concentrations of perchloric acid.

If the minima in the capacity-potential curves observed in our work were due to pseudocapacitance behavior, it is very difficult to see why the minima in capacitance-potential curves at constant pH of solution would disappear as the concentration of $KClO_4$ was raised.

On the basis of this evidence it seems reasonable that in our measurements the capacitance minimum did correspond to the potential of zero charge of platinum.

APPENDIX III-IV

Gibb's adsorption equation in the case of a polarizable platinum electrode:

Gibb's adsorption equation at constant temperature and pressure,

$$-d\gamma = \sum_i \Gamma_i \, d\bar{\mu}_i + \sum_j \Gamma_j \, d\mu_j \qquad (1)$$

γ is the interfacial tension; Γ's are the surface excesses for ionic species i and uncharged species j; $\bar{\mu}$ and μ are the electrochemical and chemical potential respectively.

$$\text{Cu} \;\big|\; \text{Pt} \;\Big|\; \begin{matrix} H^+ \; Na^+ \; OH^- \; H_2O \\ ClO_4^- \end{matrix} \;\Big\|\; \underset{\text{ref. electrode}}{H_2\text{-Pt}} \;\big|\; \text{Cu}' \qquad (2)$$

(2) represents the given system and applying (1) and to the polarizable interface of system (2), we have

$$\begin{aligned} -d\gamma = {} & (\Gamma_{Pt^+} d\bar{\mu}_{Pt^+} + \Gamma_e \, d\bar{\mu}_e) + \\ & + (\Gamma_{Na} + d\bar{\mu}_{Na^+} + \Gamma_{H^+} d\bar{\mu}_{H^+} + \Gamma_{OH^-} d\bar{\mu}_{OH^-} + \\ & + \Gamma_{ClO_4^-} d\bar{\mu}_{ClO_4^-}) + \Gamma_{H_2O} \, d\mu_{H_2O} \end{aligned} \qquad (3)$$

Equation (3) is to be transformed into one with electrode potential E with respect to hydrogen reference electrode.

Equilibrium conditions for the Pt phase are

$$\mu_{Pt} = \bar{\mu}_{Pt^+} + \bar{\mu}_e^{Pt} \tag{4}$$

$$\bar{\mu}_e^{Pt} = \bar{\mu}_e^{Cu} \tag{5}$$

The charge q^m (per unit area) is given by

$$q^m = F(\Gamma_{Pt^+} - \Gamma_e) \tag{6}$$

where F is the Faraday, Pt^+ refers to the positive ionic charge on the platinum metal. For the metal phase, one can write

$$\Gamma_{Pt^+} d\bar{\mu}_{Pt^+} + \Gamma_e d\bar{\mu}_e = \Gamma_{Pt^+} d\mu_{Pt} - \Gamma_{Pt^+} d\bar{\mu}_e^{Cu} + \Gamma_e d\bar{\mu}_e^{Cu} \tag{7}$$

Introduce (6) into (7),

$$\Gamma_{Pt^+} d\bar{\mu}_{Pt^+} + \Gamma_e d\bar{\mu}_e = \Gamma_{Pt^+} d\mu_{Pt} - \frac{q^m}{F} d\bar{\mu}_e^{Cu} \tag{8}$$

For the solution side at equilibrium

$$\mu_{NaClO_4} = \bar{\mu}_{Na^+} + \bar{\mu}_{ClO_4^-} \tag{9}$$

$$\mu_{HClO_4} = \bar{\mu}_{H^+} + \bar{\mu}_{ClO_4^-} \tag{10}$$

$$\mu_{H_2O} = \bar{\mu}_{H^+} + \bar{\mu}_{OH^-} \tag{11}$$

$$\mu_{NaOH} = \bar{\mu}_{OH^-} + \bar{\mu}_{Na^+} \tag{12}$$

$$-q^s = q^m = -F(\Gamma_{H^+} + \Gamma_{Na^+} - \Gamma_{OH^-} - \Gamma_{ClO_4^-}) \tag{13}$$

From the reference electrode,

$$\tfrac{1}{2}\mu_{H_2} = \bar{\mu}_{H^+} + \bar{\mu}_e^{Cu'} \tag{14}$$

At one atm. pressure,

$$d\bar{\mu}_{H^+} = -d\bar{\mu}_e^{Cu'} \tag{15}$$

Now, from (3) and (9) to (12), one can write

$$\Gamma_{Na^+} d\bar{\mu}_{Na^+} + \Gamma_{H^+} d\bar{\mu}_{H^+} + \Gamma_{OH^-} d\bar{\mu}_{OH^-} + \Gamma_{ClO_4^-} d\bar{\mu}_{ClO_4^-}$$

$$= \Gamma_{Na^+} d\mu_{NaClO_4} - \Gamma_{Na^+} d\mu_{HClO_4} + \Gamma_{OH^-} d\mu_{H_2O} + \Gamma_{ClO_4^-} d\mu_{HClO_4}$$

$$+ \Gamma_{Na^+} d\bar{\mu}_{H^+} + \Gamma_{H^+} d\bar{\mu}_{H^+} - \Gamma_{ClO_4^-} d\bar{\mu}_{H^+} - \Gamma_{OH^-} d\mu_{H^+} \qquad (16)$$

Substituting (13) and (15) into (16) becomes

$$= \Gamma_{Na^+} d\mu_{NaClO_4} - \Gamma_{Na^+} d\mu_{HClO_4} + \Gamma_{OH^-} d\mu_{H_2O} +$$

$$+ \Gamma_{ClO_4^-} d\mu_{HClO_4} - (\Gamma_{Na^+} + \Gamma_{H^+} - \Gamma_{ClO_4^-} - \Gamma_{OH^-}) d\bar{\mu}_e^{Cu'} \qquad (17)$$

$$= \Gamma_{Na^+} d\mu_{NaClO_4} - \Gamma_{Na^+} d\mu_{HClO_4} + \Gamma_{OH^-} d\mu_{H_2O} +$$

$$+ \frac{q^m}{F} d\bar{\mu}_e^{Cu'} + \Gamma_{ClO_4^-} d\mu_{HClO_4} \qquad (18)$$

Thus from (3), (18) and (8) together give

$$-d\gamma = \Gamma_{Pt^+} d\mu_{Pt} - \frac{q^m}{F} d\bar{\mu}_e^{Cu} + \Gamma_{Na^+} d\mu_{NaClO_4} -$$

$$- \Gamma_{Na^+} d\mu_{HClO_4} + \Gamma_{OH^-} d\mu_{H_2O} + \frac{q^m}{F} d\bar{\mu}_e^{Cu'} +$$

$$+ \Gamma_{ClO_4^-} d\mu_{HClO_4} + \Gamma_{H_2O} d\mu_{H_2O} \qquad (19)$$

$$d\bar{\mu}_e^{Cu'} - d\bar{\mu}_e^{Cu} = Fd(\phi^{Cu'} - \phi^{Cu}) = FdE^+ \qquad (20)$$

Putting (20) into (19)

$$-d\gamma = \Gamma_{Pt^+} d\mu_{Pt} + \Gamma_{Na^+} d(\mu_{NaClO_4} - \mu_{HClO_4}) + \Gamma_{ClO_4^-} d\mu_{HClO_4} +$$

$$+ \Gamma_{OH^-} d\mu_{H_2O} + q^m dE^+ + \Gamma_{H_2O} d\mu_{H_2O} \qquad (21)$$

$$= \Gamma_{Pt^+} d\mu_{Pt^+} + \Gamma_{Na^+} d(\mu_{NaClO_4} - \mu_{HClO_4}) + \Gamma_{ClO_4^-} d\mu_{HClO_4} +$$

$$+ \Gamma_{OH^-} d(\mu_{HClO_4} - \mu_{NaClO_4} + \mu_{NaOH}) + q^m dE^+ + \Gamma_{H_2O} d\mu_{H_2O}$$

$$= \Gamma_{Pt^+} d\mu_{Pt} + \Gamma_{Na^+} d(\mu_{NaClO_4} - \mu_{HClO_4}) + \Gamma_{ClO_4^-} d\mu_{HClO_4} +$$

$$+ \Gamma_{OH^-} d\mu_{HClO_4} \Gamma_{OH^-} d\mu_{NaClO_4} + \Gamma_{OH^-} d\mu_{NaOH} +$$

$$+ q^m dE^+ + \Gamma_{H_2O} d\mu_{H_2O} \qquad (22)$$

$$-d\gamma = (\Gamma_{Na^+} - \Gamma_{OH^-}) d\mu_{NaClO_4} + (\Gamma_{OH^-} + \Gamma_{ClO_4^-} - \Gamma_{Na^+}) d\mu_{HClO_4} +$$

$$+ \Gamma_{OH^-} d\mu_{NaOH} + q^m dE^+ + \Gamma_{Pt^+} d\mu_{Pt} + \Gamma_{H_2O} d\mu_{H_2O} \qquad (23)$$

$$\left(\frac{\partial E^+}{\partial \mu_{HClO_4}}\right) q^m = -\left(\frac{\partial (\Gamma_{OH^-} + \Gamma_{ClO_4^-} - \Gamma_{Na^+})}{\partial q^m}\right) \mu_{HClO_4} \qquad (24)$$

when $q^m = 0$,

Now,

$$\Gamma_{OH^-} + \Gamma_{ClO_4^-} = \Gamma_{Na^+} + \Gamma_{H^+} \qquad (25)$$

Thus, one may write

$$\left(\frac{\partial E^+}{\partial \mu_{HClO_4}}\right)_{q^m=0} = -\left(\frac{\partial \Gamma_{H^+}}{\partial \mu_{HClO_4}}\right)_{\mu_{HClO_4}} \qquad (26)$$

Similarly,

$$\left(\frac{\partial E^+}{\partial \mu_{NaOH}}\right)_{q^m} = -\left(\frac{\partial \Gamma_{OH^-}}{\partial q^m}\right)_{\mu_{NaOH}} \qquad (27)$$

Now, assume that OH^- ions are adsorbed to cause the variation of p. z. c. with pH. Now,

$$E^+_{q=0} = E_{q=0} + \frac{RT}{F} \ln a_{OH^-} + \text{const.} \qquad (28)$$

where $E^+_{q=0}$ is the potential of zero charge measured on the reversible hydrogen scale and $E_{q=0}$ is that which is measured on the normal hydrogen scale.

$$\left(\frac{\partial E^{+}_{q=0}}{\partial \mu_{NaOH}}\right) = \left(\frac{\partial E_{q=0}}{\partial \mu_{NaOH}}\right) \quad \frac{RT}{F} \frac{\partial \ln a_{OH^-}}{\partial \mu_{NaOH}} \tag{29}$$

$$\left(\frac{\partial E^{+}}{\partial \mu_{NaOH}}\right)_{q^m=0} = \frac{\partial E_{q=0}}{RT\, \partial \ln a_{NaOH}} + \frac{1}{F} \frac{\partial \ln a_{OH^-}}{\partial \ln a_{NaOH}} \tag{30}$$

As the solutions used were sufficiently dilute (below 10^{-2}N in NaOH), we can use the Debye-Hückel limiting law to express the ion activity coefficients as

$$\ln f_{\pm}^{2} = AI^{\frac{1}{2}} \quad \text{and} \quad \ln f_{-} = A'I^{\frac{1}{2}} \tag{31}$$

Putting (31) into (30),

$$\left(\frac{\partial E^{+}}{\partial \mu_{NaOH}}\right)_{q^m=0} = \frac{\partial E_{q=0}}{RT\, \partial \left[AI^{\frac{1}{2}} + \ln C_{Na^+} + C_{OH^-}\right]} + \tag{32}$$

$$+ \frac{1}{F} \times \frac{\partial A'I^{\frac{1}{2}}}{\partial \left[AI^{\frac{1}{2}} + \ln C_{Na^+} + C_{OH^-}\right]} + \frac{1}{F} \cdot \frac{\partial \ln C_{OH^-}}{\partial \left[AI^{\frac{1}{2}} + \ln C_{Na^+} + C_{OH^-}\right]}$$

In our experiments, the ionic strength was held constant and also as a result, concentration of Na^+ ions remained constant. Therefore,

$$\left(\frac{\partial E^{+}}{\partial \mu_{NaOH}}\right)_{q^m=0} = \frac{\partial E_{q=0}}{RT\, \partial \ln C_{OH^-}} + \frac{1}{F} \tag{33}$$

From (27) and (33)

$$\frac{\partial E_{q=0}}{RT\, \partial \ln C_{OH^-}} = -\left(\frac{\partial \Gamma_{OH^-}}{\partial q^m}\right)_{C_{NaOH}} - \frac{1}{F}$$

Or,

$$\frac{\partial E_{q=0}}{\partial \ln C_{OH^-}} = -\frac{RT}{F}\left[\left(\frac{\partial q_{OH^-}}{\partial q^m}\right)_{C_{NaOH}} + 1\right] \tag{35}$$

Thus, when $\left(\frac{\partial q_{OH^-}}{\partial q^m}\right)_{C_{NaOH}}$ is small, and the ionic strength is kept constant, the p. z. c. variation with pH has a slope of about $-\frac{RT}{F}$.

APPENDIX III-V

Potential of zero charge determinations by the "Friction Method".

A number of investigators have used a Herbert pendulum with a fulcrum made of glass sphere, which oscillates in a film of electrolyte.[1-3] Bowden and Young[4] used a method to determine the static coefficient of friction as a function of potential to study the effect of adsorbed gases on friction between two platinum surfaces.

The principle of the method of Bowden and Young[4] was used to determine the static coefficient of friction as a function of potential. The apparatus was designed so as to perform experiments under high purity conditions, similar to those of the capacitance measurements.

Figure V.I shows the friction vs. potential plot for platinum on platinum in 0.1 N $HClO_4$ solution. The maximum on this curve corresponds very well with the potential of zero charge values obtained by other two methods in this laboratory. The variation of potential of zero charge with pH by three different methods is shown in Figure V.2.

It can be seen that the values of potential of zero charge obtained by three methods are in good agreement. This further confirms our contention that the minimum in capacity-potential plot in dilute

solutions does correspond to the potential of zero charge on non-activated platinum electrodes.

References

1. Rehbinder and Wensrom, Acta Physicochim. URSS. 19, 36 (1944); Dokl. Akad. Nauk SSSR., 68, 329 (1949); Zhur. Fix. Khim., 12, 12 (1952); 26, 1847 (1952).

2. Bockris and Parry-Jones, Nature, 171, 930 (1953).

3. Staicopoulos, J. Electrochem. Soc., 108, 900 (1961).

4. Bowden and Young, Research 3, 235 (1950).

APPENDIX III-VI

Amount of hydrogen present in platinum electrodes used in Russian work:

It has been well established that hydrogen diffuses into platinum. Recently, the diffusion coefficient and the apparent energy of activation for the diffusion of hydrogen in platinum have been determined.[1]

$$D_{70°C} = 3.4 \times 10^{-9} \text{ cm}^2 \text{ sec}^{-1} \text{ and}$$

$$E_a = 9.6 \times 10 \text{ cal mole}^{-1}$$

The extrapolated value of the diffusion coefficient at room temperature is found to be

$$D_{27°C} = 4.57 \times 10^{-1} \text{ cm}^2 \text{ sec}^{-1}.$$

In the Russian work on the determinations of potential of zero charge on platinum, electrodes were either activated or platinized. The cathodic polarization at 40-50 mA cm^{-2} for 3-4 hours was used as the initial treatment to platinum in the work of Voropaeva, Deryagin and Kabanov.[2] Under these conditions, the electrode will absorb hydrogen according to Fick's laws of diffusion. With the boundary conditions,

$$x = 0, \; c = 0, \; t = 0$$

$$x = 0, \; c = c_0, \; t > 0$$

and assuming the electrode to be a semi-infinite solid, it can easily be shown that

$$c = c_0 \operatorname{erfc} \frac{x}{2\sqrt{Dt}} \qquad (1)$$

where c is the concentration of hydrogen as a function of distance x and time t, D is the diffusion coefficient. The concentration profile of H diffusing into Pt is shown by curve 1 in Figure VI.1 for a time of 10,000 secs corresponding to the cathod pretreatment applied to platinum by Voropaeva et al.[2]

When the electrode potential is led to more positive potentials, the surface concentration will become small and hydrogen will diffuse out of platinum. Diffusion equations can be worked out for this case, assuming a linear concentration gradient up to a certain depth of penetration which is obtained graphically. See Figure VI.1. Now the boundary conditions are

$$c = 0, \text{ at } x = 0; \; t \geq 0$$

and

$$c = c_0 \left(1 - \frac{x}{L'}\right)$$

where L' is the apparent depth of penetration. The diffusion equation for this case is found to be

$$c/c_0 = 1 - \frac{x}{L'} - \sum_{n=0}^{\infty} \operatorname{erfc} \frac{2nL' + x}{2\sqrt{Dt}} + \sum_{n=0}^{\infty} \operatorname{erfc} \frac{(n+1)2L' - x}{2\sqrt{Dt}} \qquad (2)$$

Using equation (2), c/c_0 for hydrogen diffusing out of platinum as a function of distance and time is shown in Figure VI.1. Curves (2).

However, the actual concentration profiles may be somewhat

distorted because most of the hydrogen is concentrated on islands and the transfer of bound hydrogen to free hydrogen is relatively slow.

After keeping the electrode at a positive potential for 17 minutes so that hydrogen concentration at the surface is zero, there is still more than 0.6 times the initial amount of hydrogen that went into platinum during cathodic polarization. This is seen by comparing the areas under the corresponding curves. Now integrating the concentration profiles at 3000 sec. and comparing this area with the area as if the platinum was saturated with hydrogen up to the depth of penetration, the average concentration comes out to be about $0.14\,c_0$. If c_0 is taken to be 2.7×10^{-5} g atom cc^{-1}, the average concentration is seen to be 3.8×10^{-6} g atom cc^{-1} after 50 minutes of removing H from platinum. For removal of H from Pt for about 17 minutes the concentration of H in platinum was found to be 8.6×10^{-6} g atom cc^{-1}.

References

1. Gileadi, Fullenwider, Bockris, J. Electrochem. Soc., 113, 926 (1966).
2. Voropaeva, Daryagin and Kabanov, Dokl. Akad. Nauk SSSR, 128, 881 (1959).

APPENDIX III-VII

Change in the potential of zero charge because of the presence of hydrogen:

(a) Dissolved hydrogen

First it may be observed that the value of p. z. c. of platinum obtained by us is more consistent with the work function - p. z. c. plot than the value obtained for the activated platinum (Fig. VIII.1).

Thus, it was thought that the presence of hydrogen may lower the work function and hence the p. z. c.

In Appendix VI the amount of hydrogen remained inside platinum was estimated to be about 10^{-5} g atom cc^{-1}. Now, if this amount of hydrogen is ionized, contributing these electrons to the conduction band, the Fermi level of the electron gas would be raised. Fermi level of a free electron gas is given by

$$E_F = \frac{3}{5}\left(\frac{3}{\pi}\right)^{2/3} \frac{\pi^2 h^2}{2m} \left(\frac{N}{V}\right)^{2/3} \qquad (1)$$

where m is the mass of the electron and $\frac{N}{V}$ is their concentration. Thus,

$$\frac{(E_F)_{Pt}}{(E_F)_{Pt\text{-}H}} = \frac{\left(\frac{N}{V}\right)^{2/3}_{Pt}}{\left(\frac{N}{V}\right)^{2/3}_{Pt,\,H}} \qquad (2)$$

Assuming as a first approximation, 0.30 electrons per platinum

atom, there are 1.5×10^{22} electrons cc^{-3} of platinum. The number of electrons contributed by the hydrogen present will be 6×10^{18} electrons per cc of platinum. The change of Fermi energy because of this amount of hydrogen will be smaller than 10 mV, provided the electron gas model is applicable to platinum.

(b) Adsorbed hydrogen:

If one considers an equilibrium between protons in solution and adsorbed hydrogen on the surface, then under Langmuir conditions

$$\frac{\theta}{1-\theta} = \frac{\theta_0}{1-\theta_0}\frac{C_{H^+}}{(C_{H^+})_0} \exp(V - V_0)\frac{F}{RT}$$

Now, $\theta_0 = 0.3$, $C_{H^+} = 1\ N\ H_2SO_4$; $V_0 = 0.2$ v.

Thus, in 10^{-2} N H_2SO_4, the hydrogen coverage, at $v = v_0 = 0.2$ volts is θ, $\theta << 1$.

$$\theta = \frac{0.3}{0.7} \times 10^{-2} = 0.43 \times 10^{-2} = 0.004$$

The change in surface potential because of the additional Pt - H dipoles is given by

$$\Delta\chi = 4\pi N\mu$$

where $\Delta\chi$ is change in surface potential, N is the number of dipoles per cm^2 and μ is the effective dipole moment. For $N = 5 \times 10^{+14}$ and $\mu = 0.5 \times 10^{-18}$ e. s. u., $\Delta\chi$ is seen to be about 9 mV.

Thus, the presence of hydrogen in the Russian electrodes would not give rise to the discrepancy in the values of potential of zero charge.

APPENDIX VIII

Activation of platinum and potential of zero charge

There is a large amount of evidence that suggests that the nature of the surface of platinum changes upon activation,[1,2,3] i.e., the structure of the surface of platinum changes during this procedure. Also, when the potential of the platinum electrode is held above 1.0 volt, a phase oxide of platinum is formed.[4] The oxide thickness varies linearly with potential in the range of 1.0-1.6 v (h.e.), from 1 Å to about 6 Å.[4] When the oxide is reduced, the oxygen will be converted into water. Namely, there will be water sitting in the field of a vacancy on the surface of platinum. An attempt is made here to estimate the change in the potential of zero charge of platinum when it is activated. One may write,

$$E_z - E_z^* = \{\chi^m - \chi^s\} - \{\chi^{m*} - \chi^{s*} + \delta\chi^*\} \qquad (1)$$

E_z is the potential of zero charge; * refers to the active state, χ^m and χ^s are the surface potentials of metal and solution exposed to vacuum. $\delta\chi$ is the interaction between the vacancy dipoles and the solvent dipoles.

$$\begin{aligned} E_z - E_z^* &= (\chi^m - \chi^{m*}) - (\chi^s - \chi^{s*}) - \delta\chi^* \\ &= (\chi^m - \chi^{m*}) - \delta\chi^* \end{aligned} \qquad (2)$$

The solution surface potential exposed to vacuum is the same in both cases. Further, the surface potential of the metal consists of two terms, namely,[5]

$$\chi^{m} = \chi^{m}_{sp} - \chi^{m}_{sm} \tag{3}$$

χ^{m}_{sp} is the surface potential due to the spilling of the electrons which is isotropic from crystal face to crystal face.[5] χ^{m}_{sm} is the surface potential contribution dependent upon the smoothing of the electron distribution due to the atomic arrangement at the surface of the metal. For the sake of argument, let us assume that the surface of platinum is smooth before activation, i.e., $\chi^{m}_{sm} = 0$ and χ^{m}_{sp} is the same upon activation, one has,

$$E_z - E^{*}_z = \chi^{m*}_{sm} - \delta\chi^{*}_{s} \tag{4}$$

When a vacancy is created in the surface of platinum, electron distribution around this point will be altered. The electron energy will be lowered if the electron stays in the potential well of the vacancy. Thus, the upper part of the surrounding six polyhedra will be positively charged and the vacancy will be negatively charged, giving rise to a line dipole with its positive end outwards. See Fig. VIII.1. The dipole moment is estimated as follows. The charge in the vacancy is assumed to be uniformly distributed in the lower part and the positive charge uniformly distributed in the upper half of the six surrounding polyhedra. Thus, it is seen from Fig. VIII.2 that the charge separation is half the radius of polyhedra, i.e., the radius of a platinum atom. In the case of platinum the number of free electrons is the number of electrons in

the conduction band, i.e., 0.3 electrons atom^{-1}. Thus, the dipole moment μ of the vacancy dipole is estimated to be

$$\mu = 0.3 \times \frac{1.4}{2} \times 4.8 \times 10^{-18} \text{ e.s.u.}$$

$$= 1.01 \times 10^{-18} \text{ e.s.u.}$$

Thus, the surface potential due to smoothing in the presence of vacancies,

$$\chi^{m*} = \frac{4\pi n\mu}{\varepsilon}$$

The number of vacancies created by the oxide PtO in surface of platinum is estimated to be one vacancy in every 20 atoms of platinum. This figure is obtained following a calculation that other vacancies are stable at a distance of 7Å from a given vacancy. Thus, $N = 6 \times 10^{13}$ vacancies.

$$\chi^{m*} = 4\pi \times 6 \times 10^{13} \times 1.01 \times 10^{-18} \times 300 \text{ volts}$$

$$= 0.24 \text{ volts} .$$

The change in $\delta\chi_s^*$ is obtained as an interaction term between the water dipoles and the vacancy dipoles and the change it will make in the orientation of water dipoles. This contribution is estimated as follows. The water molecules will be situated in the vacancy with their negative dipole towards the metal such that the potential of zero charge will be lowered.

The change in the surface potential because of dipole reorientation is given by

$$\delta\chi_s^* = \frac{4\pi(N\uparrow - N\downarrow)\mu}{\varepsilon}$$

When $N\uparrow - N\downarrow = 6 \times 10^{13}$ water molecules oriented in a particular direction, $\mu = 1.8$ D and $\varepsilon = 6$,

$$\delta\chi_s^* \cong -70 \text{ mv}$$

Thus, the total change in the potential of zero charge due to activation would be

$$E_z - E_z^* = 0.24\text{v} + 0.07$$
$$= 0.31 \text{ volt.}$$

Thus, it appears that the p. z. c. on active platinum is about 0. 3 more negative than that for nonactive platinum. This is in good agreement with the experimental values of p. z. c. on platinum.

References

1. Anson and King, Anal. Chem., 34, 362 (1962).

2. Shibata, Bull. Chem. Soc. Japan, 36, 525 (1963).

3. Mannan, Thesis, Univ. of Pennsylvania, 1967.

4. Reddy, Genshaw and Bockris, J. Electroanal. Chem., 8, 406 (1964).

5. Smoluchowski, Phys. Rev., 60, 661 (1941).

6. Weizer and Girifalco, Phys. Rev., 120, 837 (1960).

CAPTIONS TO FIGURES

Figure

I. 1. The concentration profile of hydrogen in the platinum electrodes prepared in Philadelphia.

II. 1. The frequency dispersion of capacity for a platinum and gold electrodes prepared in this laboratory and the expected dispersion by various models. -o- Experimental (platinum). -□- Electrolyte penetration effect. -Δ- Pseudocapacity behavior. -×- Experimental dispersion of capacity for a gold electrode.

II. 2. The dielectric relaxation model and the capacity and the resistance variation with frequency. -o- log R_p vs log f. -Δ- Calculated variation of capacity is compared with the experimental one (-×-).

III. 1. Effect of variation of the concentration of $KClO_4$ on the shape of capacity-potential plot for a Pt electrode in a 1.5×10^{-3} M $HClO_4$ solution.

III. 2. Effect of variation of the $KClO_4$ concentration on the shape of a C-E plot for a platinum electrode in a solution of pH = 10.

III. 3. Effect of change of the $HClO_4$ concentration on the shape of a C-E plot for a platinum electrode.

V. 1. Friction between two platinum surfaces as a function of potential in 0.1 M $HClO_4$.

V. 2. Potential of zero charge on Pt vs pH at constant ionic strength at 3×10^{-3} M total concentration.

VI. 1. Concentration profiles for hydrogen in a platinum electrode prepared by Voropaeva, Deryagin and Kabonov.

VII. 1. Work function versus potential of zero charge. *P. z. c. values obtained in this laboratory.

VIII. 1. Schematic diagram showing the effect of activating a platinum electrode: the electron distribution around the vacancy which is created by the anodic-cathodic activation.

VIII. 2. Diagram showing how the charge separation occurs near a vacancy, giving rise to a line dipole in opposite direction to the electron overlap.

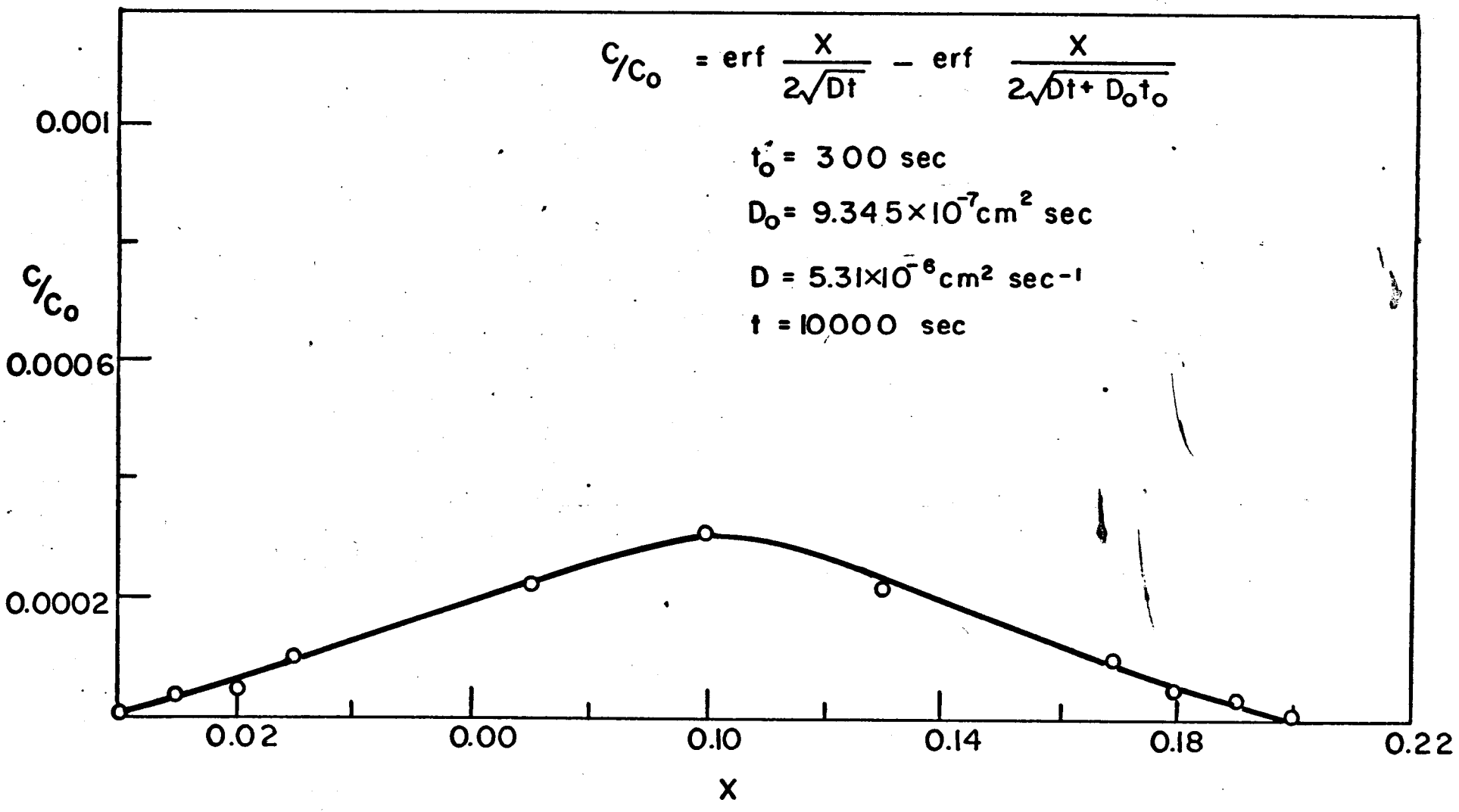

Fig. I.1 C/C_o vs distance X

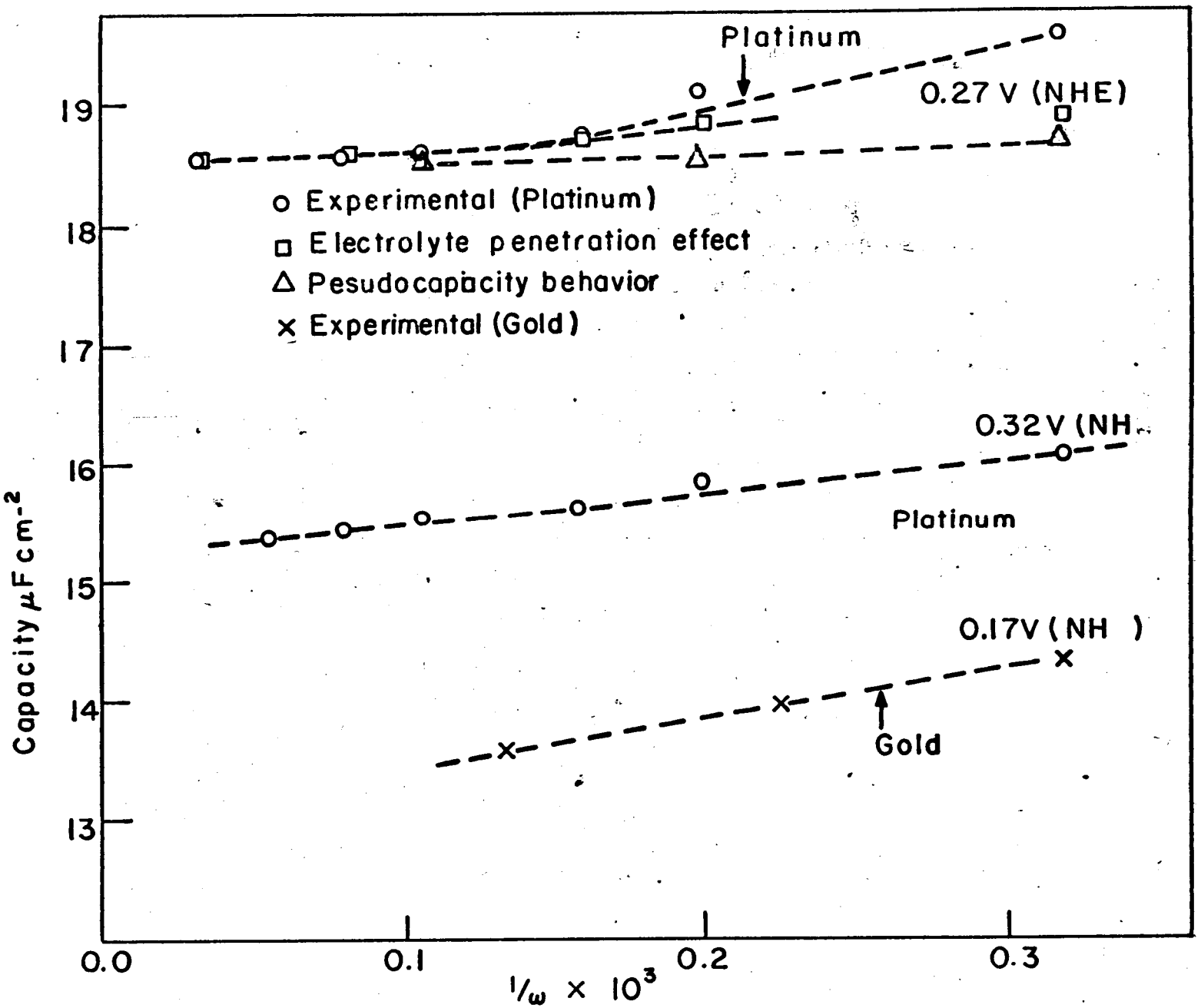

Fig.II.1 Typical frequency variation of capacity with angular frequency, for a Pt electrode in 10^{-3} N $HClO_4$. C $\mu F cm^{-2}$(geo) vs. $\frac{1}{\omega}$

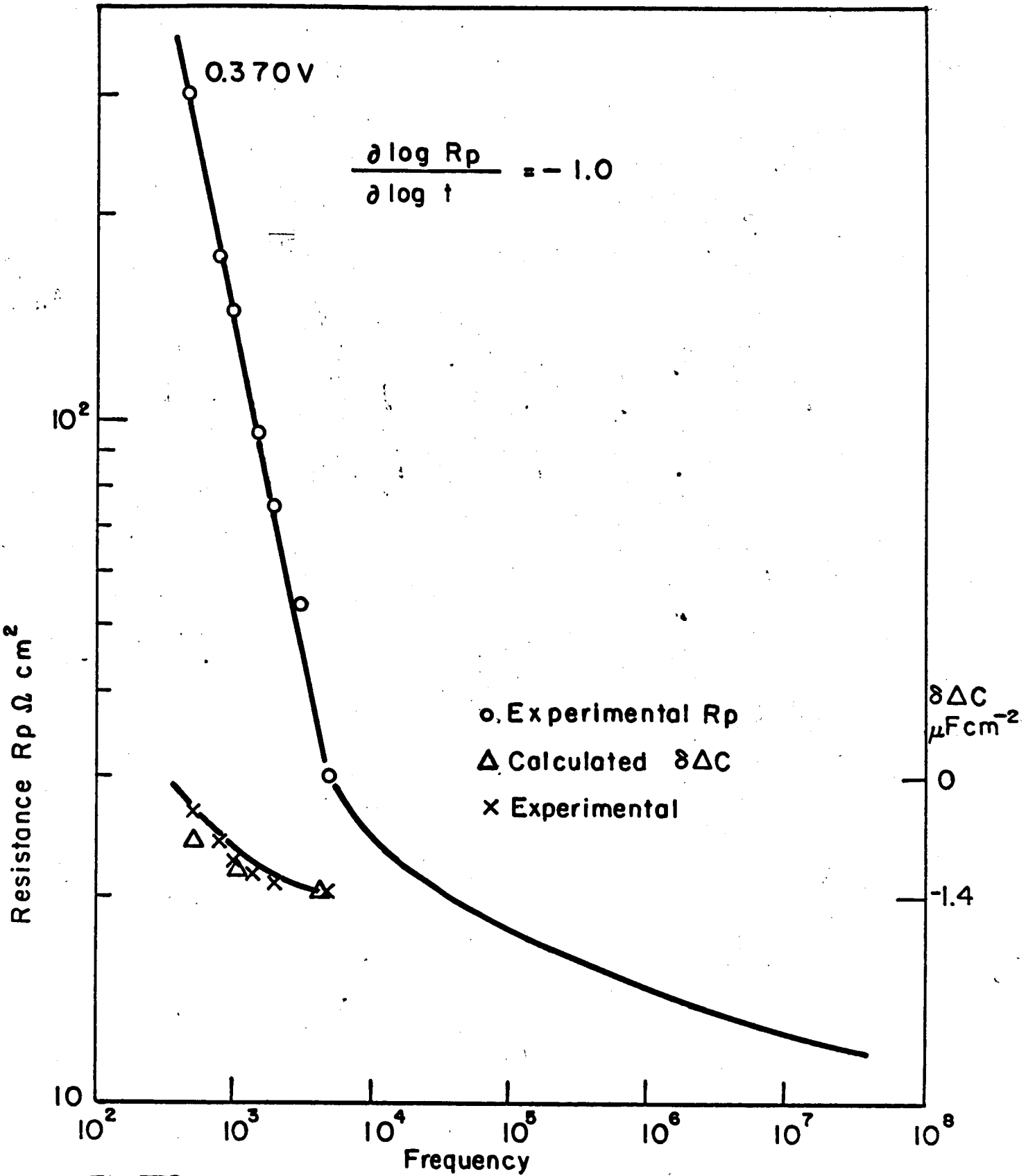

Fig II.2 Variation of capacity with frequency and the parallel resistance with frequency

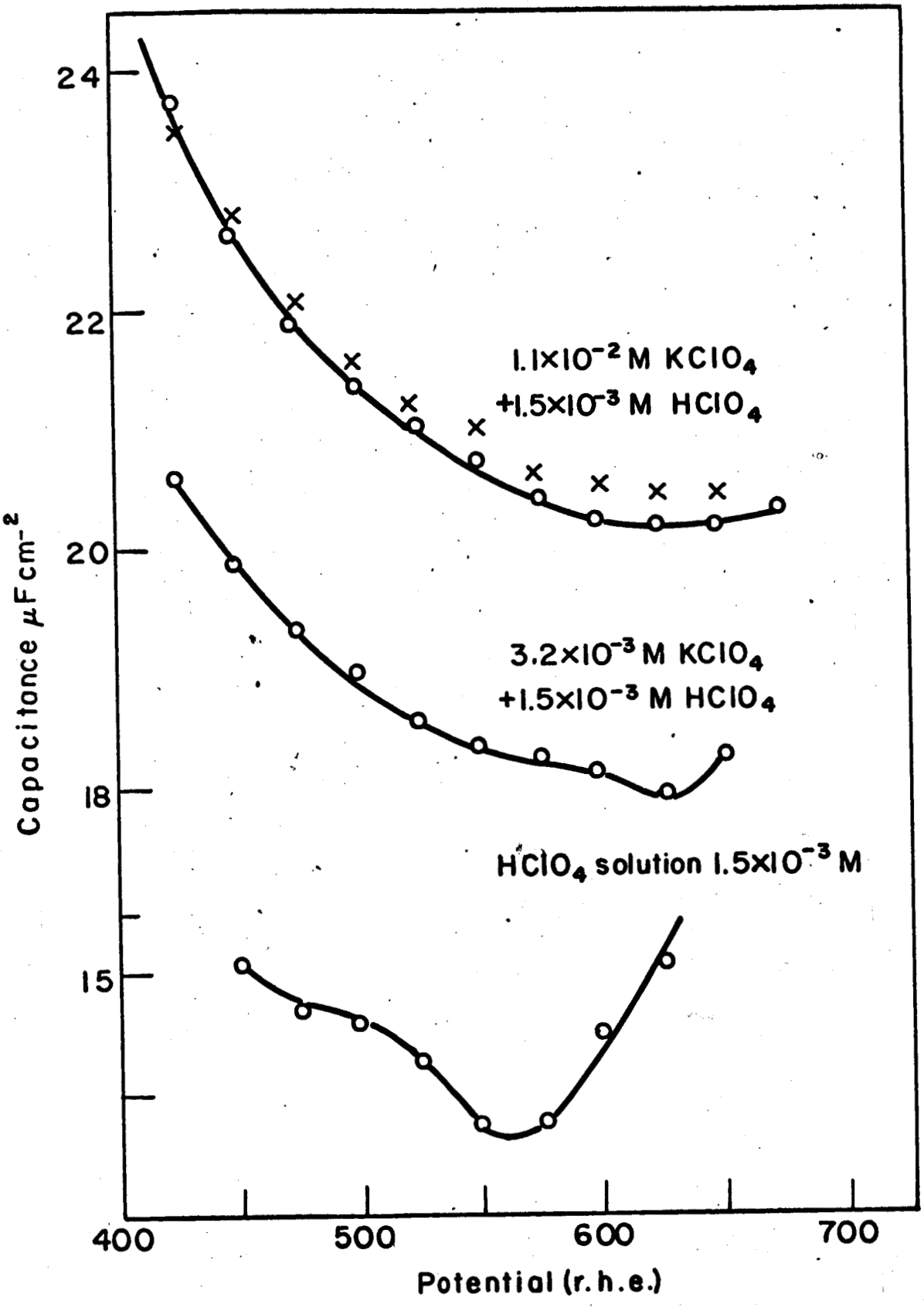
24
22
20
18
15
Capacitance μF cm⁻²
1.1×10⁻² M KClO₄
+1.5×10⁻³ M HClO₄
3.2×10⁻³ M KClO₄
+1.5×10⁻³ M HClO₄
HClO₄ solution 1.5×10⁻³ M
400
500
600
700
Potential (r.h.e.)

Fig.III.1

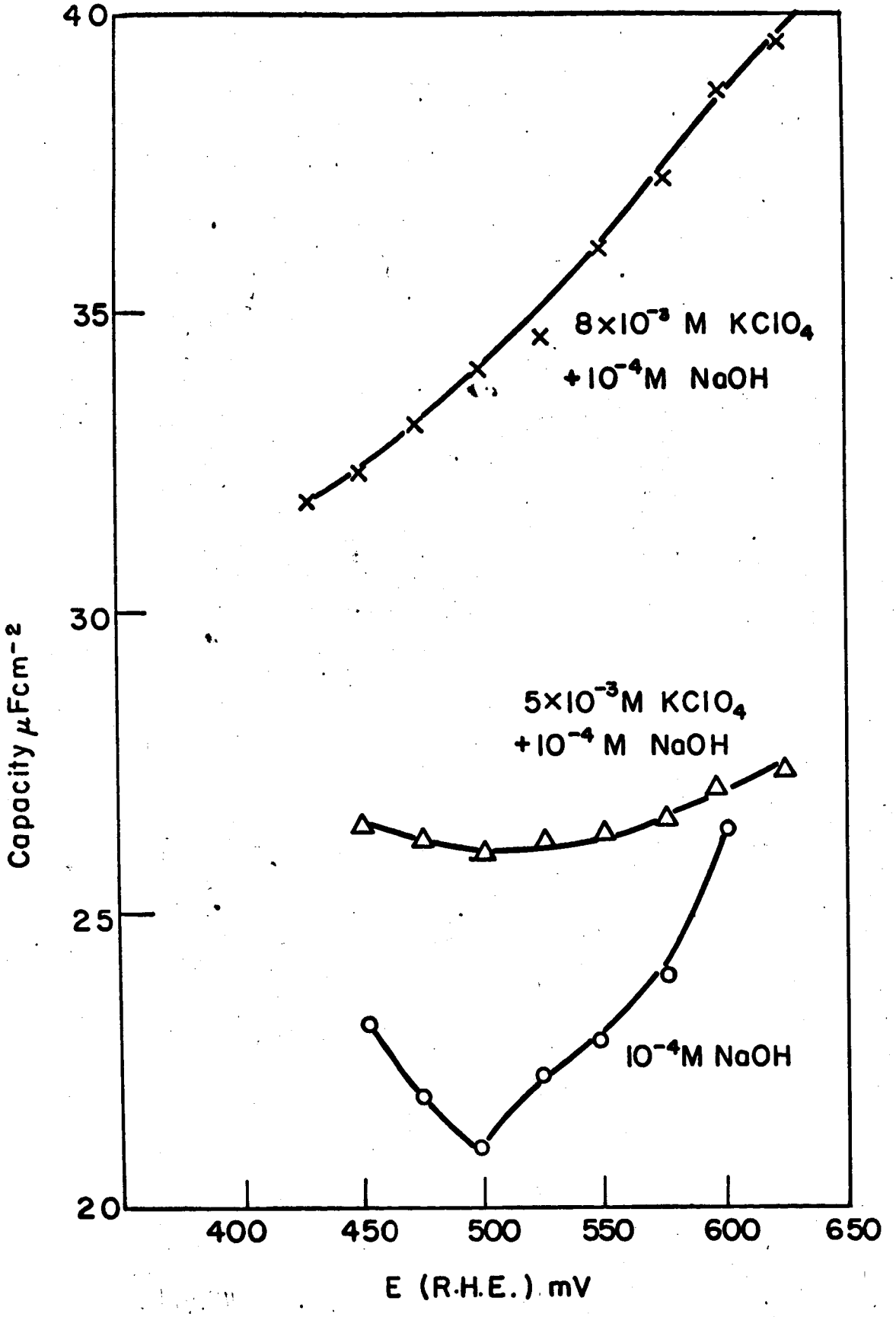
40
35
30
25
20
Capacity μFcm⁻²
8×10⁻³ M KClO₄
+10⁻⁴M NaOH
5×10⁻³M KClO₄
+10⁻⁴ M NaOH
10⁻⁴M NaOH
400
450
500
550
600
650
E (R.H.E.) mV

Fig.III.2

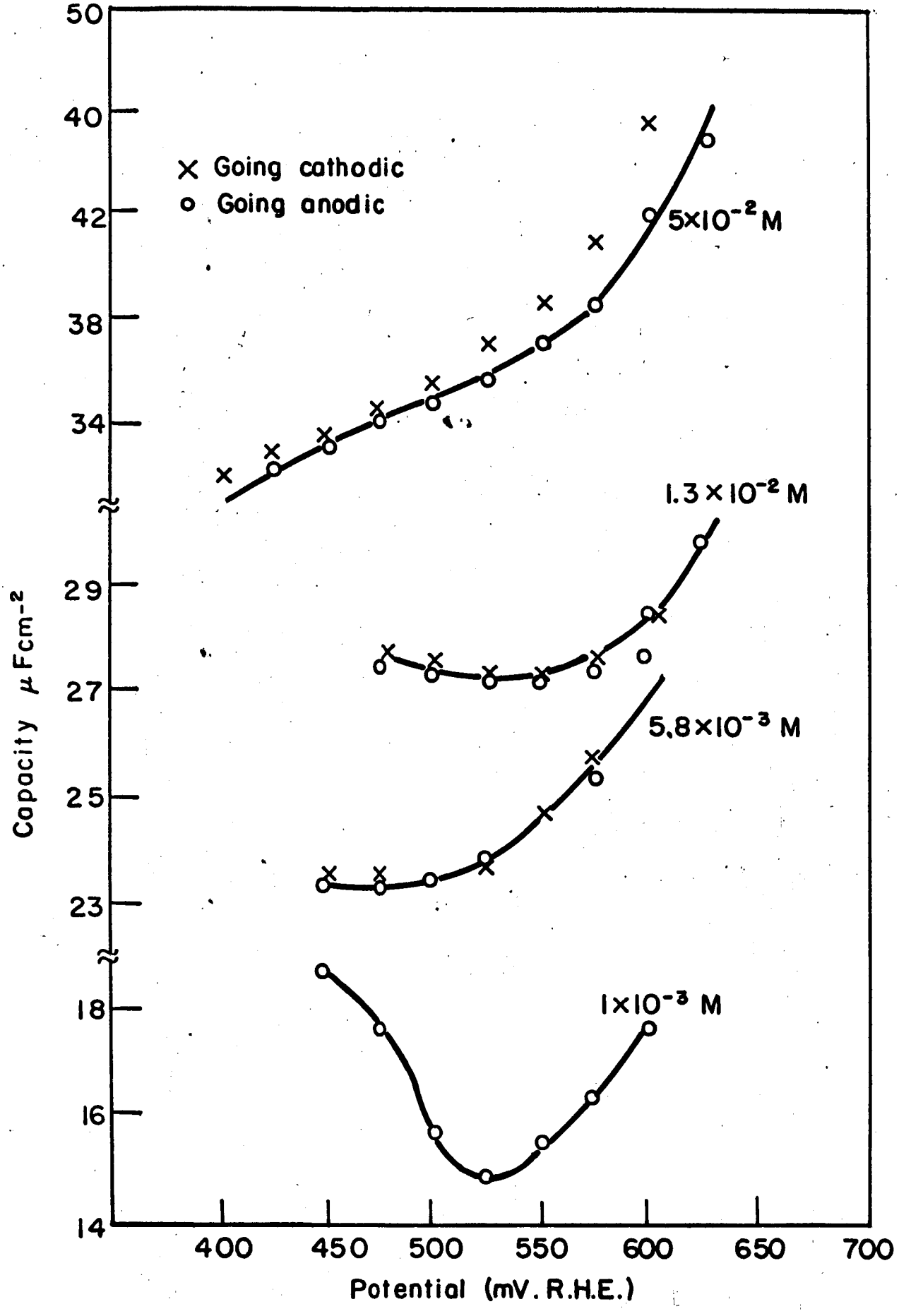
50
40
42
38
34
29
27
25
23
18
16
14
× Going cathodic
o Going anodic
5×10⁻² M
1.3×10⁻² M
5.8×10⁻³ M
1×10⁻³ M
Capacity μFcm⁻²
400
450
500
550
600
650
700
Potential (mV. R.H.E.)

Fig. III. 3

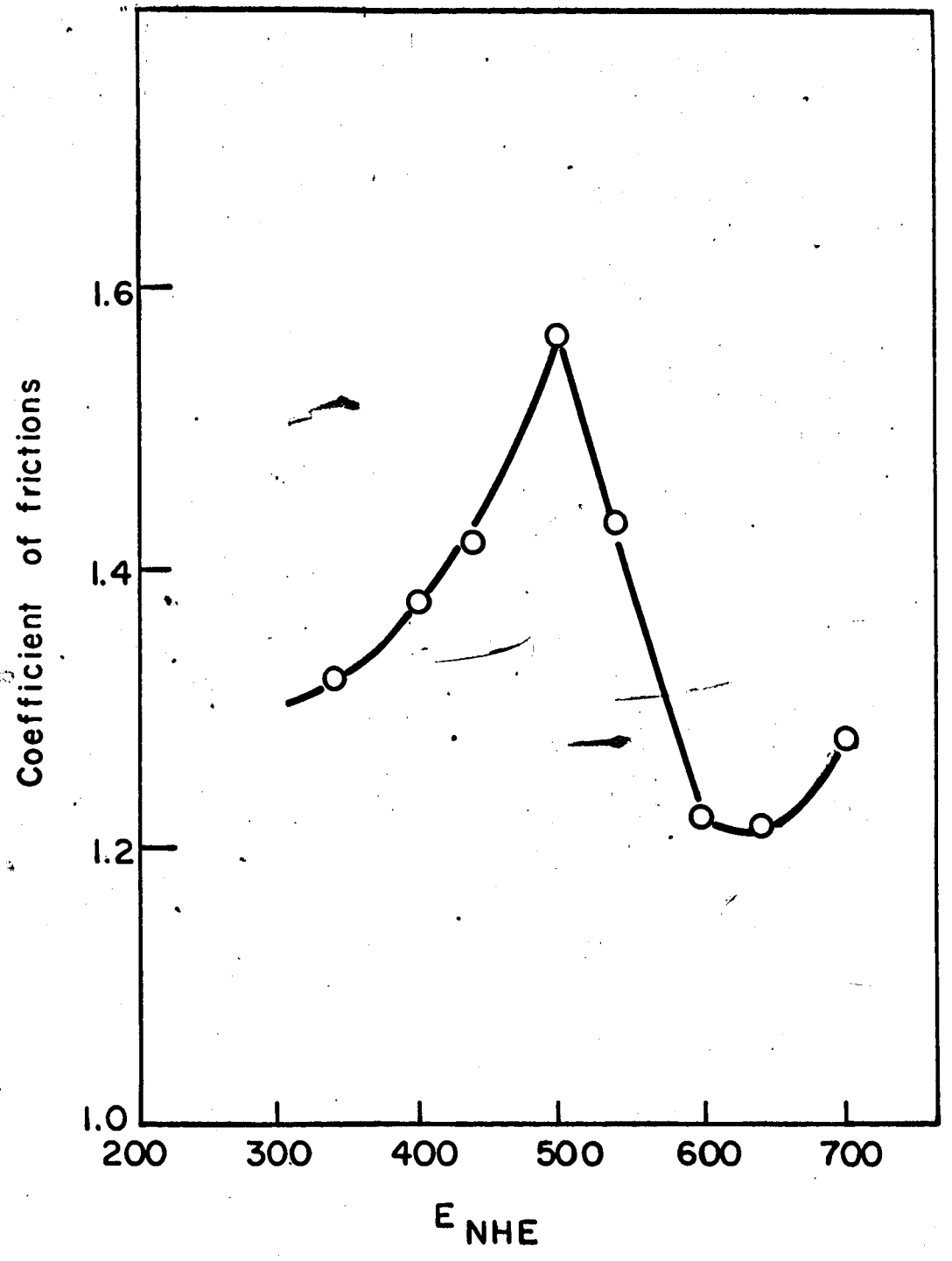

Fig.V.1 Platinum on platinum -Friction vs. Potential

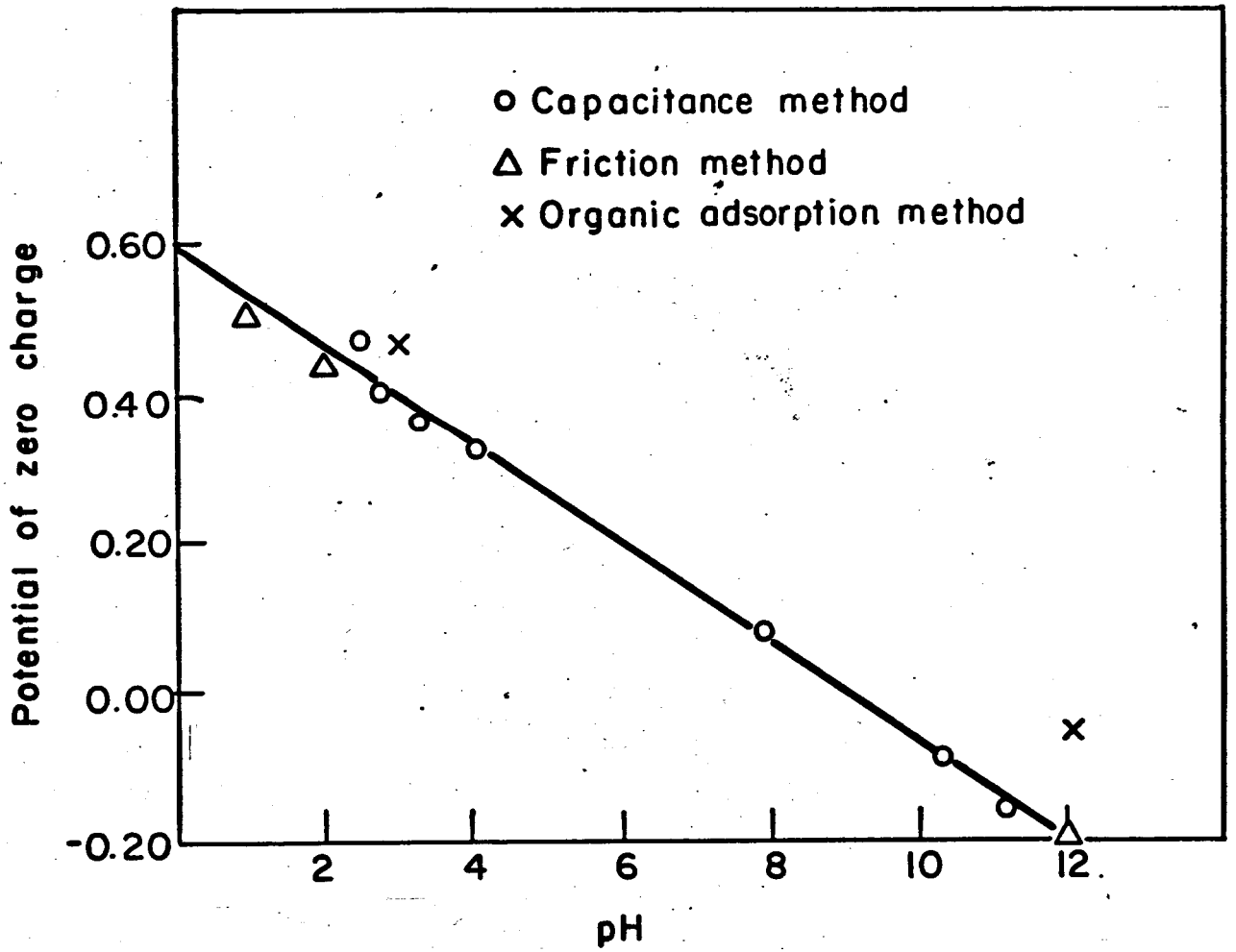

Fig.V.2 Potential of zero charge on Pt vs pH.

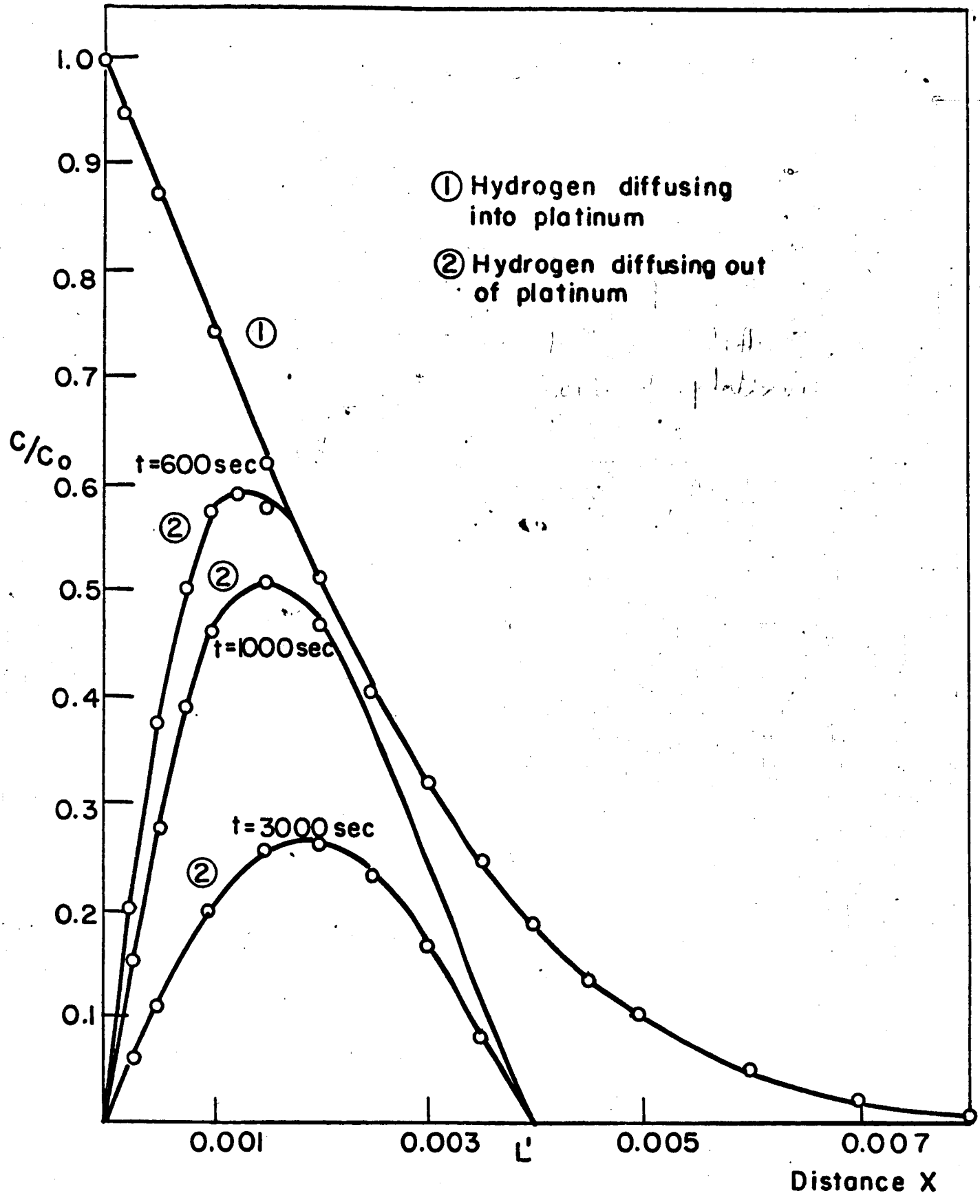

Fig.VI.1. Concentration profiles of hydrogen diffusion in platinum.

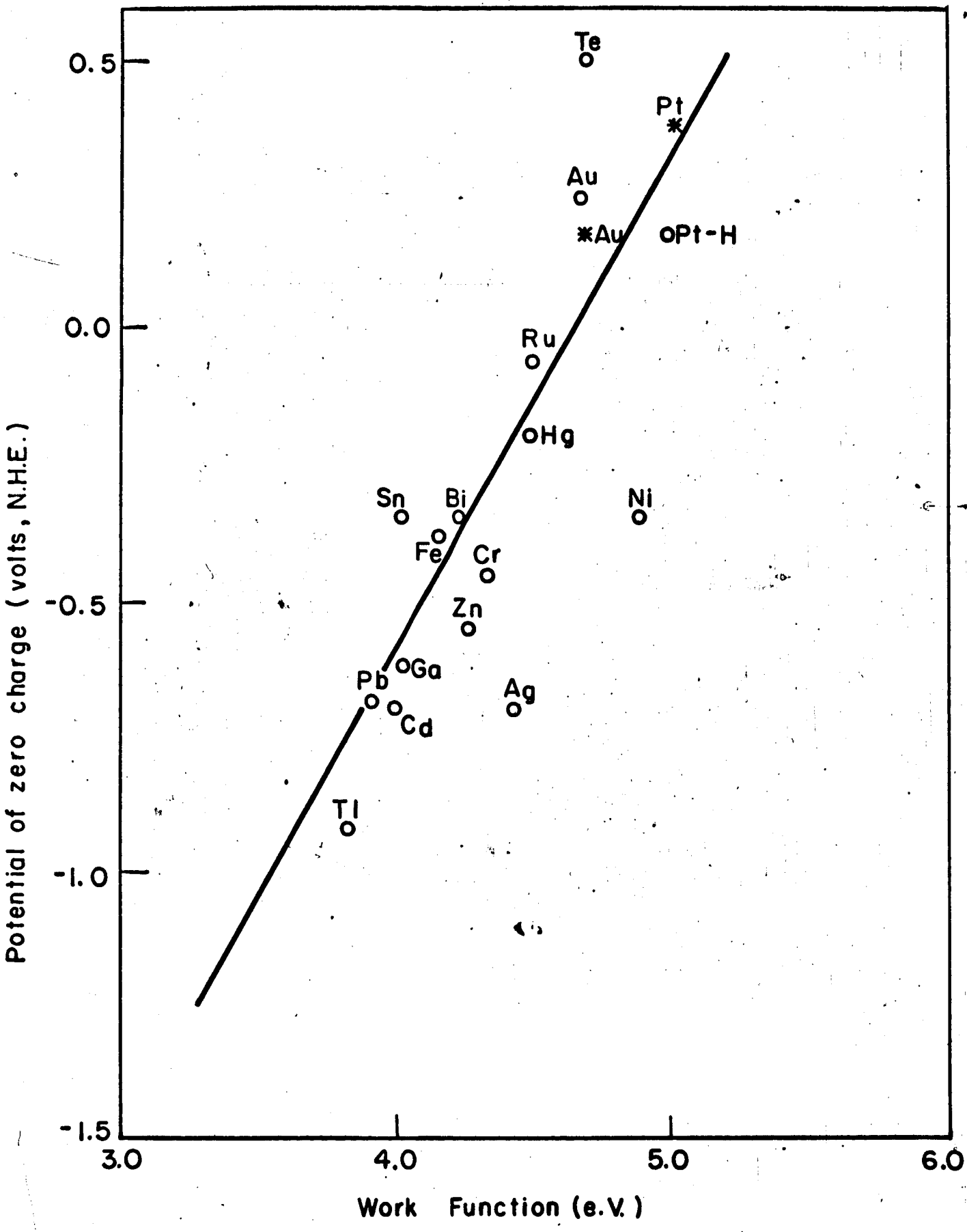
Te
Pt
Au
*Au
oPt-H
Ru
oHg
Sn
Bi
Ni
Fe
Cr
Zn
oGa
Pb
Ag
Cd
Tl
0.5
0.0
-0.5
-1.0
-1.5
3.0
4.0
5.0
6.0
Potential of zero charge (volts, N.H.E.)
Work Function (e.V.)

Fig.VII.1

(a) Before activation

(b) After activation

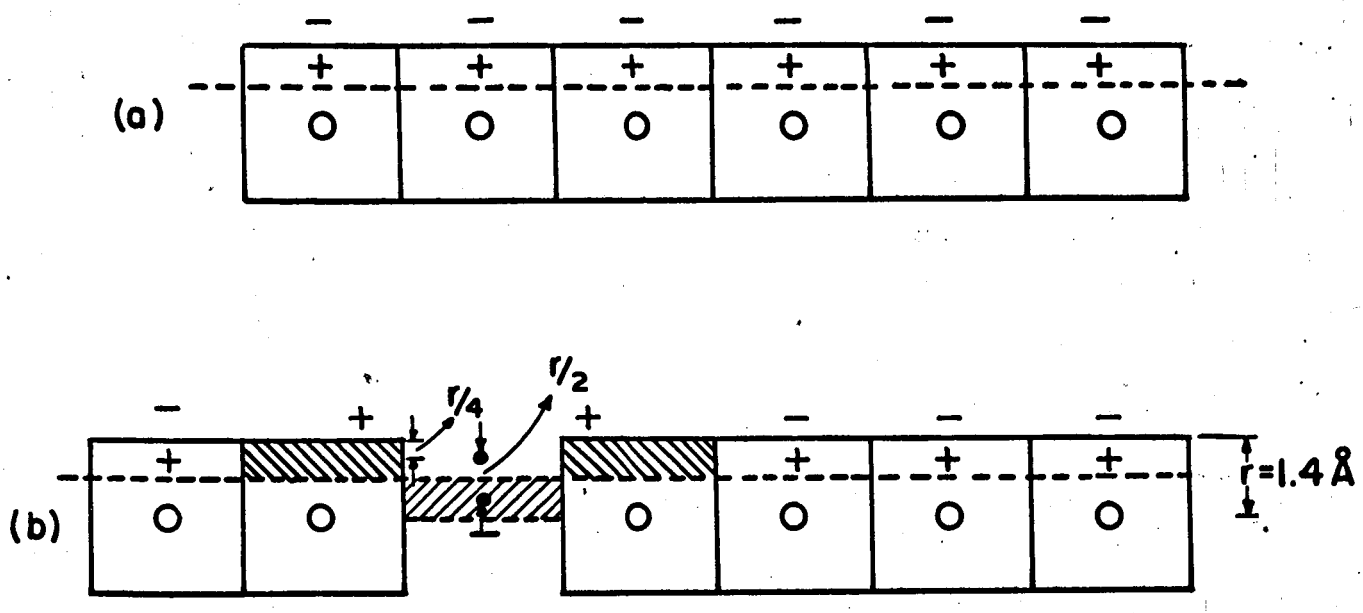

Fig. VIII I. Surface electron distribution before and after activation of platinum.

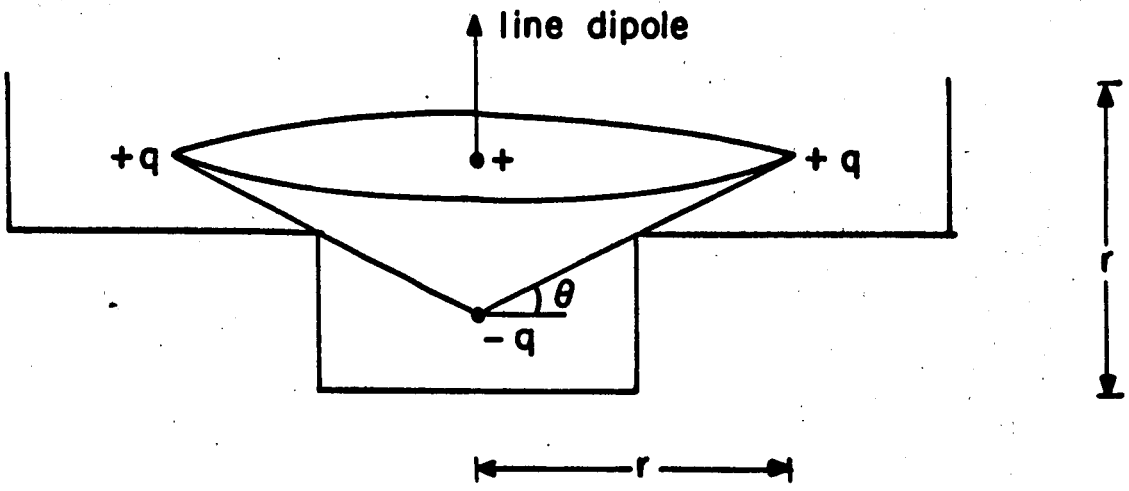

$$\text{The length of dipole} = \left\{ r^2 + \left(\frac{r}{2}\right)^2 \right\}^{1/2} \sin\theta$$

$$= \frac{\sqrt{5}}{2} r \sin\theta$$

$$\mu = q\frac{\sqrt{5}}{2} r \sin\theta = q\frac{\sqrt{5}}{2} r \times \frac{r}{2} \Big/ \frac{\sqrt{5}}{2} r$$

$$= q\frac{r}{2}$$

Fig. VIII.2 Charge separation in and around the vacancy.

SECTION IV. TRAJECTORY OF MOTION AND THE POTENTIAL ENERGY BARRIER FOR AN ION IN AN IONIC LATTICE MOVING UNDER THE INFLUENCE OF AN ELECTRIC FIELD

CONTENTS

The potential energy of a moving interstitial ion in an open lattice with fixed network is determined primarily by two factors:

a) The electric field due to the lattice ions, including polarization effects,

b) The short-range repulsive force between the moving ion and its neighbors.

1 Distribution of charge in the lattice

The first problem encountered in the attempt to assess the coulombic field is that of the amount and distribution of charge over the atoms in the lattice. The mobile atoms in the open structure systems (interstitial ions) are usually taken into the lattice in order to compensate for the stoichiometric disbalance among the atoms constituting the lattice. Ionizing, they give away the charge to atoms which need it in order to fulfill valency requirements. Thus, in alumino-silicates the interstitial alkali atom gives away an electron to an aluminum atom to complete its octet.

Hence, in the first approximation one could assume that the charge opposite to that of mobile ions is located at the aluminum lattice sites. However, this approximation would rather poorly represent reality since atoms attract electrons with different power as expressed by Pauling's electronegativity of atomic species.

Electronegativity of atomic species is related to the amount of the ionic character of a single bond between atoms A and B, with electronegativity X_A and X_B, respectively.

$$\text{Amount of ionic character} = 1 - e^{-\frac{1}{4}|X_A - X_B|^2} \qquad (1)$$

For the distribution of charge it is necessary to know the bond length, as well as the character of bonding. The length of a single bond between atoms A and B can in most cases be reasonably well calculated by use of the atomic radii r_A and r_B (as given in tables) by the equation

$$D(A - B) = r_A + r_B - c|X_A - X_B| \qquad (2)$$

(c is the Schomaker-Stevenson coefficient).

This equation gives the interatomic distance smaller than the distance should be according to sum of atomic radii of atoms A and B, if the A-B bond has some ionic character. If the actual distance between A and B atoms is even smaller than calculated according to equation (2), the remaining shortening is attributed to partial double-bond character of the bond.

The amount of double-bond character to be expected is computed from the principle of electroneutrality (1).

The percentage of ionic character of A-B bond that corresponds to the difference in electronegativity of the atoms would place a belonging negative charge on more electronegative atoms in molecules. This electric charge would be reduced to zero if each bond has a corresponding percent of double-bond characters. If each bond has the amount of ionic character corresponding to the electronegativity difference of the two atoms, the percent of ionic bond character times the number of bonds gives the value of positive charge transferred to the less electronegative atom. The additional shortening of the bond due to the double bond character gives

a bond number and the percent of double-bond character. The percent of double-bond character of each bond multiplied by number of bonds gives the amount of negative charge transferred back to less electronegative atoms. The difference between positive and negative charge gives the residual charge on the less electronegative atom.

2. Dimensions of the space from which appreciable contributions to the field strength are obtained

The limits of the space can be set up at points beyond which the sum of contributions to the field strength of all the points of an infinite lattice falls below 1% of the total field strength.

Equations (3) gives the electric field from a unit positive charge at a distance ia, $\underline{a}$ is the average distance between unit positive charges in the lattice and ε is the average dielectric constant.

$$\Delta F = \frac{e^2}{\varepsilon i^2 a^2} \tag{3}$$

If assumed that positive and negative charges are distributed periodically, the limit is determined by the condition

$$\sum_{i=1}^{n} \left\{ \frac{e^2}{\varepsilon a^2 i^2} - \frac{e^2}{\varepsilon (ai + \frac{a}{2})^2} \right\} \geq 100 \sum_{i=n+1}^{\infty} \left\{ \frac{e^2}{\varepsilon a^2 i^2} - \frac{e^2}{\varepsilon (ai + \frac{a}{2})^2} \right\} \tag{4}$$

It follows that

$$\sum_{i=1}^{n} \left\{ \frac{1}{i^2} - \frac{1}{(i - \frac{1}{2})^2} \right\} \geq 100 \sum_{i=n+1}^{\infty} \left\{ \frac{1}{i^2} - \frac{1}{(i - \frac{1}{2})^2} \right\} \tag{5}$$

This condition is fulfilled for $n \geq 5$. Hence a cube containing $> 10^3$ pairs of charges around a central ion has to be taken into account and this is independent of charge on each ion or of dielectric constant.

3. Positioning of atoms at different points in the lattice

All interactions are some function of the distance between an atom in the lattice and a point of interest.

The position of the atom is described by x, y, and z value in respect to a reference point. It is practical to place this at one corner of one unit cell of the lattice. Then, atoms of the same crystal lattice position in any other unit cell will have coordinates which are simple sums of the coordinates of the original atoms and numbers characteristic of the position of the unit cell as a whole. These numbers are simple multiples of unit cell dimensions. Such an atom is considered in a unit cell which is four unit cells away from the origin in the x-direction, two unit cells in the y-direction and is on the x axis, the coordinates of that atom should be

$$(4a_x + x),\ (2a_y + y),\ z$$

where a_x and a_y are the unit cell dimensions along x and y respectively and x, y, z are the coordinates of the corresponding atom in the basic unit cell.

4. Coulomb field in the lattice

In a practical computation a model is assumed for the charge distribution within the lattice. The volume density of charge for each ion is represented by a monopole and dipole. The influence of a nearby charge on the volume density is taken into account only by

a multiplication of the dipole moment. The charge centroid of a lattice ion is considered to remain fixed on the lattice site. In this model solutions may be formulated for the electric field acting on a mobile interstitial ion, which take into account with varying degrees of approximation the lattice self-attraction and the interaction between the lattice and the mobile ion.

i) The exact solution

A charge $Z_j e$ at lattice site j which is a vector distance $\vec{a}_{js}$ from the point s causes an electric field at s which is

$$\vec{F}_s^C = \frac{Z_j e}{a_{js}^3} \vec{a}_{js} \tag{6}$$

The dipole at lattice site j contributes the field

$$\vec{F}_s^D = \frac{3\vec{a}_{js}(\vec{\mu}_j \cdot \vec{a}_{js})}{a_{js}^5} - \frac{\vec{\mu}_j}{a_{js}^3} \tag{7}$$

In these equations the vector $\vec{a}$ is taken to point from j to s.

The total electric field strength at point s from n lattice monopoles and dipoles is

$$\vec{F}_s = \sum_{j=1}^{n} \{ \frac{Z_j e}{a_{js}^3} \cdot \vec{a}_{js} + [\frac{3\vec{a}_{js}(\vec{\mu}_j \cdot \vec{a}_{js})}{a_{js}^5} - \frac{\vec{\mu}_j}{a_{js}^3}] \} \tag{8}$$

The dipole moment of an ion is not fixed but is induced by the net electric field at that site, excluding of course the field due to the ion itself. If the net field defined this way is denoted $[\vec{F}_k]$, and if the polarizability of the ion at site k is α_k, the dipole strength will be

$$\vec{\mu}_k = \alpha_k [\vec{F}_k] \tag{9}$$

$[\vec{F}_k]$ is found from equation (8) by letting point s coincide with lattice site k and with the sum excluding k. Together (8) and (9) form a system of 3N linear equations which determine the dipole moments due to the lattice self-interaction.

$$\vec{\mu}_k = \alpha_k \sum_{\substack{j=1 \\ j \neq k}}^{n} \{ \frac{Z_j e}{a_{jk}^3} \cdot \vec{a}_{jk} + [\frac{3\vec{a}_{jk}(\vec{\mu}_j \cdot \vec{a}_{jk})}{a_{jk}^5} - \frac{\vec{\mu}_j}{a_{jk}^3}] \} \tag{10}$$

With the large numbers of atoms that have to be taken into account for a good approximation, an exact solution utilizing a present-day computer is likely to be prohibitively long. Hence, further approximation must be made.

ii) The Schottky-Jost approximation

As a first approximation it can be taken that point charges in a crystal lattice are exerting a Coulomb force through a medium of uniform dielectric constant ε, as assumed in the early works of Schottky and Jost (2, 3). Thus, at any point in the crystal the field strength would be

$$\vec{F}_s = \frac{1}{\varepsilon} \sum \frac{Z_j e}{a_{js}^3} \cdot \vec{a}_{js} \tag{11}$$

This approximation bypasses the problem of dipole induction but is rather unsatisfactory, since the largest portion of the field strength is created by the interactions with the first neighbors of the point s,

and these interactions are effected through empty space, i.e., with

$$\varepsilon = 1 \quad . \tag{12}$$

iii) The Mott-Littleton approximation

All the atoms in the lattice are divided into two blocks, (a) the moving ion and the nearest neighbors (1, 2, 3, . . . , M), and (b) the rest of the atoms in the lattice space (M+1, M+2, . . . , N) — the so-called distant atoms.

The polarization effect of the group (b) is taken into account by considering the charges outside the nearest neighbors sphere not to be in a vacuum but rather in a dielectric with a macroscopic dielectric constant ε.

The field at any point within the block (a) consists of

i) The field due to distant atoms acting through the dielectric,

ii) The field due to the charges inside the block (a) acting in vacuum,

iii) The field due to the induced dipoles within the block (a).

Thus,

$$\vec{F}_s = \frac{1}{\varepsilon} \sum_{j=M+1}^{n} \frac{Z_j e}{a_{js}^3} \cdot \vec{a}_{js} + \sum_{j=1}^{M} \{ \frac{Z_j e}{a_{js}^3} \cdot \vec{a}_{js} + [\frac{3\vec{a}_{js}(\vec{\mu}_j \cdot \vec{a}_{js})}{a_{js}^5} - \frac{\vec{\mu}_j}{a_{js}^3}] \} \tag{13}$$

Introducing (13) into (9) one obtains 3M equations with 3M dipole moments in the moving ion and the M nearest neighbors. With the known dipole moments, equation (13) can be used to find the field at any point s.

This method has the disadvantage of employing the value ε which is

not known for all the crystal species of interest and whose validity for a microscopic space of a few unit cells is questionable.

iv) The third approximation

An approximate solution to equation (9) for the dipole moments of the entire lattice segment may be obtained by iteration. Suppose the dipole moments on the right side of (9) are initially zero. Then the sum over the lattice should give an induced dipole at each lattice site due only to the monopole terms. This set of dipoles would then serve as input to the right side of (9) to obtain an improved estimate of each induced dipole on the left side. The procedure would be repeated until a satisfactory level of stability of successive dipole moments was achieved. To assist faster convergence, the monopole field in the first pass might be reduced by a dielectric constant as in equation (11). This will take into account the tendency of dipole induction to reduce the monopole field strength.

This procedure will give the dipole moments for any position of the mobile ion; however, it calls for a complete recomputation as the mobile ion is moved around the assumed starting position. It is more efficient to make a further approximation in the spirit of Mott and Littleton. As the mobile ion is moved away from the initial position the nearer dipole moments are revised but not the farther. Thus the 3M equations represented by (15) which were treated in the first iterations are reduced to a subset for the 3M nearest neighbors of the mobile ion.

$$\vec{\mu}_s = \vec{\alpha}_s[\vec{F}_s] \tag{14}$$

and

$$[\vec{F}_s] = \sum_{\substack{j=1 \\ j\neq s}}^{M} \{\frac{Z_j e}{a_{js}^3} \cdot \vec{a}_{js} + [\frac{3\vec{a}_{js}(\vec{\mu}_j \cdot \vec{a}_{js})}{a_{js}^5} - \frac{\vec{\mu}_j}{a_{js}^3}]\} + \sum_{j=M+1}^{n} \{\frac{Z_j e}{a_{js}^3} \cdot \vec{a}_{js} + [\frac{3\vec{a}_{js}(\vec{\mu}_j \cdot \vec{a}_{js})}{a_{js}^5} - \frac{\vec{\mu}_j}{a_{js}^3}]\} \tag{15}$$

The subscript s is used in (15) to indicate that the equation is to be applied not only to the ions on lattice sites but also to the mobile ion. The first sum in (15) is over the nearest ions; at each position of the mobile ion the dipole moments in this sum are to be revised. For the farther ions in the second sum the dipole moments remain constant.

The revision of the nearest dipole moments would probably be carried out by the same iterative principle applied to equation (10). With the new dipole moments (15) supplies the field acting on the mobile ion at its new position.

5. Repulsive energy interactions*

As the ions are brought closer together, so that their outer electron shells begin to overlap, repulsive force becomes operative. It is the repulsive force that opposes Coulombic attractive force between a positive and a negative ion, and causes them to come to equilibrium at a finite value of the internuclear distance.

---

*After M. Tosi: Cohesion of Ionic Solids in the Born Model (3).

The repulsive potential falls off very rapidly with increase of inter-ionic distance r. Born suggested that it could be approximated by an inverse power of r, so that the mutual potential energy of two ions could be written as:

$$E_{ij} = \frac{Z_+ Z_- e^2}{r_{ij}} + \frac{b_{ij} e^2}{r_{ij}^n} \tag{16}$$

where the second term is the repulsive energy.

The potential energy of the crystal can be written as

$$E = -\frac{Ae^2Z^2}{R} + \frac{Be^2}{R^n} \tag{17}$$

where A and B are constants for a given crystal (A = Madelung constant). So, the corresponding contribution of the repulsive energy to the lattice energy is

$$E_{rep} = \frac{Be^2}{r^n} \tag{18}$$

Born and Mayer adopted later a potential function of the form

$$E_{rep} = b \exp\left(\frac{-r}{\rho}\right) \tag{19}$$

where the new constants b and ρ replace the former B and n.

In order to retain the consistency with approximate additivity of interatomic distances, the repulsive potential, which in the case of univalent salts equals the repulsive potential energy, is expressed as

$$E_{rep(r_{1,2})} = C_{1,2}\, be^{\frac{(r_1 + r_2 - r)}{\rho}} \tag{20}$$

where r is the distance between two ions, 1 and 2, r_1 and r_2 "observed" radii of cations and anions, and constant $C_{1,2}$ is given by Pauling as:

$$C_{1,2} = 1 + \frac{Z_1}{N_1} + \frac{Z_2}{N_2} \tag{21}$$

where Z_1 and Z_2 are ionic valencies (i.e., the total charge in units of electronic charge), and N_1 and N_2 are the numbers of electrons in the outermost shell of either.

If the total repulsive energy, as a function of a nearest-neighbor distance r, is written in the form of equation (19), the evaluation of the lattice energy of an ionic crystal requires the determination of two repulsive parameters. This follows from considering only the Born repulsion of the first neighbors in the crystal.

Taking account of the Born repulsions of the second neighbors, the contribution of the Born repulsive energy to the lattice energy per molecule can be written

$$E_{rep} = Mb_{12} \exp\left(\frac{-r}{\rho}\right) + \tfrac{1}{2}M'(b_{11} + b_{22}) \exp\left(\frac{-r'}{\rho}\right) \tag{22}$$

where M and M' are the numbers of first and second neighbors, r' is the distance of the second neighbors.

Two basic assumptions are involved in equation (22). First, the repulsive energy of the crystal is written as the sum of two-body repulsive energies (this can be only approximately true as the many-body contributions to the Born repulsion arise from many-body overlap). Second, the hardness parameter is assumed to be independent of the ionic species in

a given crystal. The evaluation of the repulsive energy of an ionic crystal still requires the determination of three repulsive parameters: M_{12}, $M'(b_{11} + b_{22})$, and ρ.

The number of independent parameters in a family of salts of given structure can be reduced and individual parameters can be determined by taking account of the approximate additivity of the interionic distances. This suggests that interionic distance can be expressed as

$$r = r_1 + r_2 + \Delta \tag{23}$$

where r_1 and r_2 are characteristic lengths of the ions 1 and 2, and Δ varies slightly from crystal to crystal in the family.

The parameter b_{12} is usually written in the form:

$$b_{12} = C_{1,2}\, b \exp\left[\frac{(r_1 + r_2)}{\rho}\right] \tag{24}$$

where b is a parameter constant in the family of salts and the coefficient $C_{1,2}$ is the same as before (see equation 6).

A plausible extension of the expression (24) to the second-neighbor repulsion leads to the Born-Mayer form for the Born repulsive energy:

$$E_{rep} = MC_{1,2}\, b \exp\left[\frac{(r_1 + r_2 - r)}{\rho}\right] + \\ + \tfrac{1}{2} M'b\left[C_{11} \exp\left(\frac{2r_1}{\rho}\right) + C_{22} \exp\left(\frac{2r_2}{\rho}\right)\right] \exp\left(\frac{-r}{\rho}\right) \tag{25}$$

By regrouping of terms and by defining

$$b_1 = b^{\frac{1}{2}} \exp\left(\frac{r_1}{\rho}\right) \quad \text{and} \quad b_2 = b^{\frac{1}{2}} \exp\left(\frac{r_2}{\rho}\right) \tag{26}$$

one gets the Higgins-Mayer form for the Born repulsive energy:

$$E_{rep} = M C_{1,2}\, b_1 b_2 \exp\left(\frac{-r}{\rho}\right) + \tfrac{1}{2} M'(C_{11} b_1^2 + C_{22} b_2^2) \exp\left(\frac{-r}{\rho}\right) \qquad (27)$$

Again, the characteristic parameters b_1 and b_2 and ρ can be determined by a simultaneous fit for all salts in the family.

In the first approximation let us consider only the first neighbors. Introducing equation (20) for E_{rep} in the equation (16), one gets:

$$E = \frac{Z_+ Z_- e^2}{r} + C_{1,2}\, b \exp\left(\frac{(r_1 + r_2 - r)}{\rho}\right) \qquad (28)$$

The effect of mutual dipole induction is to add a term which tends to decrease the magnitude of the electric potential energy. This addition is discussed in the appendix.

6. Estimate of the repulsive constants from the known data on ion to ion interactions

To evaluate two Born constants one can postulate two equations in which those constants are the only unknowns, for a system similar to the system of interest inasmuch as the same type of bond is involved, for which the required experimental data are available.

Thus, data can be found for the energy of formation and the equilibrium distance between the ions for the compound in the vapor phase containing the same type of bonds.

If, for example, the energy of formation of sodium oxide vapor is known, the figure for the total potential energy can be found from these data with some additional consideration. Namely, the potential energy

is equal to the work needed to bring together from infinity to the equilibrium distance the three ions composing the oxide. If the standard enthalpy of formation of the oxide (ΔH^0_{ox}) is known as well as the standard enthalpies of forming the ions from the same reactants (e.g., metallic sodium and molecular oxygen), $\sum \Delta H^0_{ion}$, then

$$E = \Delta H^0_{ox} - \sum \Delta H^0_{ion} \quad , \tag{29}$$

which is the same potential energy as in equation (28).

The potential energy equation (28) is to be evaluated at the equilibrium distance r_0, which again is an experimentally available parameter. This is determined by the balance of the repulsive and attractive forces.

The forces which ion 1 exerts on ion 2 are

$$\vec{f}_{rep} = - \text{grad } E_{rep} = \frac{1}{\rho} E_{rep} \hat{r}_{21}$$

$$\vec{f}_{c} = - \text{grad } E_{c} = \frac{Z_1 Z_2 e^2}{r^2} \hat{r}_{21} = \frac{1}{r} E_{c} \hat{r}_{21} \tag{30}$$

where $\hat{r}$ is the unit vector pointing from 1 to 2, and E_c is the Coulomb potential, dipole contributions not considered. By balancing the forces, one obtains

$$\rho = r_0 - \frac{r_0^2 E}{Z_1 Z_2 e^2} \tag{31}$$

$$C_{1,2}\, b = \frac{\rho Z_1 Z_2 e^2}{r_0^2} \exp\left(-\frac{(r_1 + r_2 - r_0)}{r}\right) \tag{32}$$

These equations determine the range ρ and the scale b of the repulsive potential.

7. Motion of an ion in motion through the interlattice space

(a) The energy approach. The probability of finding the ion at any point in the lattice is a function of the potential energy of the ion at that point.

(b) The field approach. The energy required to reach any new position in the lattice can be determined by a line integral to that point.

The two approaches have similarities and each has its difficulties. The similarity is that each requires a re-evaluation of the lattice dipole moments as the ion is moved from position to position.

In the energy approach the mutual dipole induction between the mobile ion and the lattice leads to a modification of the potential energy expression which has not been completely solved (see the appendix). However, an approximate expression has been derived (A-7).

In the field approach an approximate line integral replaces the expression for the potential energy. The line integral could be carried out systematically from a three-dimensional field map using small steps away from the central reference position of the mobile ion, until the desired energy contours were mapped.

The energy approach is a simpler starting point for practical computation. As approximate results are obtained, the magnitude of the higher dipole corrections can be estimated and included if necessary.

The contribution to the electric potential energy of the charge $Z_s e$ by the fixed dipole $\vec{\mu}_j$ is

$$E^D = Z_s e \frac{\vec{\mu}_j \cdot \vec{a}_{js}}{a^3_{js}} \qquad (33)$$

Some of the dipole moment $\vec{\mu}$ is induced by the charge $Z_s e$. For this portion of the dipole moment a correction to the energy is to be added as discussed above and in the appendix.

8. The computer program

A computer program is being written which is to produce potential maps for a mobile ion moving in a crystal lattice. The program organization is as follows:

(a) A series of operations which generate lattice coordinates out of a unit cell, and establishes ionic charges, susceptibilities, and repulsive energy constants.

(b) An iterative procedure to obtain the dipole moments in the entire lattice, for the starting position of the mobile ion, as described in Section 4 — the third approximation.

(c) A procedure for recomputing the energy of the ion as it is moved around in the lattice cavity, with the additional approximation described in Sections 4 and 6.

9. Choice of units

It is convenient to choose units which will give the potential energy of the ion in the order of unity. Such a system is:

length a_{js} in angstroms Å

charge Ze in unit electron charge +e

susceptibility α in $Å^3$

repulsive potential b in $\frac{e^2}{Å}$

In these units the calculated dipole moments and fields will have units given by

dipole moment $\vec{\mu}$ in $Å^2$

electric field $\vec{F}$ in $\frac{e}{Å^2}$

and an expression for the potential energy of an ion of charge Z_s in the presence of fixed electric and dipole fields and the Born repulsive field is

$$E_s = \sum_j \{\frac{Z_s Z_j}{a_{js}} + Z_s \frac{\vec{\mu}_j \cdot \vec{a}_{js}}{a_{js}^3} + C_{js}\, b \exp \frac{(r_1 r_2 - a_{js})}{\rho} \qquad (34)$$

This expression has units of $\frac{e^2}{Å}$.

To obtain the potential energy in kcal/mole, the resulting energy should be multiplied by a factor of 3.3×10^2 .

Typical values for the constants might be:

$Z_j = +1$

$Z_s = -1$

$r_1 = 0.95Å$

$r_2 = 1.4Å$

$\rho = 0.3333Å$

$b = 0.0465\,(\frac{e^2}{Å})$

$C_{js} = 1$.

It should be repeated that the dipole potential in equation (34) is approximate and subject to the conditions specified for equation (33).

10. Program illustration

The following contains the listing and output from a simple program which illustrates some of the techniques discussed in the text. The program (Figs. 1 and 2) prepares and prints a potential map inside one cell of a simple two-dimensional lattice (Fig. 3). The lattice taken as an example consists of two unit cells each five angstroms square with a single negative charge at each corner of each cell. The potential which is computed is for the electric monopole force and Born repulsive force acting on a singly-charged positive ion.

Qualitative features of the obtained map (Fig. 3) are a region of equilibrium (energy minimum) near the center of the unit cell and a potential hill of 14 kilocalories per mole near the boundary between the cells. The bottom line on the map is the boundary and the second unit cell, not printed, joins along this line. Distances from one corner are labelled in angstroms along the edge of the plot.

The potential energy barrier (Fig. 4) for the jump of the mobile ion from one position of minimum energy to another is extracted from the map by plotting the computed potential energies vs. distance from a center point in the middle between the two unit cells, along the minimum energy path, which is the vertical line connecting directly the two potential energy minima and the center point.

The application of the full program to some three-dimensional lattices of certain real crystals is in progress.

APPENDIX -IV-A

Work of assembly of a system of charge and dipoles

If the dipole on one ion is induced by a second ion, the potential energy of the system is not the same as if the dipoles were of fixed strength. An expression for the potential energy can be obtained as the ions are brought together from infinity.

The monopole and dipole fields on ion -2 from ion -1 are

$$\vec{F}_2^M = \frac{q_1}{r^3}\vec{r}_{12} \qquad \text{(A-1)}$$

$$\vec{F}_2^D = \frac{3r_{12}(\vec{\mu}_1 \cdot \vec{r}_{12})}{r^3} - \frac{\mu_1}{r^5} \qquad \text{(A-2)}$$

The vector $\vec{r}_{12}$ is taken to end at ion -2 and start at ion -1. If ion -2 has no dipole moment, the field acting on ion -1 is

$$\vec{F}_1 = \frac{q_2}{r^3}\vec{r}_{21} \qquad \text{(A-3)}$$

with $r_{21} = -r_{12}$ as defined above. The dipole induced on ion -1 due to the external field acting on the ion is

$$\vec{\mu} = \alpha_1 \vec{F}_1 \qquad \text{(A-4)}$$

Equations A-2 through A-4 are a linear system similar to equations (8) and (9) in the text, but for only two ions. The solution, easily obtained, is

$$\vec{\mu} = \frac{\alpha_1 q_2}{r^3}\vec{r}_{12} \qquad \text{(A-5)}$$

$$\vec{F}_2^D = -\frac{2\alpha_1 q_2}{r^6}\vec{r}_{12} \qquad \text{(A-6)}$$

If the two ions are brought together from infinity the induced dipole acts in a way to decrease the work done, but the contribution is not as great as if the dipole were of the same fixed strength as its value when the ions are closest. The work done on the second ion against the dipole field is computed from a line integral:

$$u^D = \int_{\infty}^{r} q_2 \vec{F}_2^D \cdot d\vec{r}$$

$$= -\frac{\alpha_1 q_2^2}{4r^4} \qquad \text{A-7}$$

In the preceding derivation the ion on which work of assembly was done was considered unpolarized. If this ion has a dipole moment produced by the field from the other ion, the equations to be solved are

$$\vec{F}_2 = \frac{q_1}{r^3}\vec{r}_{12} + \frac{2\vec{\mu}_1 \cdot \vec{r}_{12}}{r^5} r_{12} \qquad \text{A-8}$$

$$\vec{F}_1 = \frac{q_2}{r^3}\vec{r}_{21} + \frac{2\vec{\mu}_2 \cdot \vec{r}_{21}}{r^5}\vec{r}_{21} \qquad \text{A-9}$$

$$\vec{\mu}_1 = \alpha_1 \vec{F}_1 \qquad \text{A-10}$$

$$\vec{\mu}_2 = \alpha_2 \vec{F}_2 \qquad \text{A-11}$$

The solution for the field magnitude at ion 2 given an increased value relative to the solution (A-6):

$$F_2\left(1 - \frac{4\alpha_1\alpha_2}{r^5}\right) = \frac{q_1}{r^2} - \frac{2\alpha_1 q_2}{r^6} \qquad \text{A-12}$$

The potential resulting from such a force law is not amenable to simple computations.

APPENDIX IV-B

Correction to repulsive energy constant for small dipole moments

Summarizing the results of the previous calculations, if an ion of charge q, and small susceptibility α, is considered stationary with its charge center coinciding with its induced dipole center, an approaching ion of charge q_2 and small susceptibility is acted upon by electric monopole and dipole forces of strength

$$f^M = \frac{q_1 q_2}{r^2} \qquad \text{A-13}$$

$$f^D = -\frac{2\alpha_1 q_2^2}{r^5} \qquad \text{A-14}$$

The contribution of each force to the potential energy of the system is

$$E^M = \frac{q_1 q_2}{r} \qquad \text{A-15}$$

$$E^D = -\frac{\alpha_1 q_2^2}{2r^4} \qquad \text{A-16}$$

The repulsive force and potential on ion -2 is

$$f^R = \frac{1}{\rho} k \exp\left(\frac{-r}{\rho}\right) \qquad \text{A-17}$$

$$E^R = k \exp\left(\frac{-r}{\rho}\right) \qquad \text{A-18}$$

k is the combination of constants given in the text:

$$k = C_{12} b \exp\frac{(r_1 + r_2)}{\rho} \qquad \text{A-19}$$

The solution for ρ and k (consequently b) requires knowing:

r_0 = equilibrium distance of the positive-negative ion pair,

E = potential energy of system at r_0, which is equal to the energy released as the charged ion pair approach each other from infinity to r_0.

The expressions for ρ and k are similar to formulas in the text modified by factors involving the ratio of the dipole potential to the monopole potential

$$\frac{E^D}{E^M} = -\frac{1}{2}\frac{q_2}{q_1}\left(\frac{\alpha_1}{r_0^3}\right) \qquad \text{A-20}$$

Having evaluated this for the ion pair, then

$$\rho = r\left\{\frac{1 + E^D/E^M}{1 + 4E^D/E^M}\right\} - r_0^2\frac{E}{q_1 q_2}\left\{\frac{1}{1 + 4E^D/E^M}\right\} \qquad \text{A-21}$$

$$k = \left\{\frac{q_1 q_2}{r_0^2} - \frac{2\alpha_1 q_2^2}{r_0^5}\right\}\rho \exp(r_0/\rho) \qquad \text{A-22}$$

Equations (A-20) through (A-22) are unsymmetrical in appearance with regard to the susceptivility of the two ions, since α_2 does not appear. This is due to the approximation in which one of the dipole fields is neglected. Therefore in the application of the equations to determine the repulsive constants the larger of the two ionic susceptibilities should be used.

The range of validity of the small dipole approximation is inherent in the original equation (A-14), in which the dipole is considered to be located at the charge center of the ion. The susceptibility α_1 measures the effective atomic volume in which the charges separate to give rise

to the dipole moment. The dipole will be near the center of the atom provided

$$\alpha_1/r_0^3 << 1 .$$

In other words, the distortion of the electron cloud should be small with respect to the distance of the other ion.

By equation (A-20) this is equivalent to requiring the dipole potential to be small with respect to the monopole potential.

Bibliography

1. L. Pauling, The Nature of the Chemical Bond, Cornell University Press, Ithaca, New York (1960).
2. C. Kittel, Introduction to Solid State Physics, John Wiley & Sons, Inc., New York, London (1960).
3. M.P. Tosi, Cohesion of Ionic Solids in the Born Model, in Solid State Physics, Vol. 16, ed. F. Seitz and D. Turnbull, Academic Press, New York and London (1964).
4. L. Pauling, Z. Krist. 67, 377 (1928).
5. M. Born and J.A. Mayer, Z. Physik 75, 1 (1932).
6. A.E. van Arkel, Molecules and Crystals, Butterworths Scientific Publications, London, 1956.

CAPTIONS

Fig. 1. Sample of the program (Part I)

Fig. 2. Sample of the program (Part II)

Fig. 3. Potential energy map as printed by the computer with equipotential contours traced out.

Fig. 4. Potential energy as a function of the distance as extracted from the map; ΔG^{0*} -activation energy barrier for the motion of the positive ion from one interstice into another in the two-dimensional model lattice.

```
626  003  VANCYCK--CSC                    FORTRAN SOURCE LIST
     ISN      SOURCE STATEMENT

      C $IBFTC POTMAP
      C     PROGRAM TO COMPUTE THE POTENTIAL AT MOBILE ION SITE DUE TO SUM
      C     OF POTENTIALS FROM LATTICE SITES.  RESULT IS PRINTED AS POTENTIAL
      C     MAP.
      C
      C-----COMPUTER SERVICES COMPANY
      C        PROGRAMMER - JAMES EARL BUTLER
      C
      C     DEFINE LATTICE LOCATIONS.  A PAIR OF COORDS FOR EACH ION.
      C     DEFINE CHARGE IN SAME ORDER ON LATTICE LOCATIONS.
      C
    1       DIMENSION A(2,6),Z(6),IE(31),XX(31)
    2       DIMENSION IPOT(13, 46)
    3       DATA A/ 2*0., 5.,0., 2*5., 5.,10., 0.,10., 0.,5. /
    4       DATA Z/6*-1./
      C
      C     DEFINE B = REPULSIVE POTENTIAL SCALE FACTOR.
      C     RHO = CHARACTERISTIC LENGTH OF REPULSIVE POTENTIAL
      C     R1 = ATOMIC RADIUS OF LATTICE IONS
      C     R2 = ATOMIC RADIUS OF MOBILE ION.
      C     QR = CHARGE ON MOBILE ION.
      C     S = LENGTH OF UNIT CELL.
      C
    5       DATA B / 0.105 /
    6       DATA R1, R2 / 0.95, 1.4 /
    7       DATA RHO / 0.208 /
   10       DATA QR/1./
   11       DATA S/5./
      C
      C     DISTANCE FUNCTION
      C
   12       R12SQ(XA, YA, ZA, XB, YB, ZB) =(XA-XB)**2+(YA-YB)**2+(ZA-ZB)**2
      C
      C     Y-GRID, DOWN.
      C     X-GRID, ACROSS.
      C
   13       DO 40 J = 1, 46
   14       Y = S*FLOAT(J-1)/45.0
   15       DO 50 K = 1, 10
   16       X = 1.0 + FLOAT(K-1)/3.0
      C
      C     SUM POTENTIALS FROM EACH LATTICE SITE AT MOBILE ION POSITION X, Y.
      C     COULOMB AND BORN REPULSIVE TERMS ONLY.
      C
   17       ENERGY=0.
   20       DO 1000 I=1,6
   21       R=SQRT(R12SQ(A(1,I),A(2,I),0.,X,Y,0.))
   22       COUL = QR*Z(I)/R
   23       BORN = B*EXP((R1 + R2 - R)/RHO)
   24       ENERGY = ENERGY + COUL + BORN
   25 1000  CONTINUE
      C
      C     CONV = SCALE FACTOR FOR ENERGY
      C
   27       DATA CONV / 330.0 /
```

FIG. I

```
2626  003  VANDYCK--CSC                    FORTRAN SOURCE LIST POTMAP
     ISN      SOURCE STATEMENT

      30          IPOT(K, J) = CONV*ENERGY
      31  50      CONTINUE
      33  40      CONTINUE
                  C
                  C     OUTPUT SECTION
                  C
      35          DIMENSION ITSELF(50)
      36          DO 200 I = 1, 50
      37  200     ITSELF(I ) = I- 1
                  C
                  C     TOP LINE
                  C
      41          WRITE(6, 20)
      42          WRITE(6, 210) (ITSELF(I), I = 1, 6)
      47  210     FORMAT(1X 5(I1, 14(1H-)), I1)
                  C
                  C     THERE ARE FIVE GROUPTS OF 9 LINES EACH.
                  C     EVERY NINTH Y-LINE IS ANOTHER ANGSTROM
                  C
      50          LINE = 1
      51          LAST = 8
      52          DO 220 I = 1, 5
      53          DO 230 J = LINE, LAST
                  C
                  C     WRITE 8 LINES WITH NO Y LABEL
                  C
      54          WRITE(6, 240) (IPOT(K, J), K = 1, 10)
      61  240     FORMAT(1X 1HI 10X 10I5, 14X 1HI)
      62  230     CONTINUE
                  C
                  C     WRITE THE NINTH LINE WITH Y-LABEL
                  C
      64          LASTP1 = LAST + 1
      65          WRITE(6, 260) I, (IPOT(K, LASTP1), K = 1, 10), I
      72  260     FORMAT(1X I1, 10X 10I5, 14X I1)
      73          LINE = LINE + 9
      74          LAST = LAST + 9
      75  220     CONTINUE
                  C
                  C     PLOT TITLE.
                  C
      77          WRITE(6, 10)
     100          WRITE(6, 30)
     101  30      FORMAT(11X 50HPOTENTIAL MAP.                              /
                 2       11X 50HUNITS OF ENERGY = KILOCAL PER MOLE.         )
     102          WRITE (6,20)
     103          CALL EXIT
                  C
     104  10      FORMAT(///)
     105  20      FORMAT ('1')
     106          END
```

FIG. II

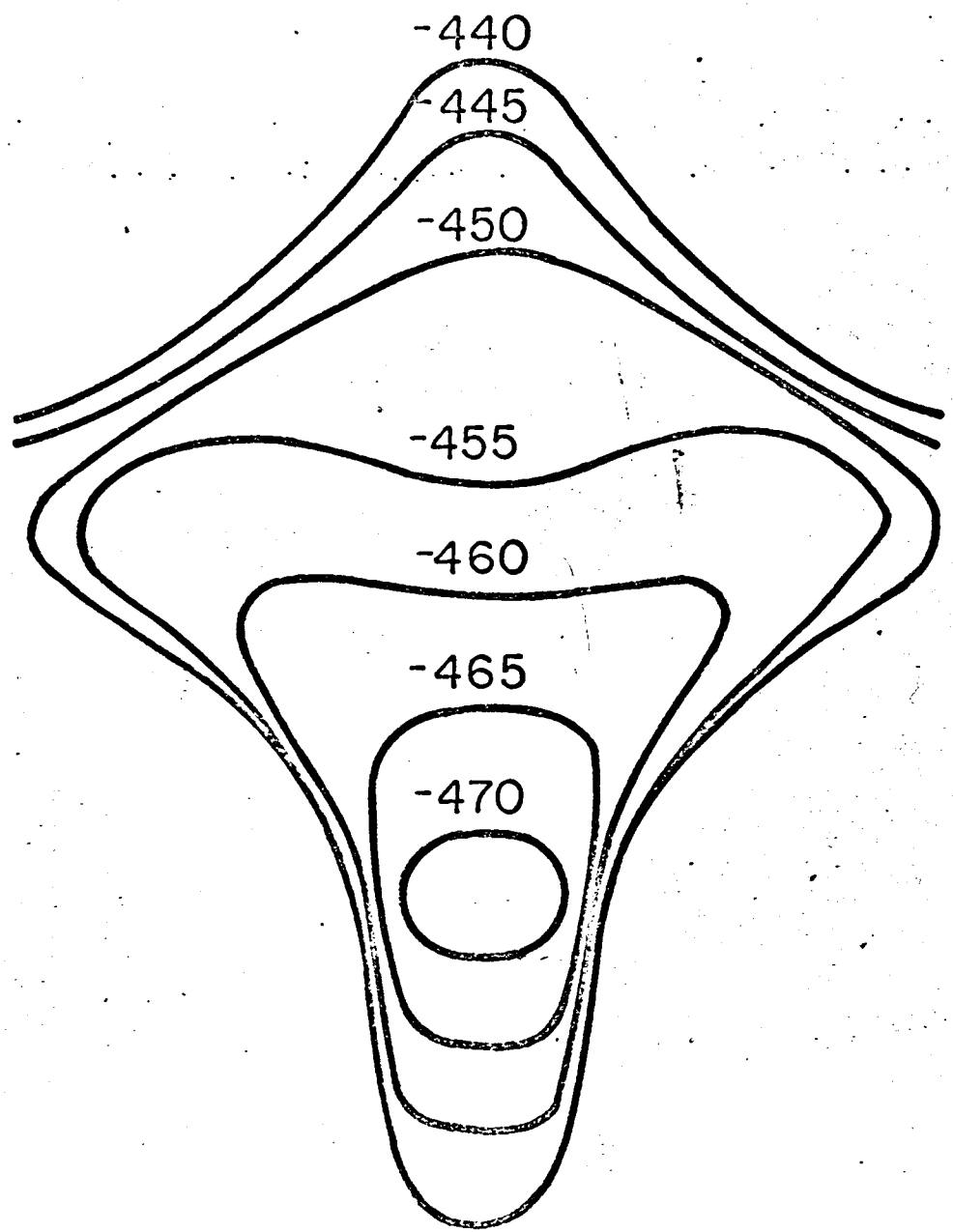

Fig. 3

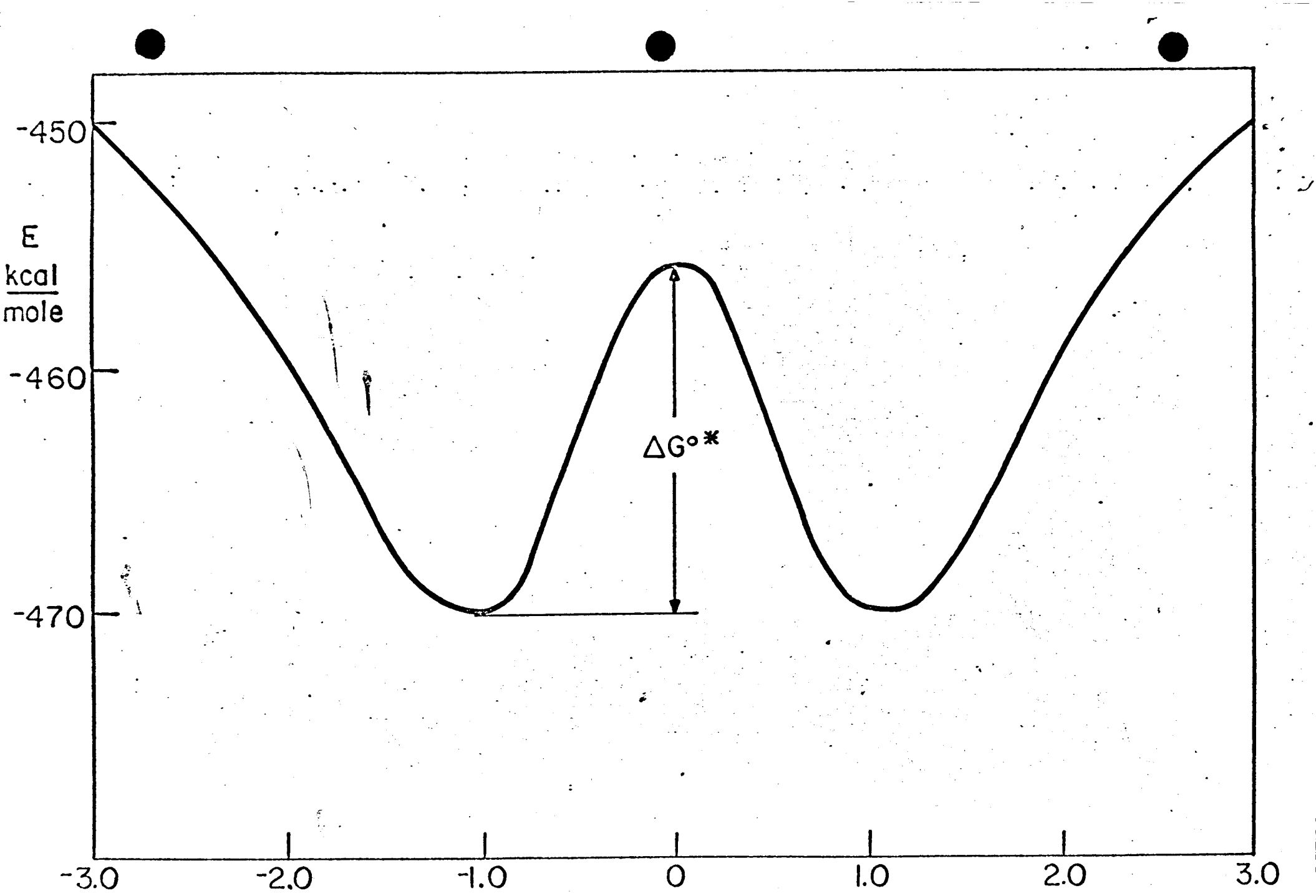

Fig.4

SECTION V. DENDRITE FORMATION ON ZINC ELECTRODE

The work of this section is being submitted as an appendix, a separately bound volume.

SECTION VI. REVERSIBILITY OF ORGANIC REACTIONS

A. Theoretical

1. The use of organic compounds in high energy secondary batteries

For a high energy battery system one desires a maximum number of electrons transferred at a maximum potential difference for a minimum weight of reactant. For the hydrogen oxygen cell two electrons are transferred for a molecular weight of 18. For an organic reaction a similar energy density may be obtained if one electron is transferred per carbon atom or its equivalent.

Some organic reactions are known to be electrochemically reversible (hydroquinone): other reactions, although not reversible in the kinetic sense, may be reversed electrochemically, as for example formate-methanol. Thus, in seeking high energy secondary batteries, organic reactions should also be considered.

2. Types of reactions desired

The type of reactions desired is that in which a large number of electrons are transferred for a reaction involving a relatively small molecule. A number of such reactions are summarized in Table 1. In choosing systems for investigation, one must also take into account the possibility of undesired side reactions (polymerization, cleavage) which prevent the reattaining of the initial compound.

TABLE 1. Theoretical ampere hour density for various reactions

Reaction	Ampere hours per pound	
	$R = CH_3$	$R = \phi$
$RNH_2 \rightleftarrows R{\equiv}N + 4H^+ + 4e^-$	1620	---
$R(NH_2)_3 + 6H_2O \rightleftarrows R(NO_2)_3 + 18H^+ + 18e^-$	1340	980
$R(NH_2)_2 + 4H_2O \rightleftarrows R(NO_2)_2 + 12H^+ + 12e^-$	1230	840
$RCH_3 + 2H_2O \rightleftarrows R\text{-}COOH + 6H^+ + 6e^-$	1150	590
$RNH_2 + 2H_2O \rightleftarrows RNO_2 + 6H^+ + 6e^-$	1130	580
$RCH_2NH_2 + H_2O \rightleftarrows RCONH_2 + 4H^+ + 4e^-$	800	400
$RSH + 3H_2O \rightleftarrows RSO_3H + 6H^+ + 6e^-$	740	460
$R_2S + 2H_2O \rightleftarrows R_2SO_2 + 4H^+ + 4e^-$	510	227
$Pb + 2H_2O \rightleftarrows PbO_2 + 4H^+ + 4e^-$	208	
$Ag + H_2O \rightleftarrows AgO + 2H^+ + 2e^-$	200	
$Hg + H_2O \rightleftarrows HgO + 2H^+ + 2e^-$	116	

3. Modification of reaction rates

With organic reactions one has the possibility of tailoring the compound to give desired properties. Thus by adding suitable substituents the kinetics of reactions may be greatly changed. This is not a hypothetical possibility but has been shown to be a real effect. This is shown in the frequent use of the modified Hammett equation.

$$E_{\frac{1}{2}} = \rho\sigma_x + E'_{\frac{1}{2}}$$

where $E_{\frac{1}{2}}$ is the half wave potential, ρ is a constant for the reacting group, σ_x is the total polar constant characteristic of the nature and position of the substituent and $E'_{\frac{1}{2}}$ is a constant. This relation has been shown to be followed in a number of reduction reactions. As an example, let us consider the reduction of aromatic aldehydes. In Table 2 the dependence of $E_{\frac{1}{2}}$ on substituent is given. The change in $E_{\frac{1}{2}}$ is about 0.2 V which, assuming a 2RT/F Tafel slope, is two orders of magnitude. A general trend for a more positive $E_{\frac{1}{2}}$ with the more negative values of σ is evident.

Such changes might be attributed to changes in the reversible potential for the reaction. Unfortunately, tabulations of the thermodynamic data for these systems are not available. However, data for the reversible potential of the nitroso-hydroxylamine couple for a number of substituents are available (Table 3). It is apparent that the changes in reversible potential are much smaller than the changes in $E_{\frac{1}{2}}$. Here again, a fairly systematic variation of E^0 with σ is evident.

TABLE 2. Effect of substituents on $E_{\frac{1}{2}}$ for benzyldehyde at pH 1.4 in 33% ethanol

R	1 $E_{\frac{1}{2}}$	2 σ
OH	-0.56	-0.357
$N(CH_3)_2$	-0.63	-0.600
H	-0.64	0
CH_3	-0.66	-0.170
C_2H_5	-0.66	-0.151
C_4H_9	-0.67	-0.161
C_3H_7	-0.70	-0.268
OCH_3	-0.72	-0.268

TABLE 3. The reversible potentials for the substituted nitrosobenzene-hydroxylamine couple

R	E^{0} [3]	σ [2]
4-$COOC_2H$	0.613	0.522
3-Cl	0.583	0.373
H	0.582	0
3-CH_3	0.579	-0.069
4-Cl	0.576	0.227
3-OCH_3	0.573	-0.115
4-CH_3	0.567	-0.170
4-OCH_3	0.554	-0.268

For a variation of substituents given in Table 2 on the half wave potential for the reduction of benzaldehyde, only two orders of magnitude variation in reduction rate was found. Since the reaction is very irreversible, an increase in rate of many orders of magnitude is required to make it reversible. When heterocyclic aldehydes are considered, a much larger variation in $E_{\frac{1}{2}}$ results (Table 4). Here a variation of 1.05 V has been observed. Again assuming a 2RT/F Tafel dependence, this corresponds to a change in rate of nine orders of magnitude. With the more active rings, the reduction reaction approaches reversibility.

For the oxidation of the reduced compound, the picture is not clear. Relatively little work has been done on the anodic reaction when compared to the reductions at the dropping mercury electrode. A simple interpretation of the dependence of half wave potentials on substituents is that electron withdrawing groups promote the reduction. On this basis for oxidation reactions, the converse should be true. Some evidence[4,5] indicates that this is true. However, if a reaction can only be made reversible in the cathodic direction, by the principle of microscopic reversibility, it must also be reversible in the anodic direction. Thus a truly reversible system would be expected. The apparent contradiction here may be resolved when one considers that substituents have effects other than electron donating or withdrawing. These include steric and mesomeric contributions. As an example, where the $E_{\frac{1}{2}}$ was made more anodic with a concurrent decrease in the potential of oxidation at Pt the oxidation and reduction of the cyanines may be considered.[7] With an

TABLE 4. Half wave potentials for reduction of some heterocyclic aldehydes

Aldehyde	$E_{\frac{1}{2}}$	pH
2-furanaldehyde	-1.33	3.6
benzaldehyde	-1.03	3.0
2-thiophene aldehyde	-0.55	3.6
2-pyrrol aldehyde	-0.95	3.1
2-pyridene aldehyde	-0.44	2.0
2-thiazole aldehyde	-0.40	2.0
2-quinoline aldehyde	-0.28	3.0

increase in the number of methylene groups separating the rings from one to seven, the $E_{\frac{1}{2}}$ increased by 0.72 V with the oxidation potential decreased by 1.01 V. Thus it is possible to simultaneously increase both cathodic and anodic rate constants. Thus, the concept of tailoring compounds with the desired redox properties has some confirmation by experiment.

4. Suggested future work

For future work the oxidation kinetics for a system known to be relatively rapid for reduction will be studied to determine if the rate of reduction is increased. The system to be studied in the immediate future will be the substituted pyridines, e.g., the system of 4-COOH, 4-CHO, 4-CH_2OH, 4-CH_3 attached to a pyridine ring. The oxidation and reduction kinetics for each stage of the reaction will be determined so that a comparison with the benzene analog may be made.

Further future work will be done with other compounts and with different electrodes.

B. Results and Discussion

1. Compounds studied

During the last period of time we have investigated the following organic compounds by means of the potential sweep method:

10^{-2} M benzenehexol, $C_6(OH)_6$, in 0.1 N H_2SO_4 at Pt electrode

10^{-2} M benzenehexol, $C_6(OH)_6$, in 1.0 N H_2SO_4 at Pt electrode

10^{-2} M cyclohexanehexone, C_6O_6, in 0.1 N NaOH at Pt and Hg electrode

$5 \cdot 10^{-2}$ M C_6O_6 in 0.1 N NaOH at Hg electrode

10^{-3} M C_6O_6 in 0.1 N H_2SO_4 and 1.0 N H_2SO_4 at Hg electrode

10^{-3} M rhodizonic acid, $C_6H_2O_6$, in 1.0 N H_2SO_4 at Hg electrode

10^{-3} M tetrahydroxy-1, 4-quinone, $C_6H_4O_6$, in 1.0 N H_2SO_4 at Pt electrode

10^{-2} M ethyl sulfone, Et_2SO_2, in 0.1 N H_2SO_4 at Hg electrode

10^{-2} M tetramethylene sulfone, $TMSO_2$, in 0.1 N H_2SO_4 at Hg electrode

10^{-2} M tetramethylene sulfoxide, TMSO, in 0.1 N H_2SO_4 at Hg electrode

10^{-2} M 2, 3 dimethyl-1, 4-benzoquinone diazine in 0.1 N H_2SO_4 at Hg electrode

10^{-2} M 2, 3 dimethyl-1, 4-benzoquinone diazine in 1.0 N H_2SO_4 at Hg electrode

10^{-3} M 2, 3 dimethyl-1, 4-benzoquinone diazine in 1.0 N H_2SO_4 at Pt electrode

(After polarization at -600 mV (Hg electrode) vs. SCE during 6 hours.)

10^{-2} M formaldehyde in 0.1 N NaOH at Hg electrode

10^{-1} M formic acid in 0.1 N NaOH at Hg electrode.

2. Cyclic hydroxy ketone

The electroöxidation of $C_6(OH)_6$ (benzenehexol) in 0.1 N and 1.0 N H_2SO_4 at Pt electrode occurs with three well expressed peaks in the potential range between 135 and 700 mV vs. SCE in course of a different sweep rate (4-900 mV/s). See Table 5.

The analysis of recorded curves shows that current peak dependence on the sweep rate at the potential of the first peak is close (Fig. 1). to the

TABLE 5. Peaks potential values, V_p, for the investigated $C_6(OH)_6 \rightarrow C_6O_6$ series*

$C_6(OH)_6$			$C_6O_2(OH)_4$		$C_6O_4(OH)_2$	C_6O_6	Sweep rate
I	II	III	I	II			$\frac{mV}{s}$
	peak			peak			
	Oxid., Pt el.		Oxid., Pt el.		Red. Hg el.	Red. Hg el.	
135	400	710	340	680	-660	-800	4
165	445	640	390	700	-705	-840	25
170	465	650	400	720	-720	-860	50
185	480	660	400	730	-740	-900	100
200	495	670	420	750	-770	-900	225
205	520	670	420	750	-780	-900	325
230	520	680	420	760	-785	-920	400
285	540	690	460	770	-800	-940	625
350	600		465	780	-790	-920	900

*All potentials are in mV vs. SCE.

values calculated for the totally irreversible diffusion-controlled reaction according to the equation derived by Delahay.[8]

$$i_p = 3{,}01 \times 10^5 n(\alpha n_a)^{\frac{1}{2}} A D_0^{\frac{1}{2}} C_0 v^{\frac{1}{2}}$$

where n is the number of electrons transferred in overall reaction and αn_a is obtained from the conventional Tafel slope:

$$\frac{dV}{d \log i} = \frac{2.3RT}{\alpha n_a F} ,$$

A is area of electrode in cm^2 and v is sweep rate in volt/sec.

The value αn_a may be determined from the slope of the line which is obtained by plotting peak potential V_p vs. sweep rate. The slope, $\frac{dV_p}{d \log v}$, is equal to $\frac{2.3RT}{2F\alpha n_a}$, and in the above case was 40 mV for the sweep rate 4-400 mV/s.

According to the experimental data the number of electrons, n, transferred during the first reaction step was two. This indicates that reaction of electrooxidation of $C_6(OH)_6$ proceeds most probably in three steps to the C_6O_6 compound, each step including 2-electron transfer according to the scheme:

$$C_6(OH)_6 \rightarrow C_6O_2(OH)_4 + 2H^+ + 2e^-$$

$$C_6O_2(OH)_4 \rightarrow C_6O_4(OH)_2 + 2H^+ + 2e^-$$

$$C_6O_4(OH)_2 \rightarrow C_6O_6 + 2H^+ + 2e^-$$

From the experimentally observed Tafel slope which is in the case of 10^{-2} M $C_6(OH)_6$ in 1.0 N H_2SO_4 equal to $2RT/3F$, it is possible to

make conclusions about the mechanism of reaction in the first reduction step.

While $\frac{2RT}{3F} = \frac{RT}{F(n + \beta n_a)}$, where n is the number of electrons transferred before the rate determining step, n_a is the rate determining step, and $\beta = \frac{1}{2}$, n has to be 1 and n_a also 1, or the reaction proceeds with a transfer of one electron overall, and one in the rate determining step.

So, the mechanism could be:

$$C_6(OH)_6 \rightleftarrows C_6O(OH)_5 + H^+ + e^-$$

$$C_6O(OH)_5 \rightleftarrows C_6O_2(OH)_4 + H^+ + e^-$$

Unfortunately, no quantitative relationship for second (or any farther) peak current has been derived thus far in the case of consecutive peak current.

Peak current, i_p, for the same concentration of $C_6(OH)_6$ in the more diluted supporting electrolyte (0.1 N H_2SO_4 instead of 1.0 N) shows the lower values, most probably due to the bigger resistive drop in the solution.

The electroreduction of 10^{-3} M C_6O_6 in 0.1 N and 1.0 N H_2SO_4 at Hg electrode proceeds in only one step. Peak potential V_p changes between -790 and -1015 mV (0.1 N H_2SO_4) and between -800 and -920 (1.0 N H_2SO_4) vs SCE in dependence on sweep rate (4-900 mV/s). The slope of the recorded i-V curve is not well reproducible. The $\frac{dV_p}{d \log V}$ value is between 75 and 107 mV; n calculated from experimental data

is less than 1 and the curve which represents i_p dependence on sweep rate lies below the curve calculated for the totally irreversible process (Fig. 2).

Peak potentials are very close to the potential of hydrogen evolution, and it is very possible that these two reactions interfere.

The electroreduction of C_6O_6 in alkaline solution (0.1 NaOH) at Pt and Hg electrodes respectively does not give good reproducibility. This may be due to the process of decomposition or polymerization of compound in alkaline media. The process of decomposition proceeds with a change in color and is faster in more concentrated solutions.

To obtain more information about the reaction path $C_6(OH)_6 \rightarrow C_6O_6$ we have investigated intermediate compounds, rhodizonic acid, $C_6C_4(OH)_2$, and tetrahydroxy-1, 4-quinone, $C_6O_2(OH)_4$.

The reduction of 10^{-3} M rhodizonic acid in 1.0 N H_2SO_4 at Hg proceeds in one step. The peak is well expressed and appears at potential between -660 and -790 mV vs. SCE (in dependence of sweep rate), or 140 mV more positive than in the case of reduction C_6O_6 (see Table 1). A quantitative interpretation of i_p and V_p values shows that this reduction proceeds again in an irreversible manner with 4-electron exchange (Fig. 3).

The electrooxidation of 10^{-3} M tetrahydroxy-1, 4-quinone in 1.0 N H_2SO_4 at Pt electrode occurs in two step reactions, as was expected. The first is, according to the quantitative analysis, an irreversible one (Fig. 4). The Tafel slope in this peak is close to 40 mV or $\frac{2RT}{3F}$, as in the case of

the first step reaction in reduction of $C_6(OH)_6$. The n and n_a values are again 1 , and the following reduction mechanism for this step may be assumed:

$$C_6O_2(OH)_4 \rightleftharpoons C_6O_3(OH)_3 + H^+ + e^-$$

$$C_6O_3(OH)_3 \rightleftharpoons C_6O_4(OH)_2 + H^+ + e^-$$

The investigation of electroöxidation of $C_6O_4(OH)_2$ and electroreduction of $C_6O_2(OH)_4$ are necessary to complete the knowledge about the mechanism of reduction and oxidation in the organic couple $C_6(OH)_6 \rightarrow C_6O_6$.

3. Sulfoxides and sulfones

In the case of electroduction of 10^{-2} M Et_2SO_2 in 0.1 N H_2SO_4 at Pt electrode, no peaks, no waves, on the i-V were obtained which could indicate any process. This is in agreement with previously done potentiometric measurements, although on the basis of the potentiometr c measurements, it was not clearly evident.

The i-V curves recorded in the course of electroreduction of 10^{-2} M TM sulfone in 0.1 N H_2SO_4 at Hg electrode with different sweep rate show well expressed peak followed by two smaller in cathodic and one peak in anodic region. The difference between the first cathodic peak and anodic peak with some potential sweep rate (between 200 and 600 mV/s) satisfied the condition

$$E\rho_{cathode} - E\rho_{anode} = \frac{2 \times 0.028}{n} [V]$$

for $n = 1$ or 2, i.e., the difference is 30-60 mV. However, the experimental i_p current is much smaller than it should be according to the concentration of the sulfone, and n calculated according to the equation for reversible process

$$i_p = 2.72 \cdot 10^5 n^{\frac{2}{3}} A D_0^{\frac{1}{2}} C_0 v^{\frac{1}{2}}$$

is less than 1. It is obvious that the peak which appeared on i-V curves during the single sweep on electrodes is due to deduction of some unidentified compound, which corresponds to an impurity concentration.

The electroreduction of TM sulfoxide in 0.1 N H_2SO_4 at Hg electrode does not occur, as in the case of sulfone, on the recorded i-V curves appears one reversible peak but peak current is at 10% of current that should be according to the TM sulfoxide concentration. This peak has to be due to some uncertain impurity in the TM sulfoxide.

4. Dimethyl benzoquinone diazine

The investigation of 10^{-2} and 10^{-3} M 2, 3 dimethyl-1, 4-benzoquinone diazine in 0,1 and 1.0 N H_2SO_4 at Hg electrode shows that reduction of the compound proceeds in three steps. The first peak is at -370 mV, the second at about -580, and the last at -1050 mV vs SCE (with 250 mV/s), while in the anodic region (reverse sweep direction) only one peak appears.

The place of the first peak does not change with sweep rate, which is an indication of a reversible process. The plot of the peak current experimentally obtained as a function of sweep rate lies between the

curves calculated for 1 and 2 electron transferred reversible process (Fig. 5).

After polarization at -600 mV vs SCE for several hours, the first two peaks disappear (compound was reduced) and investigation was continued in the same solution at Pt. In the anodic region we now obtain two peaks, the first of which varies from +260 to 360 mV (at different sweet rate), followed by one well expressed peak in cathodic region (opposite sweep direction).

A quantitative analysis of the first anodic peak shows that it corresponds to an irreversible electrode process, with two electrons transferred (Fig. 6).

5. Formic acid and formaldehyde

Investigation of the couple formic acid-formaldehyde is still proceeding. From preliminary work, the electroreduction of 10^{-1} M formic acid in 0.1 N NaOH at Hg electrode does not proceed, while the electroöxidation of 10^{-2} M formaldehyde in the same supporting electrolyte at Hg electrode occurs with one well expressed peak at the potential of about -1600 mV vs SCE,

REFERENCES

1. I. M. Kolthoff and J. J. Lingane, Polarography, Interscience, New York (1952), 682.

2. H. M. Jaffe, Chem. Rev., 53, 191 (1953).

3. W. M. Clark, Oxidation-Reduction Potentials of Organic Systems, Williams and Wilkins, Baltimore (1960), 434.

4. H. N. Simson, L. K. Nancock, and E. A. Meyers, J. Org. Chem., 30, 2578 (1965).

5. A. Zweig, W. G. Hodgson, and W. A. Jura, J. Amer. Chem. Soc., 86, 4124 (1964).

6. J. Volke, Physical Method in Heterocyclic Chemistry, Ed. A. R. Katritzky, Academic Press, New York and London (1963), Vol. 1, Chapter 6.

7. A. Stanienda, Naturwissenschaften, 47, 512 (1960).

8. P. Delahay, New Instrumental Methods in Electrochemistry, Interscience, New York (1954).

FIGURE CAPTIONS

Fig. 1 Peak current dependence on the sweep rate for the electroöxidation of 10^{-2} M $C_6(OH)_6$ in 1.0 N and 0.1 N H_2SO_4 at Hg electrode:

o experimental values

□ calculated values

Fig. 2 Peak current dependence on the sweep rate for the electroreduction of 10^{-3} M C_6O_6 in 1.0 N H_2SO_4 at Hg electrode:

o experimental values

□ calculated values

Fig. 3 Peak current dependence on the sweep rate for the electroreduction of 10^{-3} M $C_6O_4(OH)_2$ in 1.0 N H_2SO_4 at Hg electrode:

o experimental values

□ calculated values

Fig. 4 Peak current dependence on the sweep rate for the electroöxidation of $C_6O_2(OH)_4$ in 1.0 N H_2SO_4 at Pt electrode:

o experimental values

□ calculated values

Fig. 5 Peak current dependence on the sweep rate for the electroreduction of 10^{-3} M 2, 3-dimethyl-1, 4-benzoquinone diazine in 1.0 N H_2SO_4 at Hg electrode:

o experimental values

□ calculated values

Fig. 6 Peak current dependence on the sweep rate for electroöxidation reduced form of 10^{-3} M 1, 2-dimethyl-3, 4-benzoquinone diazine in 1.0 N H_2SO_4 at Pt electrode:

o experimental values

□ calculated values

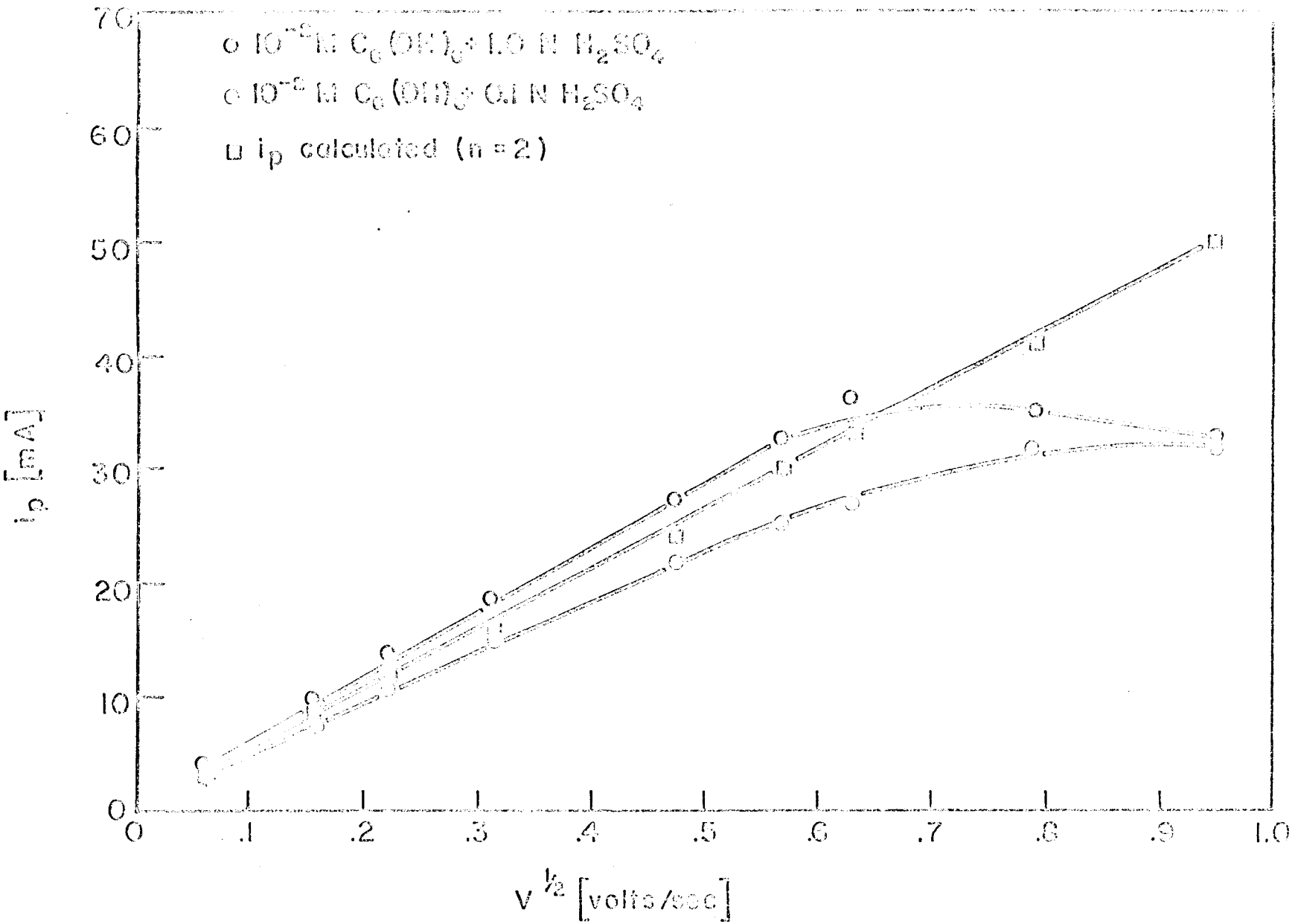
o 10^{-2} M $Co(OH)_2$ + 1.0 N H_2SO_4
o 10^{-2} M $Co(OH)_2$ + 0.1 N H_2SO_4
□ i_p calculated (n = 2)
i_p [mA]
70
60
50
40
30
20
10
0
0
.1
.2
.3
.4
.5
.6
.7
.8
.9
1.0
$V^{1/2}$ [volts/sec]

FIG. 1

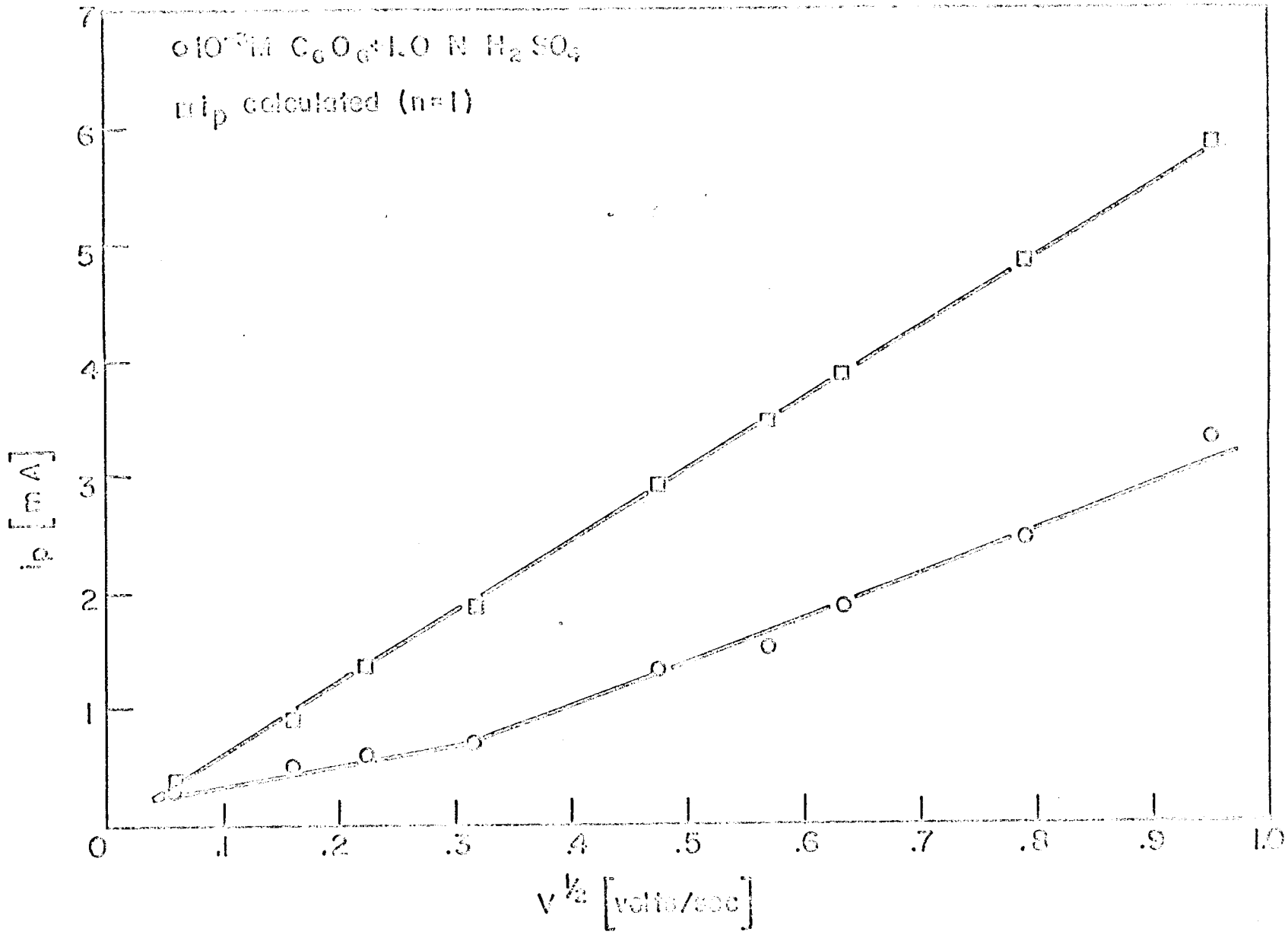
o 10^{-3} M C_6O_6 + 1.0 N H_2SO_4
□ i_p calculated (n=1)
i_p [μA]
$V^{1/2}$ [volts/sec]
0
1
2
3
4
5
6
7
.1
.2
.3
.4
.5
.6
.7
.8
.9
1.0

FIG. 2

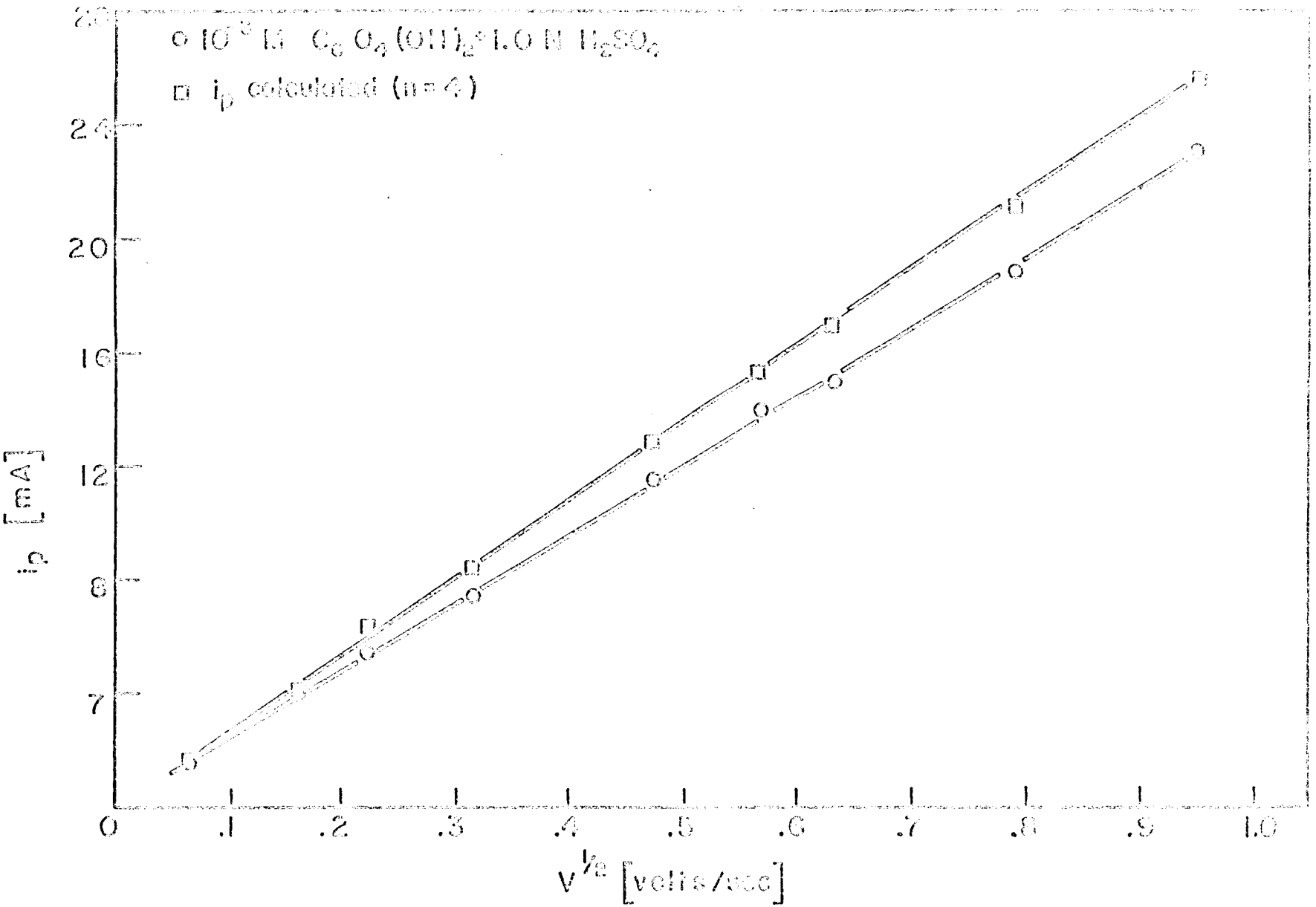
o 10^{-3} M $C_6O_4(OH)_2$ 1.0 N H_2SO_4
□ i_p calculated (n = 4)
i_p [mA]
$V^{1/2}$ [volts/sec]
0
.1
.2
.3
.4
.5
.6
.7
.8
.9
1.0
7
8
12
16
20
24

FIG. 3

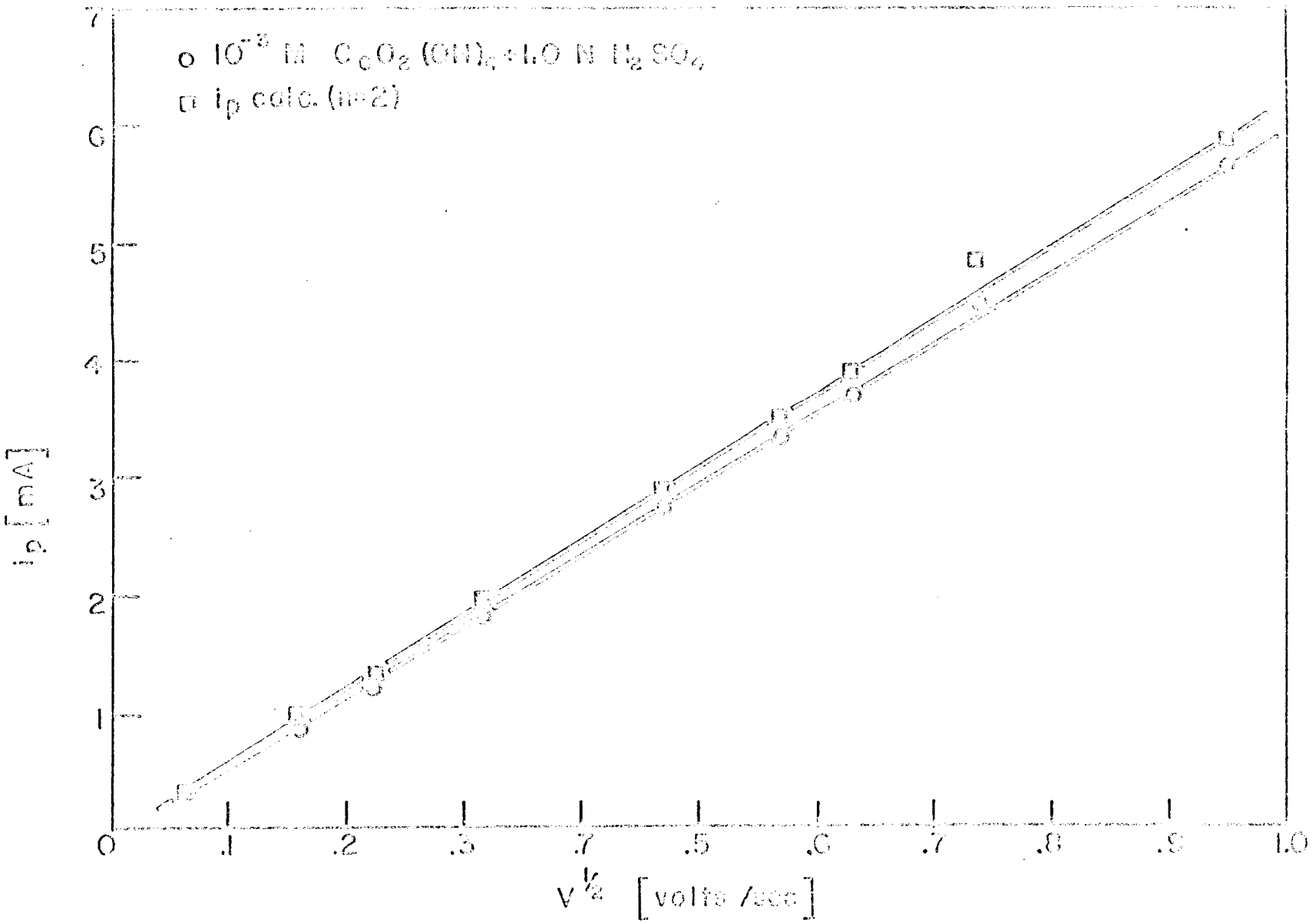
o 10^{-3} M $C_6O_2(OH)_2$ + 1.0 N H_2SO_4
□ i_p calc. (n=2)
i_p [mA]
0
1
2
3
4
5
6
7
.1
.2
.3
.4
.5
.6
.7
.8
.9
1.0
$V^{1/2}$ [volts /sec]

FIG. 4

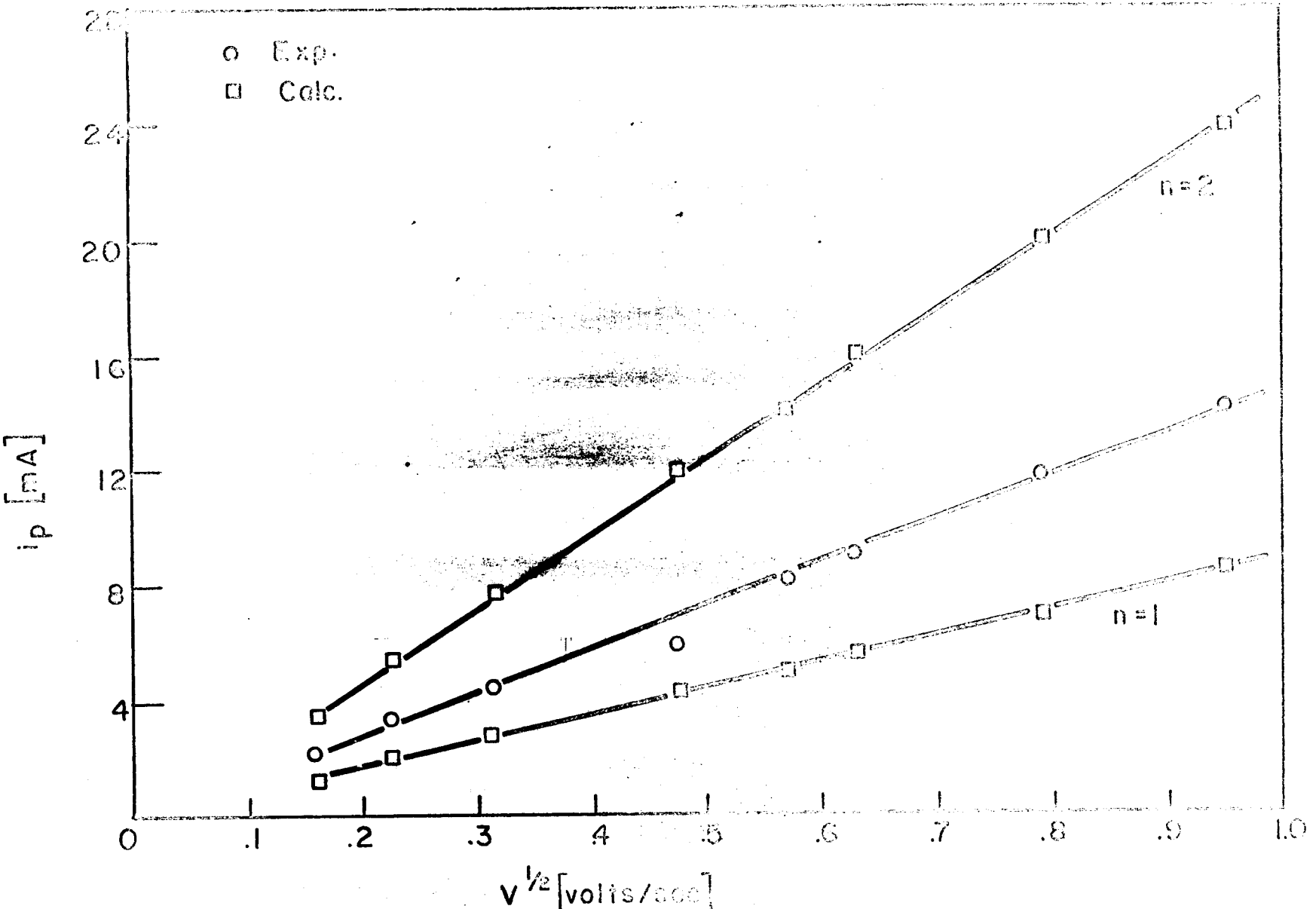

FIG. 5

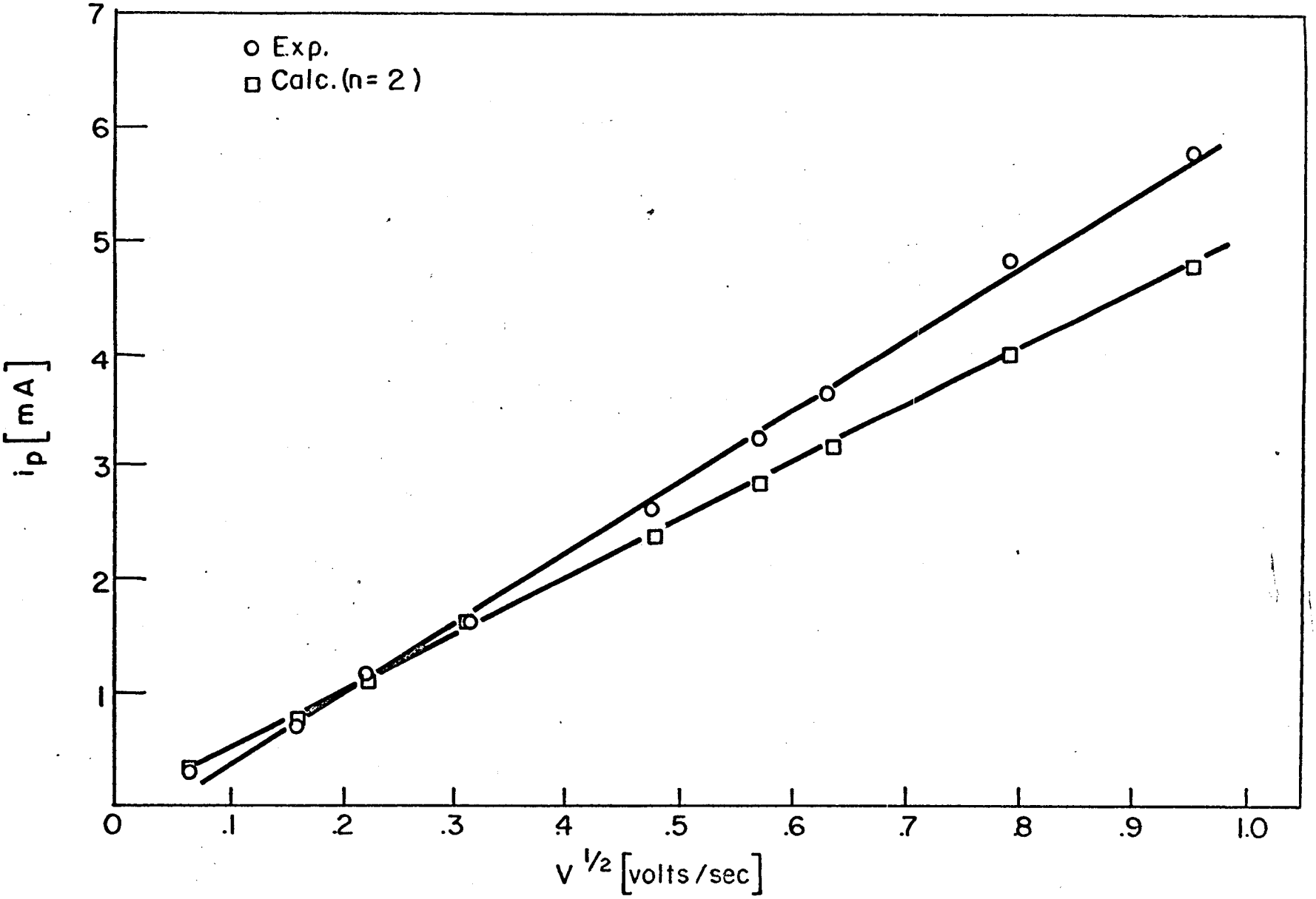

FIG. 6

SECTION VII. THE THEORY OF ELECTROCHEMICAL ENERGY CONVERSION

The book with Dr. Srinivasan (McGraw-Hill) continues to make good progress. All chapters have been submitted to the publishers, though a few references and diagrams are still missing. The publication date is Fall 1968.

SECTION VIII. MODERN ELECTROCHEMISTRY: AN INTERDISCIPLINARY APPROACH

Dr. Reddy returned to India on November 25. Finishing of editing of book being carried out by Dr. Halina Wroblowa, Professor A. Despic, Dr. C. Solomons, and Mr. J. Diggle. This editing consists largely of taking into account the various criticisms, amendments, etc., from the Bermuda conference.

Chapters 1-5 are with the publishers. Chapter 6 on molten salts being edited by Dr. C. Solomons, promised by end of December, 1967. Chapter 7, typed and has to be proofread. Chapter 8, awaits typing in final form. Chapter 9, awaits typing in final form. Chapter 10, electrocatalysis section has to be rewritten in view of completely new interpretations and results obtained by Mannan, on NASA contract. Rewriting being done by Bockris and Wroblowa. Chapter 11 to be edited by Despic, completed by February 1.

After all the chapters have been sent to the publishers, there will be a pause until the galley proofs come through. Each chapter in galley proof will be sent to an independent referee for assessment of any remaining errors and suggestions of latest material.

IX. PUBLICATIONS UNDER GRANT NsG-325

1964

1. Forces involved in the specific adsorption of ions on metals from aqueous solution, J. O' M. Bockris and T. Anderson, Electrochimica Acta, 9, 347 (1964).

2. Electrochemical kinetics of parallel reactions, E. Gileadi and S. Srinivasan, J. Electroanal. Chem., 7, 452-457 (1964).

3. Electrocatalysis, J. O' M. Bockris and H. Wroblowa, J. Electroanal. Chem., 7, 428-451 (1964).

4. Basis of possible continuous self activation in an electrochemical energy converter, J. O' M. Bockris, B. J. Piersma, E. Gileadi, and B. D. Cahan, J. Electroanal. Chem., 7, 487-490 (1964).

5. Ellipsometry in electrochemical studies, A. K. N. Reddy and J. O' M. Bockris, U. S. Dept. Comm. Natl, Bureau of Standards, Misc. Publication 256, Sept. 15, 1964, 229-244.

6. Ellipsometric study of oxygen-containing films on platinum electrodes. A. K. N. Reddy, M. Genshaw, and J. O' M. Bockris, J. Electroanal. Chem., 8, 406-407 (1964).

1965

7. Ellipsometric determination of the film thickness and conductivity during the passivation process on nickel, A. K. N. Reddy, M. G. B. Rao, and J. O' M. Bockris, J. Chem. Phys., 42, 6, 2246-2248, 15 March 1965.

8. A brief outline of electrocatalysis, J. O' M. Bockris and S. Srinivasan, 19th Annual Proceedings Power Sources Conference, May 1965.

9. Proton transfer across double layers, J. O' M. Bockris, S. Srinivasan, and D. B. Matthews, Disc. Faraday Soc., No. 39, 1965.

10. Fundamental studies of the mechanism of porous electrodes, J. O' M. Bockris, L. Nanis, and B. D. Cahan, J. Electroanal. Chem., 9, 474-476 (1965).

1966

11. The potential of zero charge on Pt and its pH dependence, E. Gileadi, S. D. Argade, and J. O' M. Bockris, J. Phys. Chem., 70, 2044 (1966).

12. The potential sweep method: a theoretical analysis, S. Srinivasan and E. Gileadi, Electrochim. Acta, 11, 321-335 (1966).

13. Electrode kinetic aspects of electrochemical energy conversion, J. O' M. Bockris and S. Srinivasan, J. Electroanal. Chem., 11, 350-389 (1966).

14. An ellipsometric determination of the mechanism of passivity of nickel, J. O' M. Bockris, A. K. N. Reddy, and B. Rao, J. Electrochem. Soc., 113, 11, 1133-1144 (1966).

1967

15. Electrocatalysis in ethylene oxidation, A. Kuhn, H. Wroblowa, and J. O' M. Bockris, Trans. Faraday Soc., 63, 1458 (1967).

16. Electrosorption, edited by E. Gileadi, Plenum Press, 1967.

17. Theory of porous gas diffusion electrodes using the thin film model, S. Srinivasan and H. D. Hurwitz, Electrochim. Acta, 12, 495 (1967).

18. Potential of Zero Charge, S. D. Argade and E. Gileadi, in Electrosorption (Ed. by E. Gileadi, Plenum Press, 1967).

19. Fundamental equations of electrochemical kinetics at porous gas-diffusion electrodes, S. Srinivasan, H. D. Hurwitz, and J. O' M. Bockris, J. Chem. Phys., 46, 3108 (1967).

20. Dependence of the rate of electrodic redox reactions on the substrate, R. J. Mannan, A. Damjanovic, and J. O' M. Bockris, J. Chem. Phys., (February 1968).

The following are in course of publication:

21. An ellipsometric study of oxide films on platinum in acid solutions, J. O' M. Bockris, A. K. N. Reddy, and M. Genshaw.

22. Chapter on Electrochemical Techniques in Fuel Cell Research, to be published in Handbook on Fuel Cell Technology, edited by C. Berger, Prentice Hall.

23. On a comparison of techniques for measuring the adsorption of organic materials on electrodic catalysts, L. Duic and J. O' M. Bockris.

OFFICIAL DISTRIBUTION LIST
FOR FUEL CELL REPORTS

July 12, 1967

NASA and JPL

National Aeronautics & Space Admin.
Scientific and Technical Information
Facility
College Park, Maryland 20740
Attn: NASA Representative
Send 2 copies plus 1 reproducible

National Aeronautics & Space Admin
Washington, D C 20546
Attn: RNW/E. M. Cohn

National Aeronautics & Space Admin
Washington, D. C. 20546
Attn: FC/A. M Greg Andrus

National Aeronautics & Space Admin.
Goddard Space Flight Center
Greenbelt, Maryland 20771
Attn: Thomas Hennigan, Code 716.2

National Aeronautics & Space Admin
Langley Research Center
Langley Station
Hampton, Virginia 23365
Attn: John Patterson

National Aeronautics & Space Admin.
Lewis Research Center
21000 Brookpark Road
Cleveland, Ohio 44135
Attn: Mr. Robert Miller

National Aeronautics & Space Admin.
Washington, D.C. 20546
Attn: Office of Technology Utilization

National Aeronautics & Space Admin.
Lewis Research Center
21000 Brookpark Road
Cleveland, Ohio 44135
Attn. M. J. Saari, MS 500-202

National Aeronautics & Space Admin.
Lewis Research Center
21000 Brookpark Road
Cleveland Ohio 44135
Attn. Mr N. D Sanders

National Aeronautics & Space Admin.
Marshall Space Flight Center
Huntsville, Alabama 35812
Attn: Mr Richard Boehme
R-ASTR-E

National Aeronautics & Space Admin
Marshall Space Flight Center
Huntsville Alabama 35812
Attn: Mr Charles Graff
R-ASTR-EAP

National Aeronautics & Space Admin.
Ames Research Center
Pioneer Project
Moffett Field California 94035
Attn. Mr Jon Rubenzer

National Aeronautics & Space Admin
Manned Spacecraft Center
Houston, Texas 77001
Attn: Mr William R Dusenbury

National Aeronautics & Space Admin.
Manned Spacecraft Center
Houston Texas 77001
Attn Mr Hoyt McBryar
EP-5 Building 16

National Aeronautics & Space Admin.
Manned Spacecraft Center
Houston Texas 77001
Attn: Mr Forrest Eastman

National Aeronautics & Space Admin.
Electronics Research Center
575 Technology Square
Cambridge, Mass. 02139
Attn: Dr. Sol Gilman

Jet Propulsion Laboratory
4800 Oak Grove Drive
Pasadena, California 91103
Attn: Mr. Aiji Uchiyama

Department of the Army

U. S. Army Engineer R&D Labs.
Fort Belvoir, Virginia 22060
Attn: Energy Conversion
Research Lab.

Commanding General
U. S. Army Electronics R&D Labs
Attn: Code AMSEL-KL-P
Fort Monmouth, New Jersey 07703

Harry Diamond Labs.
Room 300, Building 92
Conn. Ave. & Van Ness Street, N. W.
Washington, D. C. 20438
Attn: Mr. Nathan Kaplan

U. S. Army Natick Laboratories
Clothing & Organic Materials Div.
Natick, Massachusetts 01760
Attn: Leo A. Spano

Department of the Navy

Office of Naval Research
Department of the Navy
Washington, D. C. 20300
Attn: Dr. Ralph Roberts/H. W. Fox

U. S. Naval Research Laboratory
Washington, D. C. 20390
Attn: Dr. J. C. White
Code 6160

Commander, Naval Ship System Command
Department of the Navy
Washington, D. C. 20350
Attn: Mr. Bernard B. Rosenbaum

Commander, Naval Ship System Command
Department of the Navy
Washington, D. C. 20350
Attn: Mr. C. F. Viglotti

Naval Ordnance Laboratory
Department of the Navy
Corona, California 91720
Attn: Mr. William C. Spindler
Code 441

Naval Ordnance Laboratory
Silver Spring, Maryland 20910
Attn: Mr. Philip B. Cole
Code 232

U. S. Navy Marine Engineering Lab.
Special Projects Division
Annapolis, Maryland 21402
Attn: J. H. Harrison

Department of the Air Force

Wright-Patterson AFB
Aeronautical Systems Division
Dayton, Ohio 45433
Attn: James E. Cooper, APIP-2

AF Cambridge Research Lab.
Attn: CRE
L. G. Hanscom Field
Bedford, Massachusetts 01731
Attn: Francis X. Doherty
Edward Raskind (Wing F)

Rome Air Development Center
Griffiss AFB, New York 13442
Attn: Mr. Frank J. Mollura
(RASSM)

Other Government Agencies

Mr. Donald A. Hoatson
Army Reactor, DRD
U. S. Atomic Energy Commission
Washington, D. C. 20545

Office of Assistant Director
(USW & Battle Support System)
Defense Research & Engineering
3D-1048 Pentagon
Washington, D. C. 20301

Mr. D. Bienstock
Bureau of Mines
4800 Forbes Avenue
Pittsburgh, Penna., 15213

Private Organizations

Aeronutronic Division of Philco Corp.
Technical Information Services
Ford Road
Newport, California 92663

Allis-Chalmers Mfg. Co.
1100 S. 70th Street
Milwaukee, Wisconsin 53214
Attn: John W. McNeil
Mgr., Marketing Research Div.
#3349

American Cyanamid Company
1937 W. Main Street
Stamford, Connecticut 06901
Attn: Dr. R. G. Haldeman

American Machine & Foundry
689 Hope Street
Springdale,, Connecticut 06879
Attn: Dr. L. H. Shaffer
Research Division

Arthur D. Little, Inc.
Acorn Park
Cambridge, Mass., 02140
Attn: Dr. Ellery W. Stone

Aerospace Corp.
P. O. Box 95085
Los Angeles, California 90045
Attn: Tech. Library Acquisition Group

Atlantic Refining Co.
500 South Ridgeway Ave.
Glenolden, Penna. 19036
Attn: H. Shalit

Atomics International Division
North American Aviation, Inc.
8900 De Soto Avenue
Canoga Park, California 91304
Attn: Dr. H. L. Recht

Battelle Memorial Institute
505 King Ave.
Columbus, Ohio 43201
Attn: Dr. C. L. Faust

Bell Telephone Laboratories, Inc.
Murray Hill, New Jersey 07971
Attn: U. B. Thomas

ChemCell Inc.
150 Dey Road
Wayne, New Jersey 07470
Attn: Peter D. Richman

Clevite Corporation
Mechanical Research Division
540 East 105th Street
Cleveland, Ohio 44108
Attn: D. J. Berger

Consolidated Controls Corporation
15 Durant Avenue
Bethel, Connecticut 06801
Attn: Miss Carol R. Naas
(NsG-324 reports only)

G. & W. H. Corson, Inc.
Plymouth Meeting, Penna. 19462
Attn: Dr. L. J. Minnick

Douglas Aircraft Company, Inc.
Astropower Laboratory
2121 Campus Drive
Newport Beach, California 92663

Dynatech Corp.
17 Tudor Street
Cambridge, Mass. 02139
Attn: Dr. A. R. Reti

Electromite Corp.
562 Meyer Lane
Redondo Beach, Calif. 90278
Attn: R. N. Sparks

Electrochimica Corp.
1140 O'Brien Drive
Menlo Park, California 94025
Attn: Dr. Morris Eisenberg

Electro-Optical Systems, Inc.
300 North Halstead Street
Pasadena, California 91107
Attn: Martin Klein

Engelhard Industries, Inc.
497 Delancy Street
Newark, New Jersey -7105
Attn: Dr. J. G. Cohn

Esso Research and Engineering Co.
Government Division
P. O. Box 8
Linden, New Jersey 07036
Attn: Dr. C. E. Heath

The Franklin Institute
Philadelphia, Penna. 19103
Attn: Mr. Robert Goodman

Garrett Corporation
1625 Eye St., N. W.
Washington, D. C. 20013
Attn: Mr. Bowler

General Dynamics/Convair
P. O. Box 1128
San Diego, California 92112
Attn: Mr. R. P. Mikkelson
Electrical Systems Dept. 988-7

General Electric Company
Direct Energy Conversion Operation
930 Western Ave.
Lynn, Massachusetts 01901
Attn: P. Schratter

General Electric Company
Research & Development Center
P. O. Box 8
Schenectady, New York 12301
Attn: Dr. H. Liebhafsky

General Electric Company
777-14th St., N. W.
Washington, D. C. 20005
Attn: Philip C. Hargraves

General Motors Corp.
G. M. Technical Center
Warren, Michigan 48090
Attn: Library, Research Laboratories

Globe-Union, Inc.
P. O. Box 591
Milwaukee, Wisconsin 53201
Attn: J. D. Onderdonk
V. P., Marketing

Ionics, Incorporated
65 Grove Street
Watertown, Massachusetts 02172
Attn: Dr. Werner Glass

Institute for Defense Analyses
Research and Engineering Support Div.
400 Army-Navy Drive
Arlington, Virginia 22202
Attn: Dr. George C. Szego

Institute for Defense Analyses
Research & Engineering Support Div.
400 Army-Navy Drive
Arlington, Virginia 22202
Attn: Dr. R. Briceland

Institute of Gas Technology
State and 34th Streets
Chicago, Illinois 60616
Attn: Mr. B. S. Baker

Johns Hopkins University
Applied Physics Laboratory
8621 Georgia Avenue
Silver Spring, Maryland
Attn: Richard Cole

LTV Research Center
P. O. Box 5907
Dallas, Texas 75222
Attn: Madison Reed
(Contract W12, 300 only)

Johns-Manville R&E Center
P. O. Box 159
Manville, New Jersey 08835
Attn: J. S. Parkinson

Leesona Moos Laboratories
Lake Success Park
Community Drive
Great Neck, New York 11021
Attn: Dr. A. Moos

Livingston Electronic Corporation
Route 309
Montgomeryville, Penna. 18936

Lockheed Missiles & Space Company
Technical Information Center
3251 Hanover Street
Palo Alto, California

The Martin Co.
Electronics Research Department
P. O. Box 179
Denver, Colo. 80201
Attn: William B. Collins
Mail No. 1620

Midwest Research Institute
425 Volker Boulevard
Kansas City, Missouri
Attn: Physical Science Library

Monsanto Research Corporation
Boston Laboratories
Everett, Massachusetts 02149
Attn: Dr. J. O. Smith

Monsanto Research Corporation
Dayton Laboratory
Dayton, Ohio 45407
Attn: Librarian

North American Aviation Co.
S&ID Division
Downey, California 90241
Attn: Dr. James Nash

Oklahoma State University
Stillwater, Oklahoma 74075
Attn: Prof. William L. Hughes
School of Electrical Engineering

Power Information Center
University of Pennsylvania
3401 Market Street
Philadelphia, Penna, 19104

Radio Corporation of America
Astro Division
P. O. Box 800
Hightstown, New Jersey 08540
Attn: Dr. Seymour Winkler

Rocketdyne
6633 Canoga Avenue
Canoga Park, California 91304
Attn: Library, Dept. 086-306-Zone 2

Speer Carbon Company
Research & Development Laboratories
Packard Road at 47th Street
Niagara Falls, New York 14304
Attn: Dr. W. E. Parker

Stanford Research Institute
820 Mission Street
So. Pasadena, California 91108
Attn: Dr. Fritz Kalhammer

Texas Instruments, Inc.
P. O. Box 5936
Dallas, Texas 75222
Attn: Dr. Isaac Trachtenberg

TRW, Inc.
23555 Euclid Avenue
Cleveland, Ohio 44115
Attn: Dr. R.A. Wynveen

TRW Systems
One Space Park
Redondo Beach, California 90278
Attn: Dr. A. Krausz

Tyco Laboratories, Inc.
Bear Hill
Hickory Drive
Waltham, Massachusetts 02154
Attn: Dr. A.C. Makrides

Unified Science Associates, Inc.
826 S. Arroyo Parkway
Pasadena, California 91105
Attn: Dr. Sam Naiditch

Union Carbide Corporation
Electronics Division
P.O. Box 6116
Cleveland, Ohio 44101
Attn: Dr. George E. Evans

United Aircraft Corporation
400 Main Street
East Hartford, Connecticut 06108
Attn: Library

University of Pennsylvania
Electrochemistry Laboratory
Philadelphia, Penna. 19104
Attn: Prof. John O'M. Bockris

University of Pennsylvania
Institute for Direct Energy Conversion
260 Towne Building
Philadelphia, Penna. 19104
Attn: Dr. Manfred Altman

Case-Western Reserve University
Department of Chemistry
Cleveland, Ohio 44101
Attn: Prof. Ernest Yeager

Research and Development Center
Westinghouse Electric Corporation
Churchill Borough
Pittsburgh, Penna. 15235
Attn: Dr. A. Langer

Whittaker Corporation
Narmco R&D Division
3540 Aero Court
San Diego, California 92123
Attn: Dr. M. Shaw

Yardney Electric Corp.
40 Leonard Street
New York, New York 10013
Attn: Dr. George Dalin

Zaromb Research Corp.
376 Monroe Street
Passaic, N.J. 07055
Attn: Dr. S. Zaromb